CEJGSD

CENTRAL EUROPEAN JOURNAL OF GEOGRAPHY AND SUSTAINABLE DEVELOPMENT

ISSN 2668-4322
ISSN-L 2668-4322 www.cejgsd.org Vol. 4, No. 2, 2022

Romanian Geographical Society – Prahova Branch

Open access international scientific journal for theory, research
and practice of geography, sustainable development and related disciplines

Central European Journal of Geography and Sustainable Development (CEJGSD)
Volume 4, Issue 2, 2022

This journal is available online:
https://cejgsd.org/

Publisher:
ROMANIAN GEOGRAPHICAL SOCIETY-PRAHOVA BRANCH
Petroleum-Gas University of Ploiești,
39 Bucharest Avenue, Ploiești 100680, Prahova County, Romania

ISSN 2668-4322
ISSN-L 2668-4322

DOI: 10.47246/CEJGSD

Official e-mail: cejgsd@gmail.com

Periodicity: Twice a year in June and December

This journal is available online:
www.cejgsd.org

Instructions for authors can be found online at:
https://cejgsd.org/instructions-for-authors

Indexing: *Central European Journal of Geography and Sustainable Development (CEJGSD)* is available in the following journal databases and repositories:

Directory of Open Access Journals (DOAJ),
INDEX COPERNICUS INTERNATIONAL (ICI World of Journals),
CABELLS - Scholarly Analytics,
Ulrich's Periodicals Directory,
Social Science Research Network (SSRN),
ERIH PLUS (European Reference Index for the Humanities and Social Sciences),
ANVUR (Italian National Agency for the Evaluation of Universities and Research Institutes),
J-Gate,
CiteFactor,
OpenAIRE,
MIAR (Information Matrix for the Analysis of Journals),
WorldCat,
EuroPub - Directory of Academic and Scientific Journals,
Current Geographical Publications (CGP),
Elektronische Zeitschriftenbibliothek / Electronic Journals Library (EZB)
Scientific Publishing & Information Online (SCIPIO),
ResearchBib,
ROAD Directory,
Open Academic Journals Index,
DRJI - Directory of Research Journals Indexing,
Crossref,
Institutional Research Information System (IRIS),
Cosmos.

Starting from 2023, CEJGSD will be published under the auspices and with the support received from Petroleum-Gas University of Ploieşti - Faculty of Economic Sciences.

Journal Office:
Petroleum-Gas University of Ploieşti
39 Bucharest Avenue, Ploieşti 100680, J Building, Room J III 4, Prahova County, Romania
Tel: +40 728 858 022
Email: cejgsd@gmail.com

December 2022
Volume 4, Issue 2

DOI: 10.47246/CEJGSD.2022.4.2

Printed in Romania

www.cejgsd.org

CONTENT

Central European Journal of Geography and Sustainable Development
ISSN 2668-4322, ISSN-L 2668-4322
2022, Volume 4, Issue 2, Pages: 5-23
https://doi.org/10.47246/CEJGSD.2022.4.2.1

Spatial Determinants of Forest Landscape Degradation in the Kilimanjaro World Heritage Site, Tanzania

Eveline Aggrey Enoguanbhor [1,*], Evidence Chinedu Enoguanbhor [2], Eike Albrecht [1]
[1] Department of Civil Law and Public Law with references to the European Law and Environment, Brandenburg University of Technology, Cottbus – Senftenberg, Germany;
[2] Applied Geoinformation Science Lab, Department of Geography, Humboldt University of Berlin, Germany;
evelinemwambene@yahoo.com (E.A.E.); albrecht@b-tu.de (E.A.); enoguanbhor.ec@gmail.com (E.C.E.)

Received: 29 June 2022; Revised: 25 August 2022; Accepted: 20 September 2022; Published online: 3 October 2022

Abstract: Forest degradation occurs in natural World Heritage Sites (WHS) in the Global South despite the implementation of various strategic policies and the World Heritage Convention (WHC) on forest protections of the sites and this poses challenges to improve natural heritage sustainability. The current study aims to investigate spatial determinants of forest degradation in the Kilimanjaro WHS, Tanzania, to support strategic policies for forest landscape protection and natural heritage sustainability. Using remotely sensed, Digital Elevation Model, and tourism location data, we performed the supervised classification of satellite images, Digital Elevation, Euclidean distance, and linear regression modeling to identify spatial determinants of forest degradation. Our key findings indicated that while spatial determinants vary with different locations, human (tourism) activities e.g., developments of campsites, picnics, tourist routes, the historical site, and attraction areas are associated with forest degradation in the southern parts of the site. In addition to human activities, natural factors such as low levels of elevation and degrees of slope are associated with forest degradation at the site. However, in the northwest and southwest of the site, high degrees of slope are associated with the degradation. Our findings showed that while bare land surface encroached the primary forest with about 2.88%, moorland vegetation encroached the primary forest with about 16.95%, indicating a large degradation of the primary forest with about 19.83% for the past four decades. The information provided in this study is crucial to support site managers and decision-makers in strategic policies and WHC implementations on forest protection for natural heritage sustainability.

Keywords: Forest degradation, montane primary forest, spatial determinants, natural heritage sustainability, World Heritage Site, Kilimanjaro.

Citation: Enoguanbhor, E. A., Enoguanbhor, E.C., & Albrecht, E. (2022). Spatial Determinants of Forest Landscape Degradation in the Kilimanjaro World Heritage Site, Tanzania. *Central European Journal of Geography and Sustainable Development*, *4*(2), 5-23. https://doi.org/10.47246/CEJGSD.2022.4.2.1

1. INTRODUCTION

Forest degradation occurs in the Global South [1-3], including natural World Heritage Sites (WHS). For example, in the eastern part of Tanzania, including the Kilimanjaro WHS, forest degradation occurred over the years [4-7], despite various strategic policies and acts [8-10], as well as the World Heritage Convention (WHC) of 1972 [11] that made provisions for forest protection of the sites. Forest degradation in natural WHS was reported across the Global South, including Coast Atlantic Forest Reserves in Brazil, Kinabalu Park in Malaysia, Mount Wuyi in China, Iguazu National Park in Argentina [12], and Sundarbans WHS, India [13]. Such degradation poses challenges to improving heritage sustainability, which is a condition that allows the utilization of the benefits (e.g., tourism destination and income) provided by the natural WHS without compromising the current and future forest ecosystems. Also, the degradation may

* Corresponding author: evelinemwambene@yahoo.com; Tel.: +49157 5848 5545

put the heritage sites in danger if strategic measures are not put in place to protect the sites from forest degradation.

Generally, forest degradation is determined by natural and human factors [14-16]. While natural determinants are attributed to physical geographical factors e.g., topographic elevation and slope [16,17], human determinants are attributed to human factors e.g., tourism activities, transportation, agriculture, charcoal production, settlement expansion [18-21,14,22,23,15,24,17] and can be used to explain spatial patterns and determinants of forest landscape degradation. In this context, spatial determinants can, therefore, be regarded as natural and human factors that are associate with or contribute to the explanation of the location of forest landscape degradation.

Spatial determinants of forest landscape degradation vary with space and location [18]. According to Bhattarai, et al. [19] distances to roads and settlements are positively associated with forest degradation in southern Tanzania. While distances to transportation and settlement, as well as topographic elevation (altitude) between 400 and 800m above sea level, are positively associated with forest loss in the Piracicaba River basin of the States of Sao Paulo and Minas Gerais, Brazil [17], distance to settlement is negatively associated with forest landscape degradation in the Democratic Republic of the Congo [18].

Previous studies e.g., Hamunyela, et al. [4]; Kilungu, et al. [5]; Rutten, et al. [6]; Soini [7]; Allan, et al. [12]; Levin, et al. [25] on natural WHS majorly focus on impacts and human driving factors of forest degradation with little or no emphasis on spatial determinants. In the Kilimanjaro WHS, no previous study was conducted on spatial determinants of forest degradation and this makes it difficult to identify such determinants to provide useful information for strategic policy decision-makers on the montane forest landscape protection and natural heritage sustainability. The montane forest is the primary forest with dense vegetation that provides habitats for wild animals in the Kilimanjaro WHS (Figure 4) (5).

The aim of this study, therefore, is to investigate spatial determinants of primary forest degradation in the Kilimanjaro WHS, Tanzania, to support strategic policies for forest landscape protection and natural heritage sustainability. Specifically, we seek to: analyze spatial patterns of land cover types for 1976, 2000, 2012, and 2020; compute the degraded primary forest, and analyze the association between various human/natural features and the degraded primary forest to identify spatial determinants of forest degradation.

2. STUDY AREA

The study area is the Kilimanjaro WHS (Kilimanjaro National Park), located in northeast Tanzania and it covers 1686.72 km^2 (Figure 1). The site is about 300 km south of the Equator [6]. We chose the Kilimanjaro WHS because of the forest degradation over the years [5-7] and the forest landscape, particularly the montane forest as one of the outstanding universal values of the natural heritage site [11]. The Kilimanjaro National Park was established in 1973 that initially composed of the whole mountain and moorland vegetation above the montane forest and was inscribed as a natural WHS in 1987 under criteria vii, with the mountain as an outstanding universal value, which is one of the largest volcanoes in the world [11,26]. The topographic elevation of the mountain within the site ranges from 1,277 to 5,880 m above sea level at Kibo peak, which is relatively located at the center of the mountain (Figure 1). Other peaks of the mountain include Shira peak (3,952 m above sea level) and Mawenzi peak (5,130 m above sea level) located in the northwest and southeast of the Kibo peak, respectively (Figure 1). In 2005, the site was extended to include the montane forest (the natural or primary forests that serve as buffer zones and habitats for wildlife) due to human pressure on forest degradation, which is also defined as the outstanding universal value and integrity feature of the site [11,26]. As a WHS and a National Park, various strategic actions, including the Forest Act of 2002 [9], National Environmental Policy of 1997 [10], and WHC of 1972 [11] have been implemented to protect the site from forest degradation. Despite the implementation of those strategic actions, forest degradation was reported by Hamunyela, et al. [4]; Kilungu, et al. [5]; Rutten, et al. [6]; Soini [7]. As a WHS and a National Park, Mount Kilimanjaro serves as a tourism destination for national and international tourists as the site receives about 50,000 tourists annually creating tourism pressure and associated problems, including vegetation trampling, water pollution, and soil erosion [26]. Other threats associated with the WHS include yearly wildfires that destroy natural forests that serve as buffer zones and habitats for wildlife, illegal logging of forest trees, and climate change causing the melting of glaciers that may lead to the disappearance of the snow cap [26].

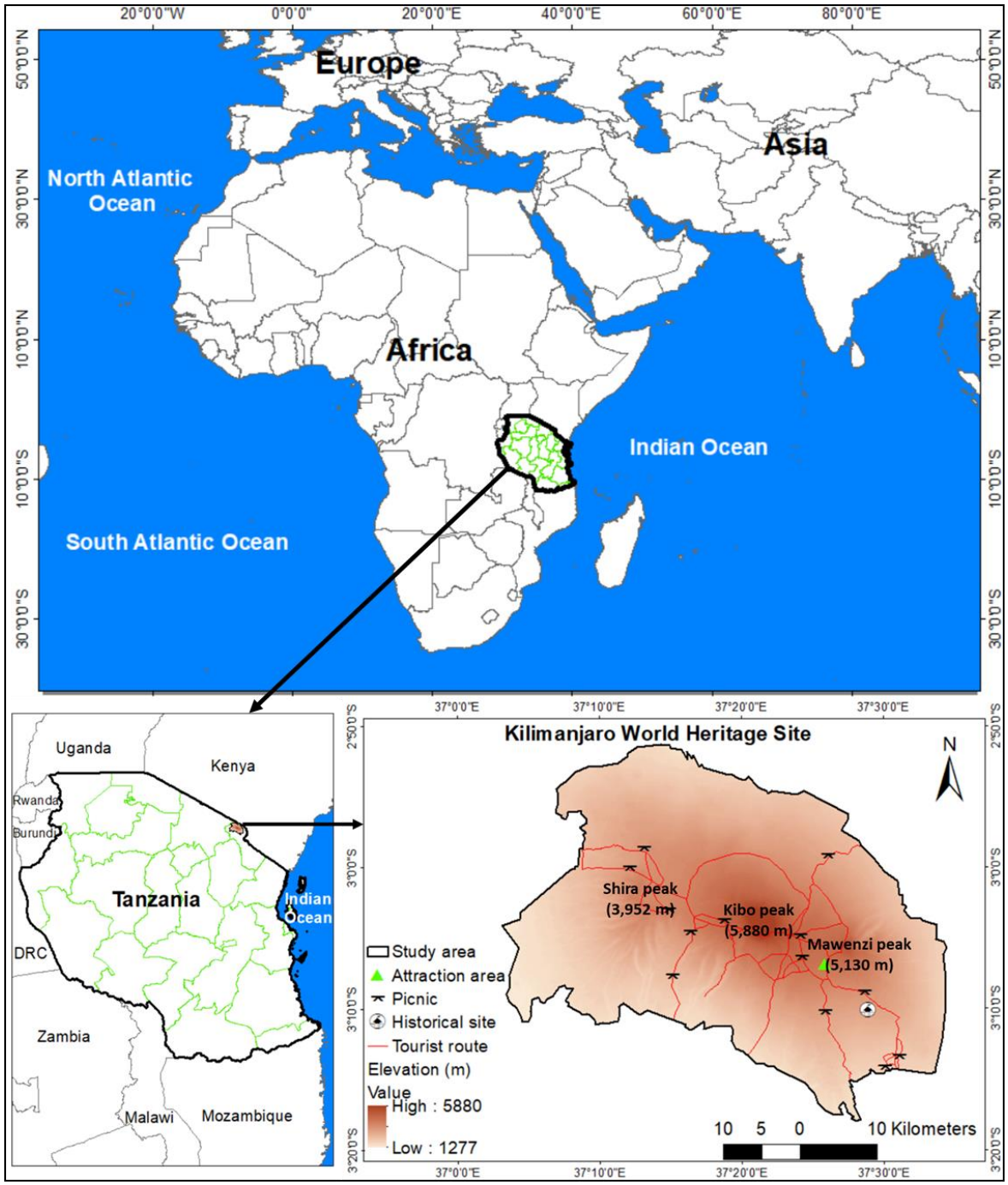

Figure 1. Maps showing the location of the Kilimanjaro World Heritage Site.
Source: Produced by authors

3. METHODS AND DATA

3.1. Data collection

We collected satellite images captured by Landsat 2 Multispectral Scanner System (MSS) in 1976 and Landsat 7 Enhanced Thematic Mapper Plus (ETM+) in 2000, 2012, and 2020 from the United States Geological Survey (USGS) [27]. The reason for collecting this set of data is due to the openly accessible platform and the coverage of the study area. Also, the set of data has been calibrated atmospherically with free cloud cover [27]. Additionally, all images were captured during precipitation seasons with heavy rainfall and snow on the Kilimanjaro Mountain and environs, which is from November to May, except that of 1976 and 2000, which were captured in January and February, respectively with little precipitations on the Kilimajaro Mountain and environs [28]. However, in January and February with little precipitations, all

types of vegetation, especially tree canopies may retain the same or similar level of green growth (chlorophyll contents) as in other months (e.g., December and March) with heavy rainfall. Furthermore, Landsat data have been deployed successfully in mapping forests to support the management of forest protections in various protected areas across the Global [29-31]. While the Landsat 2 data used for the current study is 60 m spatial resolution, that of Landsat 7 is 30 m. Table 1 summarizes the characteristics of all satellite images. An additional set of data used for the current study are tourist routes, campsites, picnics, the historical site, and the attraction area and were collected from ArcGIS online [32]. Furthermore, we collected the Digital Elevation Model (DEM) of 90 m spatial resolution from the Shuttle Radar Topography Mission (SRTM) [33].

Table 1. Summary of the remotely sensed data description.

Landsat series	Sensor	Spatial resolution	No: of bands	Date of acquisition	Sources
Landsat 2	MSS	60 m	7	21/01/1976	USGS
Landsat 7	ETM+	30 m	9	21/02/2000	USGS
Landsat 7	ETM+	30 m	9	09/03/2012	USGS
Landsat 7	ETM+	30 m	9	28/12/2020	USGS

Source: Prepared by authors.

3.2. Data analysis

To analyze spatial patterns of land cover types for 1976, 2000, 2012, and 2020, we used ArcGIS 10.8.1 to perform supervised classification of satellite images using a maximum likelihood algorithm [34-37]. The supervised classification uses training samples of the known pixels to assign pixels to different classes and the maximum likelihood algorithm uses the highest probability to assign pixels to such classes [34,38-40]. While generating training samples, we computed the Normalize Difference Vegetation Index (NDVI) [41-43] expressed as:

$$\mathbf{NDVI} = \frac{\mathbf{NIR} - \mathbf{R}}{\mathbf{NIR} + \mathbf{R}},$$

where NIR and R are the near-infrared band and red band, respectively that are used for the spectral reflectance measurements acquired in the near-infrared and visible (red) regions [43]. For Landsat 7 ETM+, band 4 is the near-infrared band with 0.772 - 0.898 μm and band 3 is the red band with 0.631 - 0.692 μm. For Landsat 2 MSS, band 6 is the near-infrared band with 0.7 - 0.8 μm and band 5 is the red band with 0.6 - 0.7 μm. While the healthy vegetation (e.g., primary forest) is reflected more in the near-infrared region due to high chlorophyll contents of the vegetation, unhealthy vegetation (e.g., moorland vegetation) and bare land surface are reflected more in the visible region due to low chlorophyll contents for moorland vegetation and lack of chlorophyll for bare land surfaces, including snow. The NDVI was grouped into three categories and based on their pixels' values for each category, 0.5 and above, 0.2 to 0.4, and 0.1 and below pixels' values were used to guide the selection of pixels' values on the composite multispectral images for healthy vegetation, unhealthy vegetation, and bare land surface, respectively. The selected pixels' values on the composite multispectral images were used to create training samples for the supervised classification, where the maximum likelihood algorithm was deployed [34-37]. We classified the land cover types into primary forest, moorland vegetation, and bare land surface as described in Table 2.

Table 2. Categories of land cover classes.

Land cover classes	Description of land cover
Primary forest	Healthy vegetation with montane and tropical rain forests
Moorland vegetation	Secondary forest, unhealthy vegetation, grasslands, shrubs, and cultivated fields
Bare land surface	Open space with alpine desert, volcanic soil, snow, wetlands, streems/rivers, rocks, and charcoal kilns

Source: Prepared by authors.

We performed accuracy assessments of the classified land cover types using simple random sampling [44] to generate 300 points and the composite images as based data for the assessments. We assessed the user accuracy (UA), producer accuracy (PA), and overall accuracy (OA) for land cover types, following Enoguanbhor, et al. [40]. The accuracy assessments are presented in Table 3.

Table 3. Accuracy assessments of land cover maps.

Land cover types	2020			2012		
	UA	PA	OA	UA	PA	OA
Primary forest	93.88%	88.46%		87.13%	86.27%	
Moorland vegetation	87.25%	89.00%	89.67%	86.87%	87.76%	86.33%
Bare land surface	88.00%	91.67%		85.00%	85.00%	
Land cover types	**2000**			**1976**		
	UA	PA	OA	UA	PA	OA
Primary forest	91.75%	85.58%		80.77%	84.00%	
Moorland vegetation	89.00%	89.00%	88.67%	84.62%	82.88%	82.67%
Bare land surface	85.44%	91.67%		81.48%	75.86%	

Source: Prepared by authors.

To compute the forest landscape degradation of the primary forest, we performed the transition change detection between 1976 and 2020 land cover types. We applied the pixel-based method and crosscheck or validated using the polygon-based method. Regarding the pixel-based method, which is the analysis based on the raster land cover maps, we first resampled the 60 m spatial resolution of the 1976 land cover map to 30 m to obtain and maintain the same pixels' sizes for both land cover maps. We applied the Land Change Modeler, an ArcGIS extension Toolbox from TerrSet (Geospatial Monitoring and Modeling Systems) to implement the transition change detection using the Multi-Layer Perceptron (MLP) Neural Network algorithm. The MLP Neural Network algorithm computes the weights of multiple input layers e.g., the 1976 and 2020 land cover maps to produce a single output layer e.g., the transitioned change detection map with the attribute information based on the number of pixels transitioned from different land cover types to others using a non-linear activation function (e.g., sigmoid) [39]. Regarding the polygon-based method to crosscheck the pixel-based method, we converted raster maps of both land cover types to vector maps and used Geoprocessing Tools, including Intersect and Union to run the transition change detection. The validation showed that both methods produced the same results with little difference. Finally, we extracted the transition from primary forest to moorland vegetation and bare land surface and used cartographic GIS overlays [45] to visualize and calculate the area of the degraded primary forest.

To analyze the association between various human/natural features and the degraded primary forest to identify spatial determinants of forest landscape degradation, we digitized locations of human features, including tourist routes, campsites, picnics, the historical site, and the attraction area. Also, we performed DEM analysis to generate parameters for the degrees of slope and levels of elevation. Additionally, we performed the Euclidean distance modeling on the digitized and extracted (degraded primary forest) maps to generate other parameters. We used all parameters to build simple and multiple linear regression models [46]. The simple and multiple linear regression modeling can be expressed as:

$$Y = \beta_0 + \beta_1 X_1 + \varepsilon$$
$$Y = \beta_0 + \beta_1 X_1 + \beta_2 X_2 + \beta_3 X_3 + \ldots + \beta_k X_k + \varepsilon \ ,$$

where Y is the dependent variable (degraded primary forest), X is the independent variable (human and natural features), β0 and β1 are intercept and coefficient, respectively and ε represents the random error terms. The independent variables were selected based on the availability of data on both human and natural features. To ensure the reduction of bias in the model, we used the Variance Inflation Factor (VIF) to calculate the multicollinearity problem and eliminated variables with 10 and above VIF values to make sure all independent variables have independent effects on the dependent variable [38,46,39,47]. After the analysis of the entire site, the site was divided into four areas, northwest, northeast, southwest, and southeast. The same analysis was performed for each of the four areas to understand the spatial determinants at the local scale and for comparative purposes between the four areas of the site.

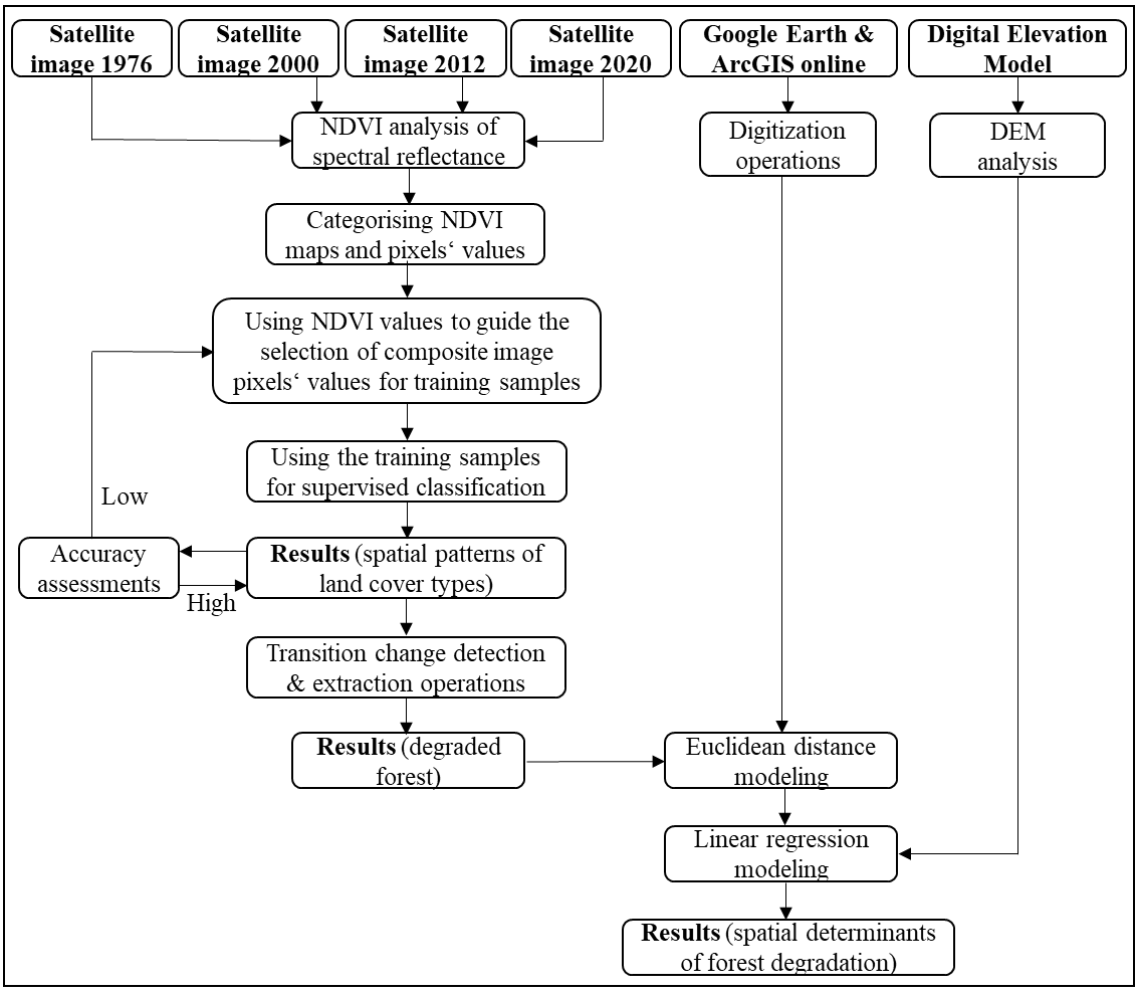

Figure 2. Materials and methods for spatial determinants of forest landscape degradation.
Source: Developed by authors.

4. RESULTS

4.1. Spatial patterns of land cover types

We analyzed the spatial patterns of land cover types for 1976, 2000, 2012, and 2020 in the Kilimanjaro WHS. Our results (Table 4 and Figure 3) showed that the primary forest are spatially distributed in the lower parts of the mountain and decreased from 1,290.64 km² (76.52%) in 1976 to 833.49 km² (49.42%) in 2020. Contrarily, the moorland vegetation is spatially distributed from the middle to upper parts of the mountain and increased from 360.08 km² (21.35%) to 453.04 km² (26.86%) in 2020. The bare land surface is mostly distributed at the mountain top, covering about 35.91 km² (2.13%) in 1976, 431.14 km² (25.56%) in 2000, 401.30 km² (23.79%) in 2012, and 400.12 km² (23.73%) in 2020. The observation in Figure 4 shows that while the bare land surface encroached on the moorland vegetation, the moorland vegetation encroached on the primary forest in the past four decades.

Table 4. Calculated areas of land cover types in km²

Land cover classes	1976	2000	2012	2020
	Area km²	Area km²	Area km²	Area km²
Bare land surface	35.91	431.14	401.30	402.12
Moorland vegetation	478.08	393.99	437.10	441.04
Primary forest	1172.64	861.45	848.20	843.49
Total	**1,686.63**	**1,686.58**	**1,686.62**	**1,686.65**

Source: Prepared by authors.

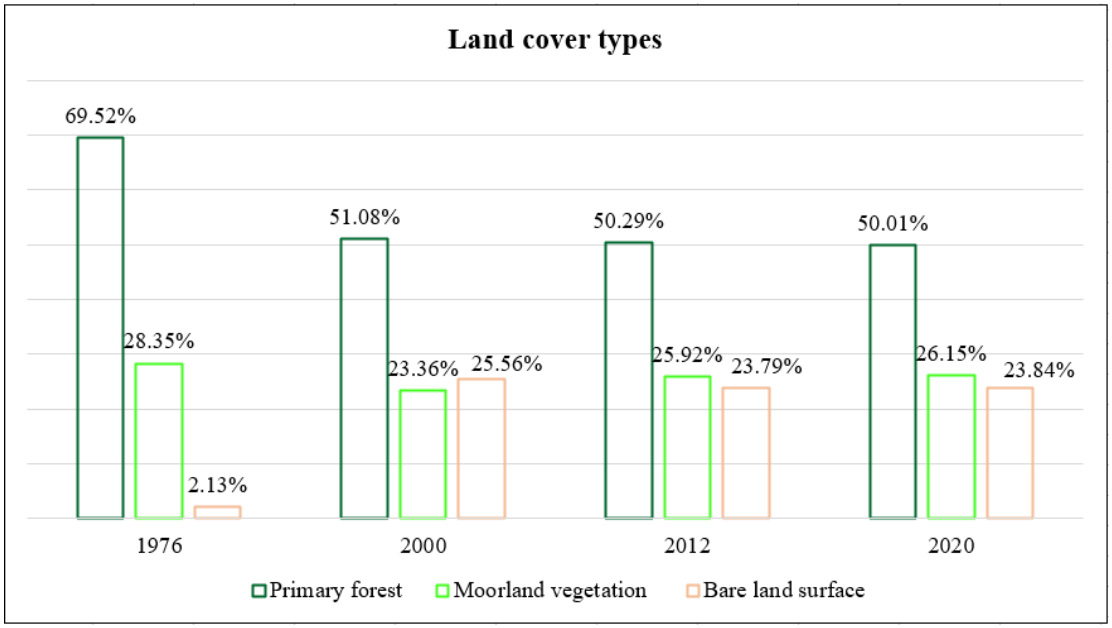

Figure 3. Calculated area of land cover types in percentage.
Source: Produced by authors.

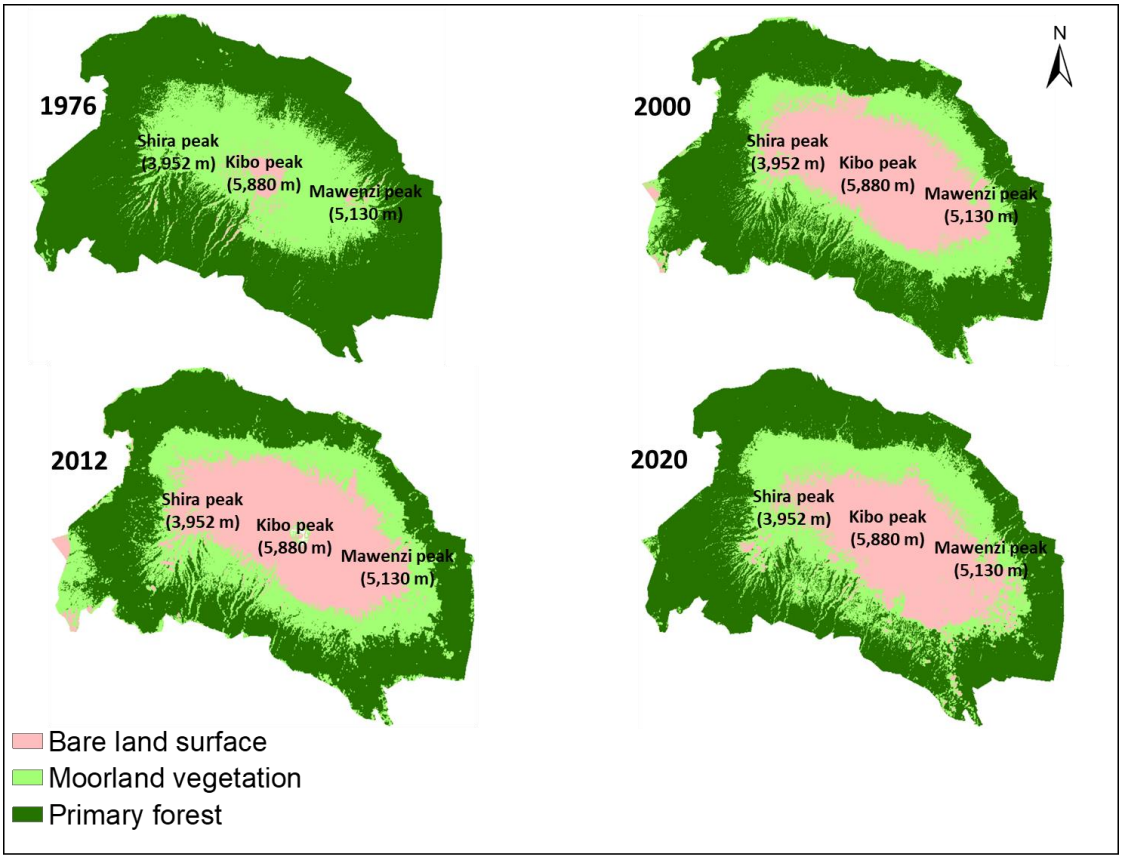

Figure 4. Spatial patterns of land cover types.
Source: Produced by authors.

4.2. Degraded primary forest

We computed the degraded primary forest through a transition mapping process. The transition mapping showed the highest transition that occurred between the primary forest and other land cover types is the moorland vegetation (Figure 5a). While about 16.95% of the primary forest transitioned into

the moorland vegetation, 2.88% transitioned into the bare land surface. Our result in Figure 5b shows that the primary forest that was degraded from 1976 to 2020 is about 19.83% of the total area.

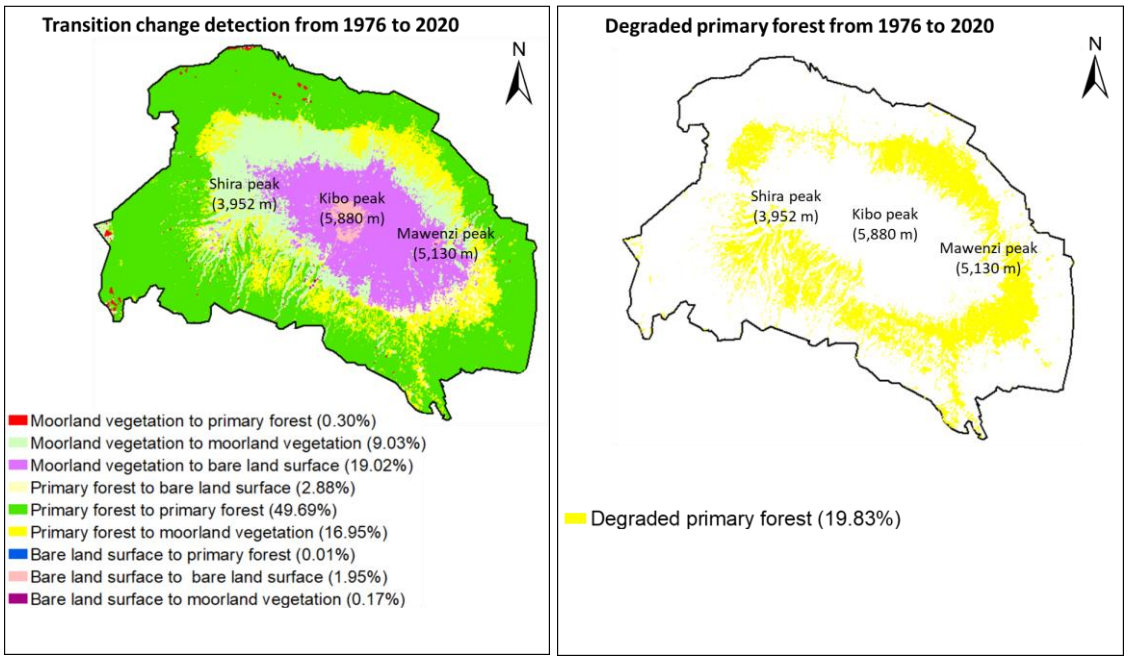

(a) **(b)**

Figure 5. Spatial patterns of (**a**) land cover transitions and (**b**) the degraded primary forest.
Source: Produced by authors.

4.3. Associations between human/natural features and the degraded primary forest

Considering the entire scale of the site, we analyzed the association between various human/natural features and the degraded primary forest to identify spatial determinants of forest degradation in the Kilimanjaro WHS (Table 5 and Figure 6). Our results at the simple linear regression level of the whole site (Table 5) showed that distances to the locations of human activities, including tourist routes, campsites, picnic locations, the historical site, and the attraction area are negatively associated with the degraded primary forest. The level of elevation and the degrees of slope as natural features are positively associated with the degraded primary forest, with slope having the highest coefficient.

Table 5. Spatial determinants of the degraded primary forest of the Kilimanjaro WHS.

	Independent variables	Simple linear regression			Multiple linear regression				
		Coef.	P-value	Std. error	Coef.	P-value	Std. error	Initial VIF	Final VIF
1	Dist. to tourist route	-0.010	0.000***	0.003	0.007	0.151	0.005	6.818	5.955
2	Dist. to campsite	-0.010	0.000***	0.003	0.154	0.000***	0.005	6.171	5.339
3	Dist. to picnic	-0.018	0.000***	0.003	-0.002	0.684	0.004	3.765	3.457
4	Dist. to the historical site	-0.001	0.147	0.000	-	-	-	18.106	-
5	Dist. to attraction area	-0.013	0.000***	0.001	-	-	-	22.116	-
6	Level of elevation	0.603	0.001***	0.011	1.109	0.000***	0.013	3.260	1.972
7	Degrees of slope	4.026	0.005 ***	1.434	-0.182	0.000***	0.012	1.130	1.122

Residual standard error = 796.1 on 9994 degrees of freedom (multiple linear regression)
Multiple R-squared = 0.414, Adjusted R-squared = 0.4139 (multiple linear regression)
P-value = 0.000*** (multiple linear regression)

Source: Prepared by authors.

The results at the multiple linear regression level (Table 5) showed that while the degrees of slope and distance to picnic are negatively associated with the degraded primary forest, distances to tourist routes, campsites, and the level of elevation are positively associated. Distances to the historical site and the attraction area were eliminated from the model due to the problem of multicollinearity in the initial VIF. The final VIF indicated that the final model eliminated the multicollinearity problem and the low standard errors associated with all variables indicated good models' fit.

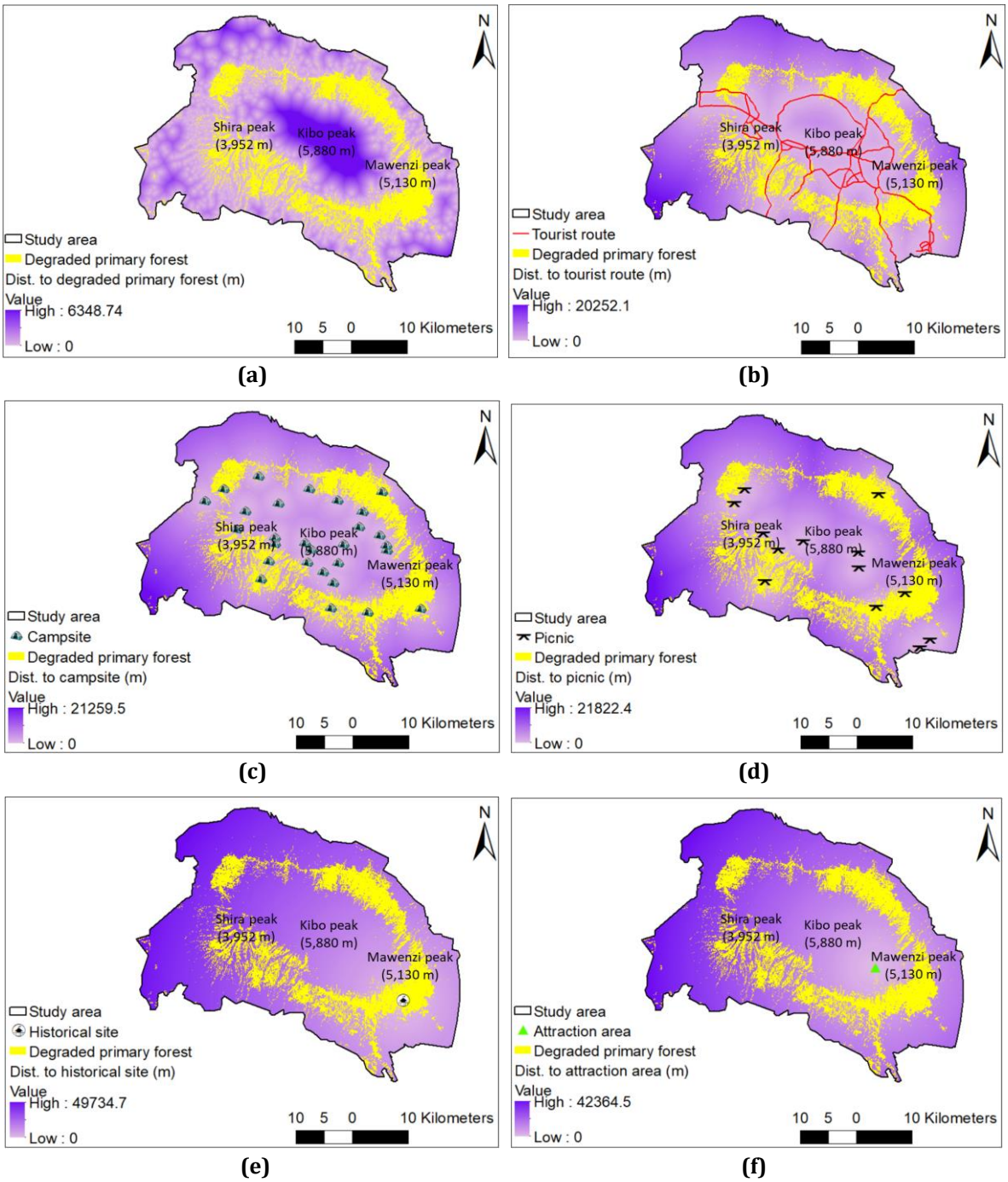

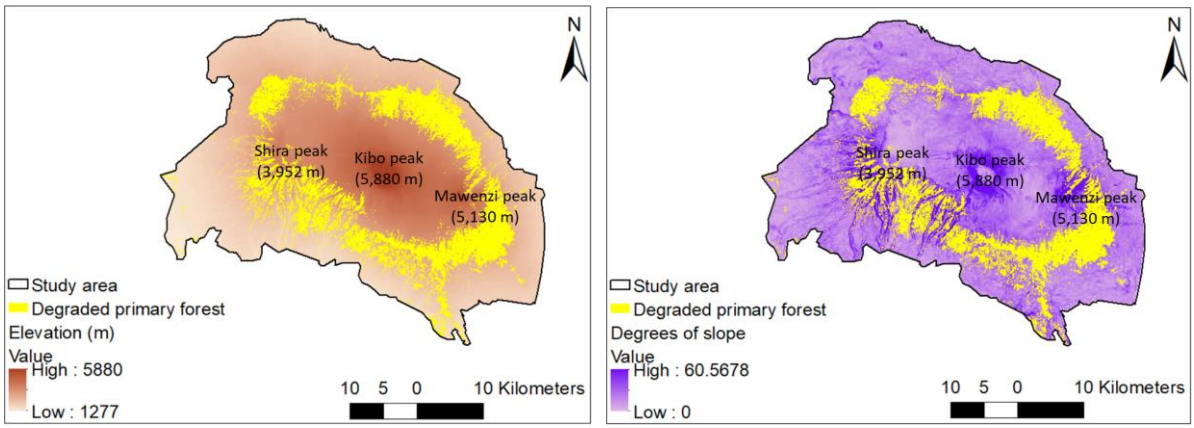

(g) **(h)**

Figure 6. Maps showing Euclidean distances to (**a**) degraded primary forest, (**b**) tourist route, (**c**) campsite, (**d**) picnic, (**e**) historical site, and (**f**) attraction area, (**g**) level of elevation, and (**h**) the degrees of slope. Source: Produced by authors.

Our results at the simple linear regression level of the northwest Kilimanjaro WHS (Table 6) showed that while distances to tourist routes, campsites, and picnic locations are positively associated with the degraded primary forest, that of the historical site and attraction area are negatively associated. The level of elevation and the degrees of slope as natural features are positively and negatively associated respectively. The multiple linear regression level showed that the degrees of slope remains negative and the distance to picnic remains positive. Other variables were excluded from the model due to problems of multicollinearity indicated by VIF values above 10. Low standard errors associated with all variables indicated good models' fit.

Table 6. Spatial determinants of the degraded primary forest in northwest Kilimanjaro NWHS.

	Independent variables	Simple linear regression			Multiple linear regression				
		Coef.	P-value	Std. error	Coef.	P-value	Std. error	Initial VIF	Final VIF
1	Dist. to tourist route	0.040	0.000***	0.005	-	-	-	10.603	-
2	Dist. to campsite	0.065	0.000***	0.006	-	-	-	10.256	
3	Dist. to picnic	0.029	0.000***	0.005	0.026	0.000***	0.005	5.467	1.027
4	Dist. to the historical site	-0.045	0.000***	0.003	-	-	-	1008.795	-
5	Dist. to attraction area	-0.046	0.000***	0.003	-	-	-	1056.567	-
6	Level of elevation	0.407	0.000***	0.027	-	-	-	13.964	
7	Degrees of slope	-15.844	0.000***	3.374	-13.162	0.000***	3.404	1.202	1.027
Residual standard error = 948.5 on 2564 degrees of freedom (multiple linear regression)									
Multiple R-squared = 0.018, Adjusted R-squared = 0.017 (multiple linear regression)									
P-value = 0.000*** (multiple linear regression)									

Source: Prepared by authors.

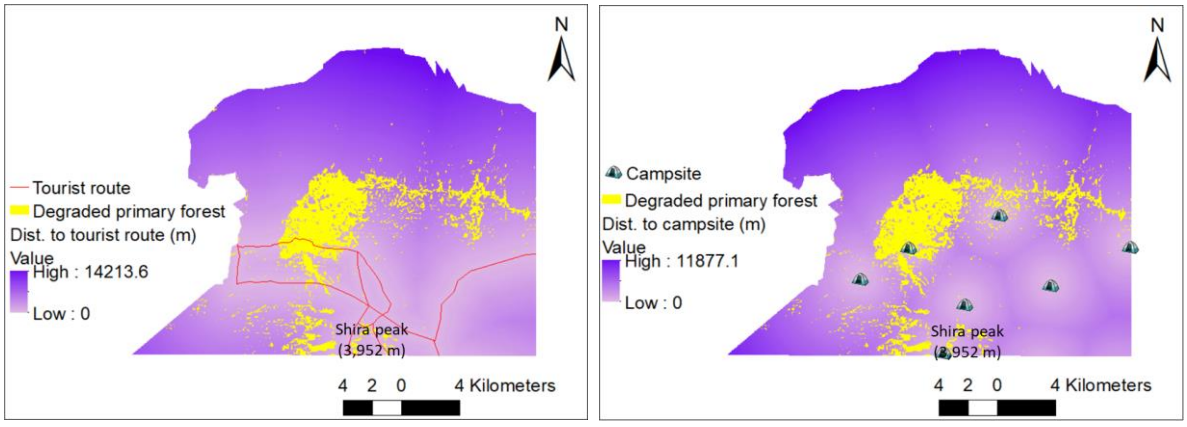

(a) **(b)**

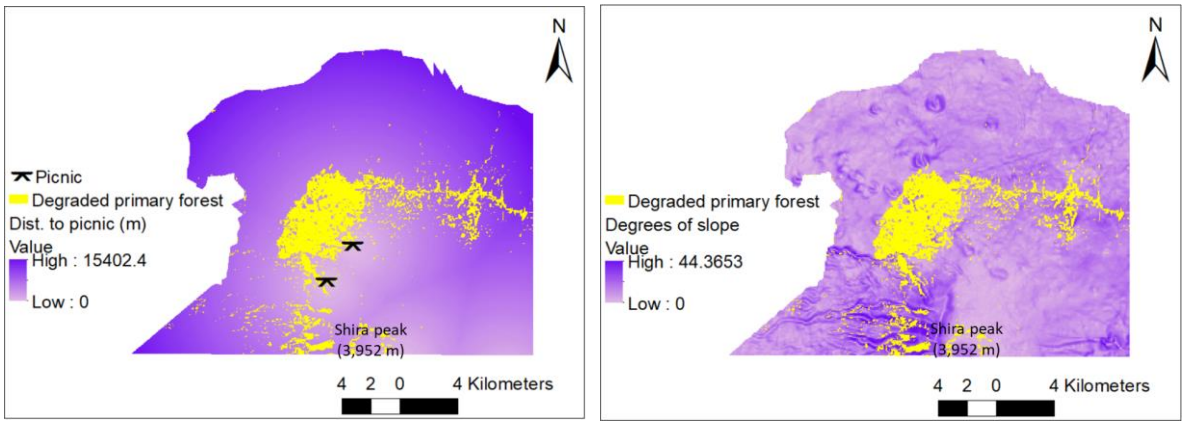

(c) **(d)**

Figure 7. Maps showing relationships between the degraded primary forest and Euclidean distances to (**a**) tourist routes, (**b**) campsites, (**c**) picnics, and (**d**) degrees of slope in the northwest Kilimanjaro WHS. Source: Produced by authors**.**

In the northeast Kilimanjaro WHS, the results (Table 7) showed that while distances to tourist routes and campsites are positively associated with the degraded primary forest, that of the picnic, the historical site, and attraction area are negatively associated. The natural features: level of elevation and the degrees of the slope are positively associated, with slope having the highest coefficient. The multiple linear regression showed that the degrees of slope remains positive and the distance to picnics remains negative. Other variables were excluded from the model due to problems of multicollinearity indicated by VIF values above 10. Low standard errors associated with all variables indicated good models' fit.

Table 7. Spatial determinants of the degraded primary forest in northeast Kilimanjaro NWHS.

	Independent variables	Simple linear regression			Multiple linear regression				
		Coef.	P-value	Std. error	Coef.	P-value	Std. error	Initial VIF	Final VIF
1	Dist. to tourist route	0.011	0.362	0.012	-	-	-	15.557	-
2	Dist. to campsite	0.013	0.337	0.013			-	14.542	
3	Dist. to picnic	-0.001	0.928	0.001	-0.004	0.547	0.007	1.786	1.000
4	Dist. to the historical site	-0.026	0.000***	0.006	-	-	-	88.774	-
5	Dist. to attraction area	-0.061	0.000***	0.006	-	-	-	125.941	-
6	Level of elevation	1.096	0.000***	0.029			-	11.305	
7	Degrees of slope	152.800	0.000***	4.730	0.015	0.000***	4.731	2.272	1.000
Residual standard error = 824.1 on 1523 degrees of freedom (multiple linear regression)									
Multiple R-squared = 0.407, Adjusted R-squared = 0.406 (multiple linear regression)									
P-value = 0.000*** (multiple linear regression)									

Source: Prepared by authors.

Table 8. Spatial determinants of the degraded primary forest in southwest Kilimanjaro NWHS.

	Independent variables	Simple linear regression			Multiple linear regression				
		Coef.	P-value	Std. error	Coef.	P-value	Std. error	Initial VIF	Final VIF
1	Dist. to tourist route	0.027	0.000***	0.002	-	-	-	27.819	-
2	Dist. to campsite	0.028	0.000***	0.002	-	-	-	35.903	-
3	Dist. to picnic	0.023	0.000***	0.002	-	-	-	13.329	-
4	Dist. to the historical site	0.013	0.000***	0.001	-	-	-	674.671	-
5	Dist. to attraction area	0.012	0.000***	0.001	-	-	-	850.934	-
6	Level of elevation	0.067	0.000***	0.014	-	-	-	12.522	-
7	Degrees of slope	-18.210	0.000***	1.201	-	-	-	1.333	-

Source: Prepared by authors.

In the southwest Kilimanjaro NWHS, the results (Table 8) showed that distances to all the identified human activities are positively associated with the degraded primary forest. The level of elevation and the

degrees of slope as natural features indicated positive and negative associations respectively. The multiple linear regression modeling was not performed due to problems of multicollinearity associated with all independent variables, except the degrees of slope.

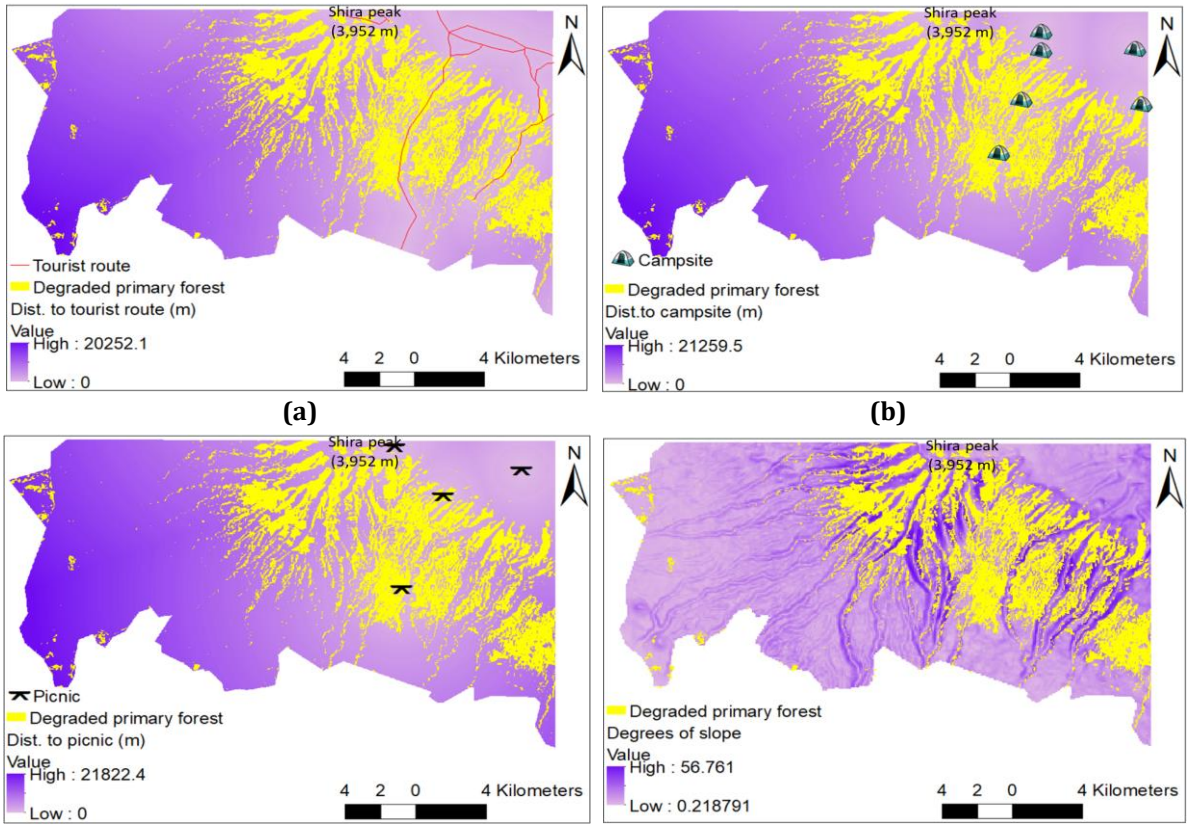

Figure 9. Map showing relationships between the degraded primary forest and (**a**) tourist routes, (**b**) campsites, (**c**) picnics, and (**d**) the degrees of slope.
Source: Produced by authors.

In the southeast Kilimanjaro WHS, the results (Table 9) showed that while distances to tourist routes, campsites, picnics, and the attraction area are negatively associated with the degraded primary forest, that of historical site is positive. The level of elevation and the degrees of slope as natural features are positively associated, with slope having the highest coefficient. The multiple linear regression showed that distances to picnic and the historical site remain negatively and positively associated respectively. While the initial VIF indicated the absence of multicollinearity problem, low standard errors associated with all variables indicated good models' fit.

Table 9. Spatial determinants of the degraded primary forest in southeast Kilimanjaro NWHS.

	Independent variables	Simple linear regression			Multiple linear regression				
		Coef.	P-value	Std. error	Coef.	P-value	Std. error	Initial VIF	Final VIF
1	Dist. to tourist route	-0.156	0.000***	0.009	0.048	0.000***	0.009	2.740	-
2	Dist. to campsite	-0.123	0.000***	0.009	0.066	0.000***	0.007	2.428	-
3	Dist. to picnic	-0.158	0.000***	0.008	-0.187	0.000***	0.009	3.765	-
4	Dist. to the historical site	0.150	0.000***	0.005	0.135	0.000***	0.009	2.718	-
5	Dist. to attraction area	-0.058	0.000***	0.005	0.138	0.000***	0.006	4.042	-
6	Level of elevation	0.826	0.000***	0.018	0.012	0.000***	0.033	6.604	-
7	Degrees of slope	21.969	0.000***	2.973	-0.318	0.000***	0.020	1.486	-
	Residual standard error = 705.5 on 3397 degrees of freedom (multiple linear regression)								
	Multiple R-squared = 0.6992, Adjusted R-squared = 0.6986 (multiple linear regression)								
	P-value = 0.000*** (multiple linear regression)								

Source: Prepared by authors.

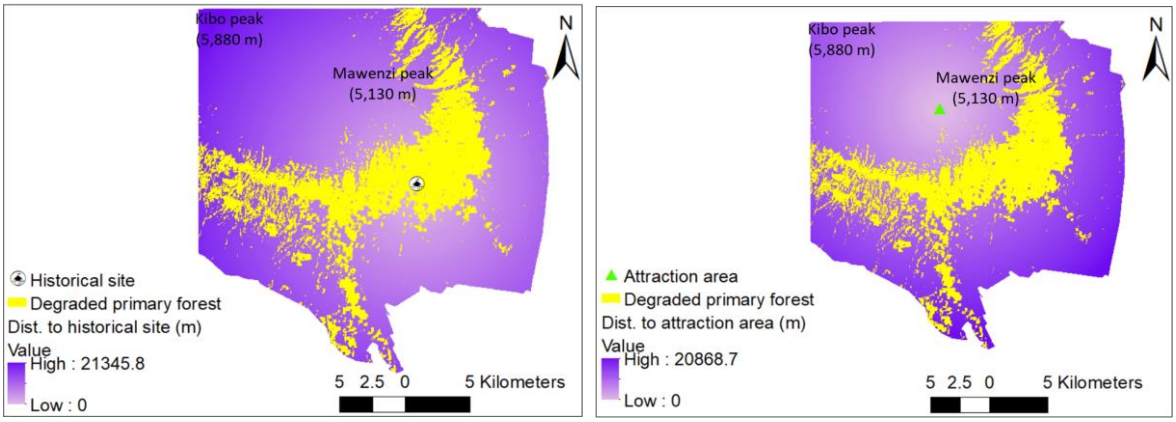

(a) **(b)**

Figure 10. Maps showing relationships between the degraded primary forest and Euclidean distances to (**a**) the historical site and (**b**) the attraction area.
Source: Produced by authors**.**

5. DISCUSSION

Our study provides the first comprehensive investigation of spatial determinants of forest degradation in the Kilimanjaro WHS, Tanzania to support strategic policies for forest landscape protection and natural heritage sustainability.

5.1. Findings

Considering the scale of the site holistically, our findings (Table 5) show that the topographic elevation and slope as natural features are positively associated with forest degradation, indicating the lower the level of elevation and degrees of slope, the higher the likelihood of forest degradation. The results are similar to the findings from Htun, et al. [48] and Freitas et al. [49] who reported forest degradation at the low level of elevation and degrees of slope in the Popa Mountain Park, Central Myanmar, and the Plateau of Ibiuna, near Sao Paulo, Brazil, respectively. Other human factors are associated negatively, indicating the farther from those locations, the higher the likelihood of forest degradation. This could be due to the scale of the entire study area. Comparison of spatial determinants at the local scale, the degrees of the slope are negatively associated with forest degradation in the northwest and southwest Kilimanjaro WHS, indicating the higher the degrees of slope, the higher the likelihood of forest degradation in those areas. This can be visualized in Figures 7d and 9d. Considering previous studies e.g., Htun et al. [48] and Freitas et al. [49] that report the degradation of the forest at the low degrees of slope, other factors other than the degrees of slope may be responsible for forest degradation in the northwest and southwest Kilimanjaro WHS. Distances to tourist routes, campsites, and picnics are positively associated with forest degradation in the northwest area, indicating the closer the locations of those tourist activities in the northwest, the higher the likelihood of forest degradation. These are visualized in Figures 7a, b, and c). Contrarily, distances to the historical site and the attraction area are negatively associated with forest degradation in the same northwest. In the northeast Kilimanjaro WHS, our findings (Table 7) show the only human features that are positively associated with forest degradation are tourist routes and campsites but in the southwest, all the identified human features are associated with forest degradation positively, indicating the contribution of tourism activities on forest degradation. These are visualized in e.g., Figures 9a, b, and c. These results support the findings from Pongpattananurak [50] who reported the impact of tourism on forest degradation in the overlapping area between Thap Lan National Park and the Thai Samakkhi subdistrict of Thailand. In the southeast, the only human feature that is positively associated with forest degradation is the attraction area. However, picnic turned out to be the only human feature that is negatively associated at the multiple linear regression level in the same southeast area.

Our findings on spatial patterns of land cover types (Table 4 and Figures 3 and 4) show the primary forest was about 69.52% in 1976 and decreased to 50.01% in 2020. This result is consistent with those of

Hamunyela, et al. [4] and Kilungu, et al. [5], who reported a decrease in primary (montane) forest in the Kilimanjaro WHS, Tanzania. Also, the result is similar to those of Adeyemi & Owolabi [51]; Sievers, et al. [13]; Zeb [52], and Htun, et al. [48] who showed decreasing primary/mangrove/dense/closed forests in Effan Forest Reserve in Nigeria, Sundarbans natural WHS in India, the District Chitral in Pakistan, and Popa Mountain Park in Central Myanmar, respectively. Also, the result is similar to those of Morin, et al. [29] and Ullah, et al. [53] who reported reductions in forest land cover in the Dilijan National Park of Armenia and Teknaf Wildlife Sanctuary of Bangladesh, respectively. However, the result differs from the report from Liu, et al. [54] who showed increasing forestland in the Jiuzhaigou natural WHS, China. The study shows a little decrease in the forest between 2000, 2012, and 2020 and this may be associated with the stronger implementation of strategic policies and WHC on forest protection as the primary forest was included in the site in 2005 [11]. Our study showed that the moorland vegetation decreased from 1976 to 2000 and started increasing from 2000 to 2020. The moorland vegetation increase is similar to those of Kilungu, et al. [5]. Our observation shows that while the bare land surface encroached into the moorland vegetation, the moorland vegetation encroached into the primary forest over the years. This can be visualized on spatial patterns of land cover types (Figure 3) and the transition mapping (Figure 4a). The computation of the transition mapping shows that about 19.83% of the study area has been degraded within the primary forest between 1976 and 2020 (Figure 4b).

5.1. Implications of the findings

One implication of our findings is the clarification that spatial determinants of forest degradation in the Kilimanjaro WHS vary with different locations in the site, similar to the report from Shapiro et al. [18] for the Democratic Republic of the Congo and Zeb [52] for the District Chitral, Pakistan. This would help site managers to look beyond the reports deduced from the holistic viewpoint of the entire site in general to specific areas of the site in particular when implementing the WHC and other strategic policies for forest protection and natural heritage sustainability. For example, considering the site as a protected area that allows tourism activities, tourist routes, development of campsites, and picnics pose threats to the primary forest in the southwest area and the historical site and attraction areas pose threats in the southeast area. This may be the case for other natural WHS that serve as tourism destinations in Sub-Saharan Africa and other parts of the Global South. Human activities such as the development of campsites and picnics have the possibility of causing fire outbreaks that can degrade forest landscapes [26,55,56]. Tourism is one of the major activities posing a significant threat to forest protection [50,57,5,58,59].

An important implication of our findings is the decrease in primary forests that may be associated with the loss of habitats for wildlife in those areas, which may lead to wildlife migration/extinction and a decrease in tourism demand [11,60]. Also, the decrease in primary forest may put the site in danger, considering the forest as one of the outstanding universal values of the natural heritage [11]. Additionally, degradation of the primary forest may expose the site to denudation and increases soil erosion that may later develop into gully erosions [26]. Gully erosions may affect existing tourist routes, which may lead to the development of additional routes with additional negative impacts on forest protection and wildlife disturbances.

The positive implication of our findings shows that various strategic policies and WHC implementations on forest protection may have improved over the last two decades, considering a slight decrease in the primary forest from 2000 to 2020. In 2005, the Kilimanjaro WHS was expanded from the initial boundary of the moorland vegetation of the mountain to the primary (montane) forest of the mountain [11,26] and that may have enhanced the protection of the primary forest. However, there is a need to regenerate forest within lower parts of moorland vegetation for effective forest protection due to the encroachment of moorland vegetation into the primary forest between 1976 and 2020. Regeneration of forests in those areas would improve forest and natural heritage sustainability, as well as habitat protection for wildlife on the site.

Such spatial information is crucial for site managers and decision-makers in strategic policies and WHC implementations on forest protection in the Kilimanjaro WHS, Tanzania and other natural WHS found in Sub-Saharan Africa, as well as other parts of the Global South. By integrating various methods to derive new findings on, e.g., how human (various tourism activities) and natural (elevation and degrees of

slope) factors determine spatial patterns of forest degradation at different scales in a WHS, our study, therefore, contributes to Heritage Studies and Management for natural heritage sustainability.

5.3. Limitations and recommendations

One limitation of the current study is the non-availability of data related to other uses of the site. This makes it impossible to identify additional human factors (e.g., illegal logging) [61,26] in the site as spatial determinants of forest degradation. Also, the use of 30 m spatial resolution of remotely sensed data did not allow the identification of the locations of such illegal logging. However, the openly accessible remotely sensed data are useful for monitoring primary forest trends of the Kilimanjaro WHS at no cost. Additionally, our inability to obtain 100% accuracies shows that there are some misclassifications of land cover types despite the high accuracies obtained for the current study.

Based on the limitations of the current study and the findings, we recommend the following: First, the information on spatial determinants of forest degradation provided in the current study should be considered when implementing strategic policies and WHC on forest landscape protection of the site. For example, tourism activities such as the development of campsites and picnics that are associated with forest degradation should be monitored effectively to prevent further degradation (e.g., fire outbreaks). Second, the strategic policies and WHC implementations on forest landscape protection can still be improved to regenerate forest along the lower parts of the moorland vegetation to compensate for the loss of primary forest over the years. This can be done by initiating forest regeneration programs within the context of the strategic policies and WHC. Finally, future research should be conducted by integrating high spatial resolution remotely sensed data and additional data on other uses of the site (including illegal logging), as well as the qualitative survey-based data to investigate spatial determinants and other driving factors of forest landscape degradation of the site.

6. CONCLUSIONS

Our study investigated spatial determinants of forest degradation in the Kilimanjaro WHS, Tanzania to support strategic policies for forest landscape protection and natural heritage sustainability. The analysis of spatial patterns of land cover types showed a decrease in primary forest and a decrease in moorland vegetation over the years. The computation of transition mapping showed the encroachments of bare land surface into moorland vegetation and that of moorland vegetation into the primary forest, indicating a large area of primary forest degraded over the years. While spatial determinants of the degraded primary forest vary with different locations in the site, human (tourism) activities, including locations of tourist routes, campsites, picnics, the historical site, and the attraction area are mostly associated with the degradation of forest in the southern parts of the site.

The study showed that spatial determinants of forest degradation in the Kilimanjaro WHS vary with different locations in the site, similar to the report from previous studies in the Democratic Republic of the Congo and the District Chitral, Pakistan. Additionally, while tourism activities such as tourist routes, development of campsites, and picnics pose threats to the primary forest in the southwest area, the historical site and the attraction area of tourism activities pose threats to the same forest category in the southeast area of the site. For sustainable protection of the forest landscape in the Kilimanjaro WHS, additional efforts are required to intervene the lost primary forest by regenerating the forest in the lower parts of the moorland vegetation. By investigating the spatial patterns of primary forest of a protected WHS and how distances to various tourist activities (e.g., the attraction area, picnic locations, campsites, tourist routes, and the historical site), as well as other environmental factors (e.g., topography), are associated with the degradation, this paper contributes to Heritage Studies and Management for natural heritage sustainability.

Spatial information provided in the current study is crucial to support site managers and decision-makers in strategic policies and WHC implementations on forest landscape protection for natural heritage sustainability of the Kilimanjaro WHS, Tanzania and other sites located in the Global South. Future research is required to integrate high spatial resolution satellite images and additional location data e.g., illegal logging, as well as qualitative survey-based data to investigate other driving factors along with spatial determinants of forest landscape degradation.

ACKNOWLEDGMENT

We acknowledge Paul and Maria Kremer Stiftung for the PhD scholarship awarded to the first author that contributed financially to the success of this article. Also, we appreciate the United States Geological Survey (USGS) for making the remotely sensed data used in this study freely available and accessible.

REFERENCES

1. Pinage, E. R., Bell, D. M., Longo, M., Gao, S., Keller, M., Silva, C. A., Ometto, J. P., Köhler, P., Frankenberg, C., & Huete, A. (2022). Forest structure and solar-induced fluorescence across intact and degraded forests in the Amazon. *Remote Sensing of Environment*, 274, 112998. https://doi.org/10.1016/j.rse.2022.112998
2. Fitz, J., Adenle, A. A. & Speranza, C. I. (2022). Increasing signs of forest fragmentation in the Cross River National Park in Nigeria: Underlying drivers and need for sustainable responses. *Ecological Indicators*, 139, 108943. https://doi.org/10.1016/j.ecolind.2022.108943
3. Marzo, T. D., Gasparri, N. I., Lambin, E. F., & Kuemmerle, T. (2022). Agents of Forest Disturbance in the Argentine Dry Chaco. *Remote Sensing, 14*(7), 1758. https://doi.org/10.3390/rs14071758
4. Hamunyela, E., Brandt, P., Shirima, D., Do, H. T. T., Herold, M., & Roman-Cuesta, R. M. (2020). Space-time detection of deforestation, forest degradation and regeneration in montane forests of Eastern Tanzania. *International Journal of Applied Earth Observation and GeoinformationInt*, 88, 102063. https://doi.org/10.1016/j.jag.2020.102063
5. Kilungu, H., Leemans, R., Munishi, P. K.T., Nicholls, S., & Amelung, B. (2019). Forty Years of Climate and Land-Cover Change and its Effects on Tourism Resources in Kilimanjaro National Park. *Tourism Planning & Development*, 16, 235–253. https://doi.org/10.1080/21568316.2019.1569121
6. Rutten, G., Ensslin, A., Hemp, A., & Fischer, M. (2015). Forest structure and composition of previously selectively logged and non-logged montane forests at Mt. Kilimanjaro. *Forest Ecology and Management*, 337, 61–66. http://dx.doi.org/10.1016/j.foreco.2014.10.036
7. Soini, E. (2005). Land use change patterns and livelihood dynamics on the slopes of Mt. Kilimanjaro, Tanzania. *Agricultural Systems*, 85, 306–323. https://doi.org/10.1016/j.agsy.2005.06.013
8. Magessa, K., Wynne-Jones, S., & Hockley, N. (2020). Does Tanzanian participatory forest management policy achieve its governance objectives? *Forest Policy and Economics*, 111, 102077. https://doi.org/10.1016/j.forpol.2019.102077
9. URT (United Republic of Tanzania), (2002). *The Forest Act, 2002*. Dar Es Salaam: URT.
10. URT (United Republic of Tanzania), (1997). *National Environmental Policy*. Dar Es Salaam: URT, Vice president office.
11. UNESCO (United Nations Educational, Scientific and Cultural Organization) (2021). *Convention Concerning the Protection of the World Cultural and Natural Heritage.* Retrieved from https://whc.unesco.org/en/conventiontext/
12. Allan, J. R., Venter, O., Maxwell, S., Bertzky, B., Jones, K., Shi, Y., & Watson, J. E. M. (2017). Recent increases in human pressure and forest loss threaten many Natural World Heritage Sites. *Biological Conservation*, 206, 47–55. http://dx.doi.org/10.1016/j.biocon.2016.12.011
13. Sievers, M. Chowdhury, M. R., Adame, M. F., Bhadury, P., Bhargava, R., Buelow, C., Friess, D. A., Ghosh, A., Hayes, M. A., McClure, E. C., Pearson, R. M., Turschwell, M. P., Worthington, T. A. & Connolly, R. M. (2020). Indian Sundarbans mangrove forest considered endangered under Red List of Ecosystems, but there is cause for optimism. *Biological Conservation*, 251, 108751. https://doi.org/10.1016/j.biocon.2020.108751
14. Tarazona, Y., & Miyasiro-Lopez, M. (2020). Monitoring tropical forest degradation using remote sensing. Challenges and opportunities in the Madre de Dios region, Peru. *Remote Sensing Applications: Society and Environment*, 19, 100337. https://doi.org/10.1016/j.rsase.2020.100337
15. Zimbres, B., Machado, R. B., & Peres, C. A. (2018). Anthropogenic drivers of headwater and riparian forest loss and degradation in a highly fragmented southern Amazonian landscape. *Land Use Policy*, 72, 354–363. https://doi.org/10.1016/j.landusepol.2017.12.062
16. Kanade, R., & John, R. (2018). Topographical influence on recent deforestation and degradation in the Sikkim Himalaya in India; Implications for conservation of East Himalayan broadleaf forest. *Applied Geography*, 92, 85–93. https://doi.org/10.1016/j.apgeog.2018.02.004
17. Molin, P. G., Gergel, S. E., Soares-Filho, B. S., & Ferraz, S. F. B. (2017). Spatial determinants of Atlantic Forest loss and recovery in Brazil. *Landscape Ecology*, 32, 857–870. https://doi.org/10.1007/s10980-017-0490-2

18. Shapiro, A. C., Bernhard, K. P., Zenobi, S., Müller, D., Aguilar-Amuchastegui, N., & Annunzio, R. (2021). Proximate Causes of Forest Degradation in the Democratic Republic of the Congo Vary in Space and Time. *Frontiers in Conservation Science*, 2, 690562. https://doi.org/10.3389/fcosc.2021.690562
19. Bhattarai, S., Dons, K., & Pant, B. (2020). Assessing spatial patterns of forest degradation in dry Miombo woodland in Southern Tanzania. *Cogent Environmental Science*, 6, 1801218. https://doi.org/10.1080/23311843.2020.1801218
20. Yahya, N., Bekele, T., Gardi, O., & Blaser, J. (2020). Forest cover dynamics and its drivers of the Arba Gugu forest in the Eastern highlands of Ethiopia during 1986 – 2015. *Remote Sensing Applications: Society and Environment,* 20, 100378. https://doi.org/10.1016/j.rsase.2020.100378
21. Sedano, F., Lisboa, S., Duncanson, L., Ribeiro, N., Sitoe, A., Sahajpal, R., Hurtt, G., & Tucker, C. (2020). Monitoring intra and inter annual dynamics of forest degradation from charcoal production in Southern Africa with Sentinel – 2 imagery. *International Journal of Applied Earth Observation and Geoinformation,* 92, 102184. https://doi.org/10.1016/j.jag.2020.102184
22. Shigaeva, J., & Darr, D. (2020). On the socio-economic importance of natural and planted walnut (Juglans regia L.) forests in the Silk Road countries: A systematic review. *Forest Policy and Economics*, 118, 102233. https://doi.org/10.1016/j.forpol.2020.102233
23. Viccaro, M., Cozzi, M., Fanelli, L., & Romano, S. (2019). Spatial modelling approach to evaluate the economic impacts of climate change on forests at a local scale. *Ecological Indicators,* 106, 105523. https://doi.org/10.1016/j.ecolind.2019.105523
24. Sulaiman, C., Abdul-Rahim, A. S., Mohd-Shahwahid, H. O., & Chin, L. (2017). Wood fuel consumption, institutional quality, and forest degradation in sub-Saharan Africa: Evidence from a dynamic panel framework. *Ecological Indicators*, 74, 414–419. http://dx.doi.org/10.1016/j.ecolind.2016.11.045
25. Levin, N., Ali, S., Crandall, D., & Kark, S. (2019). World Heritage in danger: Big data and remote sensing can help protect sites in conflict zones. *Global Environmental Change*, 55, 97–104. https://doi.org/10.1016/j.gloenvcha.2019.02.001
26. IUCN (International Union for Conservation of Nature), (2020). *Kilimanjaro National Park - 2020 Conservation Outlook Assessment.* https://worldheritageoutlook.iucn.org/explore-sites/wdpaid/17761
27. USGS (United States Geological Survey) (2021). *USGS Science for a changing world.* https://glovis.usgs.gov/app
28. Weather & Climate. *Climate in Mount Kilimanjaro: monthly precipitation* (2022). https://weather-and-climate.com/average-monthly-Rainfall-Temperature Sunshine, Mount+Kilimanjaro-tz,Tanzania
29. Morin, N., Masse, A., Sannier, C., Siklar, M., Kiesslich, N., Sayadyan, H., Faucqueur, L., & Seewald, M. (2021). Development and Application of Earth Observation Based Machine Learning Methods for Characterizing Forest and Land Cover Change in Dilijan National Park of Armenia between 1991 and 2019. *Remote Sensing,* 13, 2942. https://doi.org/10.3390/rs13152942
30. Valožić, L., & Cvitanović, M. (2011). Mapping the Forest Change: Using Landsat Imagery in Forest Transition Analysis within the Medvednica Protected Area. *Hrvatski Geografski Glasnik,* 73, 245–255. https://doi.org/10.21861/hgg.2011.73.01.16
31. Shaharum, N. S. N., Shafria, H. Z. M., Gambo, J., & Abidin, F. A. Z. (2018). Mapping of Krau Wildlife Reserve (KWR) protected area using Landsat 8 and supervised classification algorithms. *Remote Sensing Applications: Society and Environment,* 10, 24–35. https://doi.org/10.1016/j.rsase.2018.01.002
32. KINAPA (Kilimanjaro National Park). (2017). *KINAPA tourism facilities*. ArcGIS online inbuilt.
33. Jarvis, A., Reuter, H. I., Nelson, A. & Guevara, E. (2008). *SRTM Tile Grabber*. https://dwtkns.com/srtm/
34. Vijayalakshmi, S., Kumar, M., & Arun, M. (2021). A study of various classification techniques used for very high-resolution remote sensing [VHRRS] images. Materials Today: *Proceedings*, 37, 2947–2951. https://doi.org/10.1016/j.matpr.2020.08.703
35. Campbell, J. B., & Wynne, R. H. (Eds.) (2011). *Introduction to Remote Sensing*. New York: The Guilford Press.
36. Lu, D., Weng, Q., Moran, E., Li, G., & Hetrick, S. (2011). Remote Sensing Image Classification. In: Q. Weng, (Ed.), *Advances in Environmental Remote Sensing: Sensors, Algorithms, and Applications* (219–240). Boca Raton: Tailor & Francis Group.
37. Tso, B., & Mather, P. M. (2009). *Classification methods for remotely sensed data*. Boca Raton: CRC Press.
38. Enoguanbhor, E. C. (2021). *Urban land dynamics in the Abuja city-region, Nigeria: integrating GIS, remotely sensed, and survey-based data to support land use planning*. PhD Thesis, Berlin: Humboldt-Universität zu Berlin. https://doi.org/10.18452/23620

39. Enoguanbhor, E. C., Gollnow, F., Walker, B. B., Nielsen, J. O., & Lakes, T. (2022). Simulating Urban Land Expansion in the Context of Land Use Planning in the Abuja City-Region, Nigeria. *GeoJournal*. 87, 1479–1497. https://doi.org/10.1007/s10708-020-10317-x
40. Enoguanbhor, E. C., Gollnow, F., Nielsen, J. O., Lakes, T., & Walker, B. B. (2019). Land Cover Change in the Abuja City-Region, Nigeria: Integrating GIS and Remotely Sensed Data to Support Land Use Planning. *Sustainability*, *11*(5), 1313. https://doi.org/10.3390/su11051313
41. Jiang, L., Liu, Y., Wu, S., & Yang, C. (2021). Analyzing ecological environment change and associated driving factors in China based on NDVI time series data. *Ecological Indicators*, 129, 107933. https://doi.org/10.1016/j.ecolind.2021.107933
42. Kwan, C., Gribben, D., Ayhan, B., Li, J., Bernabe, S., & Plaza, A. (2020). An Accurate Vegetation and Non-Vegetation Differentiation Approach Based on Land Cover Classification. *Remote Sensing, 12*(23), 3880. MDPI AG. https://doi.org/10.3390/rs12233880
43. Ezaidi, F., Aydda, A., Kabbachi, B., Althuwaynee, O. F., Ezaidi, A., Haddou, M. A., Idoumskine, I., Thorpe, J., Park, H-J., & Kim, S-W. (2022). Multi-temporal Landsat-derived NDVI for vegetation cover degradation for the period 1984-2018 in part of the Arganeraie Biosphere Reserve (Morocco). *Remote Sensing Applications: Society and Environment,* 27, 100800. https://doi.org/10.1016/j.rsase.2022.100800
44. Olofsson, P., Foody, G. M., Herold, M., Stehman, S. V., Woodcock, C. E., & Wulder, M. A. (2014). Good practices for estimating area and assessing accuracy of land change. *Remote Sensing of Environment*, 148, 42–57. https://doi.org/10.1016/j.rse.2014.02.015
45. Enoguanbhor, E. C., Gollnow, F., Walker, B. B., Nielsen, J. O., & Lakes, T. (2021). Key Challenges for Land Use Planning and its Environmental Assessments in the Abuja City-Region, Nigeria. *Land*, *10*(5), 443. https://doi.org/10.3390/land10050443
46. Fotang, C., Bröring, U., Roos, C., Enoguanbhor, E. C., Dutton, P., Tédonzong, L. R. D., Willie, J., Yuh, Y. G., & Birkhofer, K. (2021). Environmental and anthropogenic effects on the nesting patterns of Nigeria–Cameroon chimpanzees in North-West Cameroon. *American Journal of Primatology, 83,* e23312. http://doi.org/10.1002/ajp.23312
47. Visser, S., & Jones III, J. P. (2010). Descriptive Statistics. In B. Gomez, J. P. Jones III (Eds.) *Research Methods in Geography: A Critical Introduction* (279–296). West Sussex: Blackwell Publishing Lt.
48. Htun, N. Z., Mizoue, N., & Yoshida, S. (2013). Changes in Determinants of Deforestation and Forest Degradation in Popa Mountain Park, Central Myanmar. *Environmental Management,* 51, 423–434. https://doi.org/10.1007/s00267-012-9968-5
49. Freitas, S. R., Hawbaker, T. J., & Metzger, J. P. (2010). Effects of roads, topography, and land use on forest cover dynamics in the Brazilian Atlantic Forest. *Forest Ecology and Management*, 259, 410–417. http://dx.doi.org/10.1016/j.foreco.2009.10.036
50. Pongpattananurak, N. (2018). Impacts from tourism development and agriculture on forest degradation in Thap Lan National Park and adjacent areas. *Agriculture and Natural Resources,* 52, 290–297. https://doi.org/10.1016/j.anres.2018.09.013
51. Adeyemi, A. A., & Owolabi, F. M. (2021). Land-use/Land-cover Changes and Deforestation in Effan Forest Reserve, Kwara State, Nigeria. *Preprints*, 2021080356. https://doi.org/10.20944/preprints202108.0356.v1
52. Zeb, A. (2019). Spatial and temporal trends of forest cover as a response to policy interventions in the district Chitral, Pakistan. *Applied Geography*, 102, 39–46. https://doi.org/10.1016/j.apgeog.2018.12.002
53. Ullah, S. M. A., Tani, M., Tsuchiya, J., Rahman, M. A., & Moriyama, M. (2022). Impact of protected areas and co-management on forest cover: A case study from Teknaf Wildlife Sanctuary, Bangladesh. *Land Use Policy*, 113, 105932. https://doi.org/10.1016/j.landusepol.2021.105932
54. Liu, J., Wang, J., Wang, S., Wang, J., & Deng, G. (2018). Analysis and simulation of the spatiotemporal evolution pattern of tourism lands at the Natural World Heritage Site Jiuzhaigou, China. *Habitat International,* 79, 74–88. https://doi.org/10.1016/j.habitatint.2018.07.005
55. Riva, M. J., Daliakopoulos, I. N., Eckert, S., Hodel, E., & Liniger, H. (2017). Assessment of land degradation in Mediterranean forests and grazing lands using a landscape unit approach and the normalized difference vegetation index. *Applied Geography,* 86, 8–21. http://dx.doi.org/10.1016/j.apgeog.2017.06.017
56. Minja, G. (2014). Vulnerability of Tourism in Kilimanjaro National Park and the livelihoods of adjacent communities to the impacts of climate change and variability. *European Scientific Journal,* 1010, 1857–7881. https://eujournal.org/index.php/esj/article/view/4428

57. Li, J., Bai, Y., & Alatalo, J. M. (2020). Impacts of rural tourism-driven land use change on ecosystems services provision in Erhai Lake Basin, China. *Ecosystem Services,* 42, 101081. https://doi.org/10.1016/j.ecoser.2020.101081
58. Delgado-Aguilar, M. J., Hinojosa, L., & Schmitt, C. B. (2019). Combining remote sensing techniques and participatory mapping to understand the relations between forest degradation and ecosystem services in a tropical rainforest. *Applied Geography,* 104, 65–74. https://doi.org/10.1016/j.apgeog.2019.02.003
59. Brandt, J. S., Radeloff, V., Allendorf, T., Butsic, V., & Roopsind, A. (2019). Effects of ecotourism on forest loss in the Himalayan biodiversity hotspot based on counterfactual analyses. *Conservation Biology*, 33, 1318–1328. https://doi.org/10.1111/cobi.13341
60. Larsen, F., Hopcraft, J. G. C., Hanley, N., Hongoa, J. R, Hynes, S., Loibooki, M., Mafuru, G., Needham, K., Shirima, F., & Morrison, T. A. (2020). Wildebeest migration drives tourism demand in the Serengeti. *Biological Conservation*, 248, 108688. https://doi.org/10.1016/j.biocon.2020.108688
61. Sullivan, M. K., Biessiemou, P. A. M., Niangadouma, R., Abernethy, K., Queenborough, S. A., & Comita, L. (2022). A decade of diversity and forest structure: Post-logging patterns across life stages in an Afrotropical forest. *Forest Ecology and Management*, 513, 120169. https://doi.org/10.1016/j.foreco.2022.120169

Central European Journal of Geography and Sustainable Development
ISSN 2668-4322, ISSN-L 2668-4322

2022, Volume 4, Issue 2, Pages: 24-49
https://doi.org/10.47246/CEJGSD.2022.4.2.2

Assessment of the impact of the Dniester Hydropower Complex on hydrological state of the Dniester River

Ana Jeleapov *,

Institute of Ecology and Geography, Chisinau, 1 Academiei Street, MD-2028, Republic of Moldova;
anajeleapov@gmail.com

Received: 15 May 2022; Revised: 17 October 2022; Accepted: 21 October 2022; Published online: 27 October 2022

Abstract: Operation of the Dniester Hydropower Complex (DHC), build on the middle course of the Dniester River in the middle of the '80s of the last century and extended during last decades, on one hand, produces low-cost energy and contributes to local and regional economical development, but on the other hand, leads to modification of river flow and ecosystems in the downstream, creating a series of dilemmas that are difficult to manage and solve by bazinal countries, Ukraine and the Republic of Moldova. This research aims to assess the changes in flow, phases of the hydrological regime, water temperature and sediments' regime due to the DHC operation. Main utilized approach was comparative analysis of hydrological time series recorded at the stations situated upstream and downstream of the DHC, for two representative time periods: before and after construction of this hydropower complex. As a result, it was estimated that the mean annual flow downstream the DHC decreased by 9.2%. Seasonal flow changed mainly by significant decrease in February-April (February - 18%, March - 40%, April - 27%), and increase in the autumn months, by 10-14%. Minimum flows upstream of the DHC, increased by 52%, and downstream have doubled, reaching 107 m^3/s (compared to 51 m^3/s, before the DHC construction). Maximum annual flow, in the upstream part, in the second period, has slightly increased, while towards the downstream part, there is a reduction of this parameter by about 30%. One of the direct impacts of the DHC operation is hydropeaking effect. Intraday level amplitude downstream of the DHC amounts to 52 cm and the length of the sector that is influenced by this effect is over 100 km. Also, a long river sector is subject to water thermal modifications: when upstream the average annual water temperature has risen by 0.8°C, in the downstream it has diminished by 0.44°C. On a monthly scale, there is a decrease in the water temperature in the spring-summer period, and an increase in the autumn-winter period downstream of the DHC. Sediment transport process was also altered significantly. Due to the DHC operation, suspended sediments decreased by 92-98% downstream of it. The significant decrease in sediment volumes is specific to all months of the year. The reduction of sediment transport has increased the transparency of water, which, as a result, influences the development of the aquatic ecosystems.

Key words: Dniester Hydropower Complex, the Dniester River, flow regime, hydrological alteration, reservoirs

Citation: Jeleapov, A. (2022). Assessment of the impact of the Dniester Hydropower Complex on hydrological state of the Dniester River. *Central European Journal of Geography and Sustainable Development*, *4*(2), 24–49. https://doi.org/10.47246/CEJGSD.2022.4.2.2

1. INTRODUCTION

The power of rivers is used by humans for different needs for centuries. However, its intensive utilization began only 140 years ago by development of hydropower plants (HPP). From the'80s of the 19th century when the first HPPs were built, till now thousands of these structures were constructed and supply with energy millions of people and industries. Nowadays, worldwide there are over 65 ths. of large

* Corresponding author: anajeleapov@gmail.com; Tel.: +373-68-473-729

HPPs with installed capacity of 1,330 GW, and continues to grow with 1-1.5%/year [1]. Large development of HPPs is specific for East Asia and Pacific Region, Europe, South and Central Asia, etc. Main countries by hydropower production are China, Brazil, Canada, the United States, and Russia [1]. Rapid increase of HPPs construction was caused by certain advantages related to hydropower. Relative low-cost of HPPs and renewable and free source for energy – river flow – remains to be main reasons of continuing raise of hydropower use. Also, reservoirs formed as a result of the dams' construction across the rivers have a positive influence on the local or regional economic development, being a valuable source of water for irrigation, industry, recreation, fishery. So far, hydropower is a leading renewable source of energy, with a share of 58% (over 4,300 TWh) from total electricity generated by renewable sources in 2020 (7500 TWh) [2], and the increasing trend in hydropower production show global interest in further development of this sector.

However, as a consequence of a high increase of HPPs construction on rivers, the problem of their impact on river flow and downstream ecosystems has raised. In this context, large number of studies was developed in order to evaluate the HPPs effects [3-20]. Thus, a comprehensive study performed by a group of authors in 2015 [4] shows that, on a global basis, 48% of river volume is moderately to severely impacted by either flow regulation or river fragmentation, or both. Assuming completion of all dams planned and under construction, this number would nearly double to 93%, largely due to major dam construction in the Amazon Basin [4]. As a result of flow regulation and river fragmentation due to dam construction, many other consequences appeared. The most important of them are the following: loss of connectivity between the upstream and downstream parts of the river which stops the migration of fish and other aquatic organisms; reduction the sediments that, on the one hand, accumulate in the reservoir and lead to its siltation during the time, and, on the other hand, cause a more transparent water downstream of the dams, leading to abundant growth of aquatic plants and water quality secondary alteration; changes of surface and ground water connectivity; alteration of the river thermal regime, usually due to flow evacuation from lower water layers of the reservoirs with constant water temperature; appearance of hydropeaking effect downstream of dams due to turbine operation - effects that determine reduction of biodiversity and invasion of new species for which new hydrological conditions are favorable [19,20]. Also, due do alteration of natural resources (water and food from rivers), the quality of life of population situated downstream of dams decreases. The decline of fish number and species denote less food resources for people. Colder water discharged from HPPs leads to changes in agriculture practice, especially reduction of irrigation surfaces, as well as worsening of tourism sector. Hydropeaking and secondary water alteration cause difficulties in water abstraction for humans' supply.

Actual legislation in the field of water resources and protection, namely the EU Water Framework Directive (Directive 2000/60/EC) [21] and its implementation guidelines, stipulates that hydromorphological alteration, especially expressed by river lateral and longitudinal connectivity loses, cause substantial impacts on river flow and its biodiversity, thus, activities to decrease human impact must be applied in order to improve water bodies status/potential. Water managers have a challengeable responsibility, on the one hand, to find and implement the best practices in order to protect rivers with their ecosystems and, on the other hand, to provide the necessary water to supply the socio-economic needs. However, it should be clear that increasing global population, need in water and non-fuel energy resources, and different global and regional crises must not cause a greater impact on waters.

Operation of the Dniester Hydropower Complex (DHC), build on the middle course of the Dniester River in the middle of '80 of the last century and extended during last decades, also rises the controversy between various experts and even states (e.g., Ukraine and the Republic of Moldova), creating a series of dilemmas that are difficult to manage and solve. Several studies were performed so far in order to evaluate the effects of the DHC on downstream status of the river, most of which are mainly oriented to estimation of water quality and biodiversity state [22-26] and only a few researches were developed to demonstrate the changes of water flow characteristics [27,28,29]. In this context, the present study focuses only on the evaluation of hydrological alterations of the Dniester River, that, as a consequence, cause ecosystems and economic losses in its downstream part. Main objectives are: i) identification of changes in flow parameters: mean annual, seasonal and monthly flow, minimum and maximal flows; ii) estimation of hydrological regime phases modifications: spring and summer floods, low flow; iii) analysis of hydropeaking effect; iv) assessment of water temperature regime and v) evaluation of sediment

transport processes alteration. All parameters were evaluated comparatively for two representative time periods: before (pre-) and after (post-) the DHC construction.

2. STUDY AREA

The Dniester River is located in the Eastern part of Europe and flows through Ukraine and the Republic of Moldova (Figure 1). The river length is 1362 km and the basin area is 72,100 km2. Over 70% of the basin is situated in Ukraine, 27% belong to Republic of Moldova, and 0.34% - to Poland. The basin is conventionally divided in three parts: the Upper Part represents the region from Dniester spring to confluence with Zolota Lypa River (nearby Zalischyky Village), the Middle Part is assigned to the region from Zolota Lypa River to Dubasari Town (in general situated in Podolia Plateau), and the Lower Part is characterized by plain relief. The Upper part lays in Carpathians and represents only 30% of the basin area, but due to the high amounts of precipitations, 70% of Dniester runoff is generated in this area. Precipitations over basin area decrease constantly from 1300-1000 mm in the Upper part to 450-500 in the Lower Part [30,31].

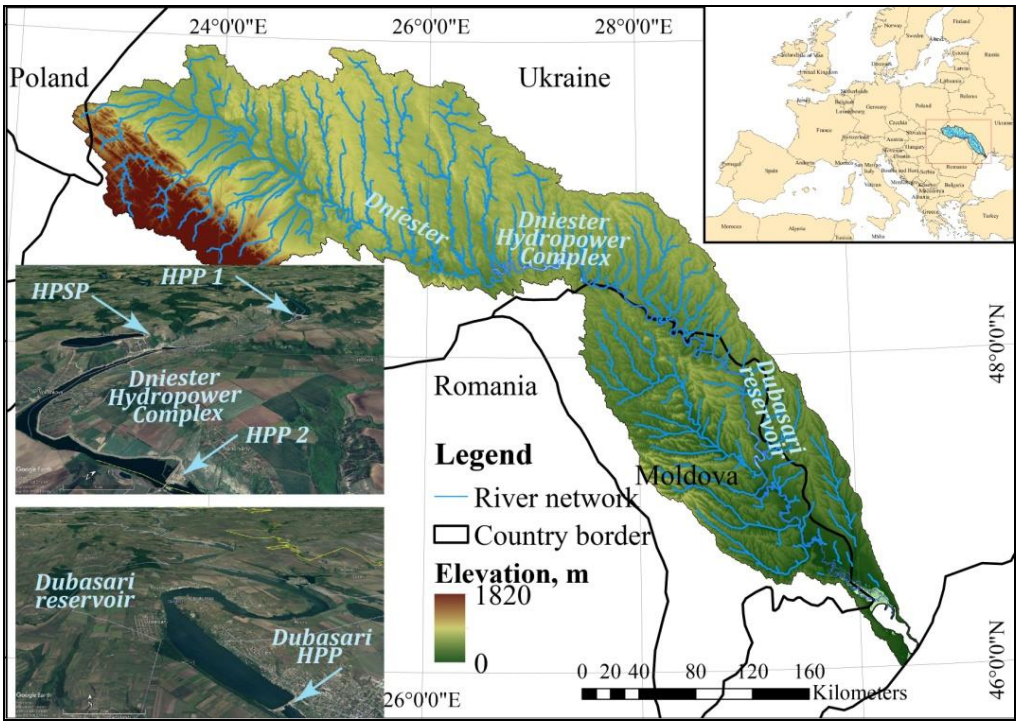

Figure 1. The Dniester River Basin.
Source: elevation extracted from [32], images extracted from [33].

The flow of the Dniester River is regulated by 3 reservoirs situated on the stream and one positioned lateral to the river. Three of these reservoirs form the Dniester Hydroelectric Complex: the Dnestrovsk reservoir with HPP-1, the buffer reservoir with HPP-2, the artificial reservoir with pumped storage hydroelectric power plant (HPSP). First reservoirs from this complex (the Dnestrovsk reservoir with HPP-1 and the buffer reservoir), were built during the years 1981-1983. The main functions of the Dnestrovsk reservoir are flood reduction, water supply, electricity production. Its length is 194 km, water volume at normal retention level (NNR) - 2.6 km^3, HPP-1 has a height of 54 m, and is equipped with 6 turbines, with capacity of 702 MW. Buffer reservoir was built to reduce hydropeaking effect caused due to operation of HPP-1 turbines. However, during the years 1999-2002, the dam was equipped with 3 turbines, with capacity of 40.8 MW, thus at present HPP-2 is also a producer of flow pulsation effect. After turbines installation and HPSP construction, the function of the buffer reservoir has been changed, currently it is used for electricity generation, water supply and attenuation hydropeaking effect from upper reservoirs. Its volume at NNR is 37 mil. m^3, with intentions from Ukrainian part to increase its value to 58 mil. m^3. Its length is 19.8 km, the average depth is 6 m. 9 km downstream of HPP-1, another reservoir with HPSP was built by damming. It is located on the upper right side of the river at approx. 150 m above the Dniester water level. The volume of water at NNR is 41.4 mil. m^3 [34,35,36]. HPSP is equipped with 3 turbines that were installed during the years 2013-2016, the capacity is of 972 MW in turbine mode and 1263 MW in pumping mode. Recently, the fourth turbine was installed (324 MW in turbine

mode and 421 MW in pumping mode), and the construction of other 3 turbines (with a capacity of 972 MW in turbine mode and 1263 MW in pumping mode) is planned by Ukraine for next decade. As a result of the operation of all 7 turbines, the total capacity will be 2268 MW in turbine mode and 2947 MW in pumping mode [37]. At the end of the HPSP construction, it will be ranked 4th in the world [38]. The reservoirs' location and the original form of the Dniester River bed can be seen in Figure 2.

It should be noted that there is one more reservoir with dam with HPP constructed on the Dniester River, called Dubasari. It is situated in the Republic of Moldova. In comparison with DHC, it has a low impact on river regulation due to relatively small water volume, and high reservoir siltation. HPP was built in 1954, and is equipped with 4 turbines with a capacity of 48 MW [39].

3. METHODS

The main group of methods for assessment of changes in river hydrological regime due to HPP operation includes the direct ones that are based on the analysis of measurement data from the hydrologic monitoring network. Main designs that are usually applied are: (1) Paired-Before–After Control–Impact (BACIP), (2) Before–After (BA), (3) Control–Impact (CI), (4) Hydrological Classification (HC) and (5) Predicted Hydrological indices (HP) [7]. Also, one of modern approaches is determination of main Hydrological Alteration Indicators and Environment Flow Components [8-9], which is applied, in most of the cases, for estimation of impact of reservoirs operation on river flow [11,12,29 etc.]. This approached is performed using the special software IHA [40], where 33 IHA characteristics (monthly mean values, annual minima and maxima of 1, 3, 7, 30, 90 days and their date of occurrence, etc.), are calculated, as well as Environmental Flow Components (minimum monthly flow, extreme low flow, flow pulses, small and large floods) for pre- and post-impact periods. From all existing approaches, the best way to assess the anthropogenic impacts on river flow is the analysis of hydrological information for pre- and post-impact, pre/post-control periods. Thus, the comparative analysis of the hydrological data collected in natural conditions of the Dniester River flow generation, as well as during the impact of the DHC operation reflects the tendency of flow change determined by the human factor.

The hydrological regime of the Dniester River consists of flow characteristic phases: spring floods, pluvial floods, summer - autumn and winter low flows. Thus, these characteristic phases, as well as hydrologic indicators (e.g. multiannual flow, seasonal and average monthly flow, multiannual and monthly suspended sediments and water temperature) were assessed, time series being differentiated over 2 time periods, pre-DHC (before the DHC operation) and post-DHC (after the DHC operation). The focus of the study was also on evaluation of hydropeaking effect, which was performed using water level data from immediate proximity up to 140 km downstream of HPPs in order to understand the extension of this phenomenon.

3.2. Data

The basic approach of the study was to analyze and establish the hydrological characteristics at the Zalischyky station, situated upstream of the DHC, as well as those at the stations located downstream of the DHC: Mogilev-Podolsky, Naslavcea, Unguri, Soroca, Grushka, Sanatauca, Camenca, Dubasari, Bender. The time series was considered mainly from 1950 till 2020. In order to assess the impact of DHC on hydrological regime, from the whole time series, homogeneous data series were used for two times periods: the first one – the period of natural flow for the years 1950-1980 (before the DHC or pre DHC), and the second period – the regulated flow from the 1987 till 2020 (after the DHC construction or post DHC). The analysis was performed both in time profile, highlighting the trends of change over time, as well as in space profile, the focus being on the changes of characteristics from upstream to downstream of DHC.

The hydrological information used in the study was provided by the responsible data organizations in Moldova and Ukraine: the Hydrometeorological Service (SHS) [41,42] and State Water Agency, data were collected through UNDP in Moldova, Ministry of Environment of the Republic of Moldova, the Commission on Sustainable Use and Protection of the Dniester River Basin (the Dniester Commission). The table below summarizes the hydrological information used to assess the hydrological status of the Dniester River as a result of the impact of DHC.

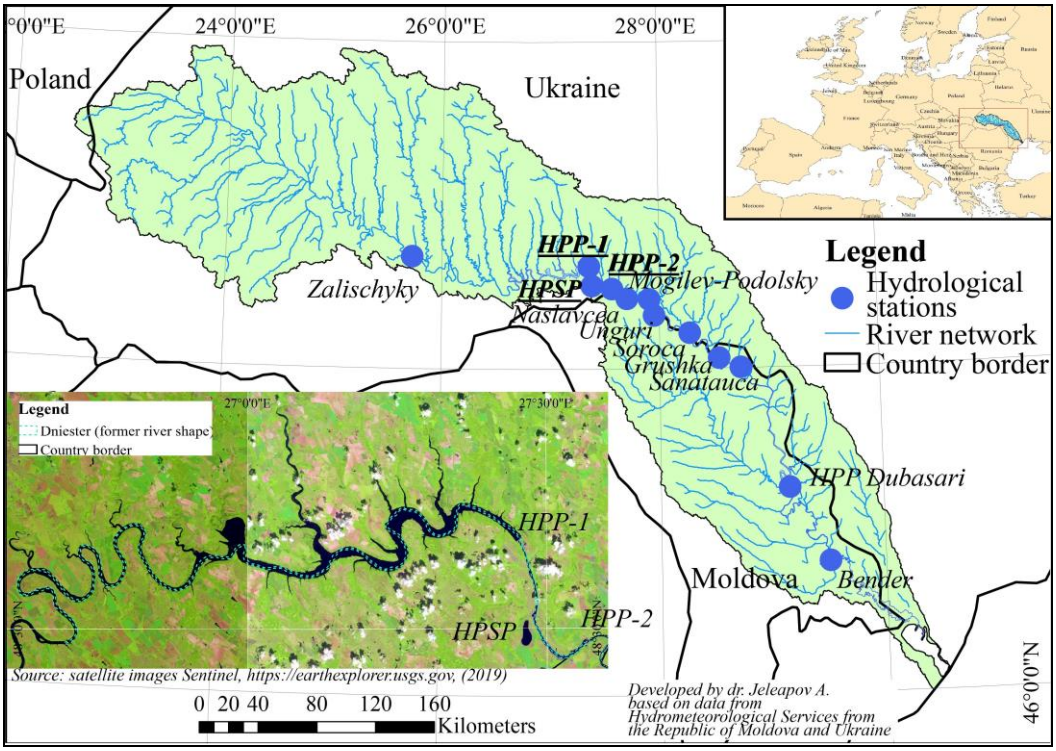

Figure 2. Location of the hydrologic stations on the Dniester River considered in the study.

Table 1. List of hydrological stations and data used for the study [based on 41,42].

Hydrologic station	Basin surface till station (km²)	Distance till river mouth (km)	Data used for the study	Time period
Data from SHS Ukraine				
Zalischyky	24,600	936	Daily/monthly flow (discharges), monthly water temperature, monthly suspended sediments	1950-2016
Reservoir with HPP-1	40,500	677.7	Daily/monthly flow (discharges), levels	1982-2020
Mogilev - Podolsky	43,000	630	Daily/monthly flow (discharges), monthly water temperature, monthly suspended sediments	1950-2016
Data from SHS Moldova				
Naslavcea	-	653	Water levels (from 15 to 15 minutes)	2013-2020 (some missing data)
Unguri	-	627.4	Water levels (from 15 to 15 minutes)	2013-2020 (some missing data)
Soroca	47,000	550	Water levels (from 60 to 60 minutes)	2017-2020 (some missing data)
Grushka	48,700	509	Daily/monthly flow (discharges), monthly water temperature, monthly suspended sediments	1968-2020
Sanatauca	49,000	473	Water levels (from 60 to 60 minutes)	2017-2020 (some missing data)
Camenca	49,000	473	Daily/monthly flow Water temperature	1952-1966 1951-1977, 1993-2015
HPP Dubasari	53,600	351	Daily/monthly flow (discharges), monthly water temperature, monthly suspended sediments	1956-2020
Bender	66,100	214	Daily/monthly flow (discharges), monthly water temperature, monthly suspended sediments	1950-2020

4. RESULTS AND DISCUSSIONS

4.1. Hydrological regime

4.1.1. The dynamic of multiannual flow and volume

First hydrological indicators that were evaluated and compared are average flow and volume. Thus, for two considered time periods, upstream of the DHC, at Zalischyky, approximately equal values are observed: 7022 mil.m^3 and 6964 mil.m^3. Downstream of the DHC at Mogilev-Podolsky, both river flows and volumes decrease: the volumes have decreased from 8753 mil. m^3 to 7952 mil. m^3 or by 800 mil. m^3 which is 9.2%. The decrease of water resources continues towards the river mouth: at Bender the average flows before the DHC construction were 320 m^3/s and after its construction the value decreases to 272 m^3/s, and volumes diminished from 10089 to 8579 mil. m^3 or with 1.5 km^3 of water, i.e. 15% (Figures 3 and 4).

As usual, the volumes of water in the basin increase with its area. Thus, in natural regime, the increase in volumes from Zalischyky was by 25% to Mogilev-Podolsky, by 34% to Grushka and by 44% to Bender. During the second period, the flow increase changed, being only by 14% to Mogilev-Podolsky (10% less than in the previous period), and only by 23% to Bender which is by 2 times lower than in the period pre DHC (Figure 5). Thus, if, in the previous period at Zalischyky about 70% of water resources were formed and towards Mogilev-Podolsk the value increased to 87%, at present, in the upper part of the basin towards Zalischyky, 81% of water flow is already formed and towards Mogilev-Podolsky, it increases to about 90%. This means that in the limits of the Republic of Moldova only about 10% of the water resources of the Dniester River are generated.

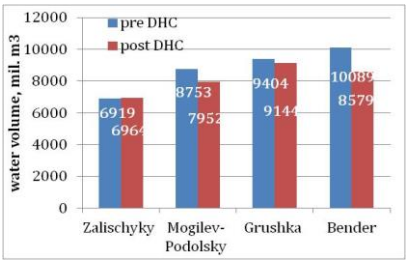

Figure 3. Average annual flow.

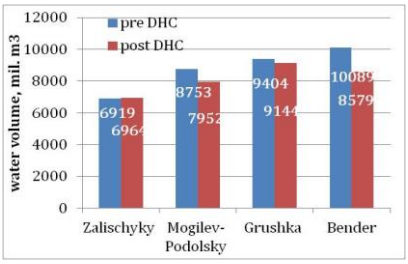

Figure 4. Average annual volume.

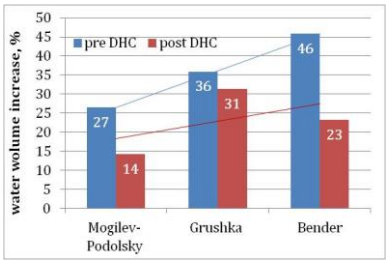

Figure 5. Share of volume increase with basin area in comparison with Zalischyky.

The increase of water losses for the sector from DHC to the river mouth can be explained by several factors, including water use for various economic needs, decrease in water resources brought by tributaries and slope runoff, declining ground water supply, the increase of evaporation rate caused by rising temperatures in recent decades due to climate change, etc. Future climate change scenarios show that for the upper part of the Dniester River basin, on the territory of Ukraine, where the main water volumes are formed, due to climate change the water resources would decreases by 5-10%, while in the downstream part, in the Republic of Moldova, the decrease would be more substantial, of about 20-25% [43]. This fact makes middle and lower part of the river more vulnerable to assurance with water resources, and more dependent to releases from DHC.

4.1.2. The dynamic of seasonal and monthly flow and volume

An important analyzed indicator is the seasonal flow. In natural regime, the seasonal flow is distributed as follows: 34% (17% each season) is generated in the autumn and winter. The most important resources are formed in the spring - 37% and in the summer - 30%, namely: at Zalischyky, 325 m^3/s (2573 mil. m^3) and 261m^3/s (2074 mil. m^3), and at Mogilev-Podolsky, 413 m^3/s (3274 mil. m^3) and 312 m^3/s (2474 mil. m^3) respectively. During the DHC operation, a redistribution of the share of water volumes is observed. Upstream, the volumes decreased by 3% in summer and increased by 2% in autumn and winter. Downstream of the DHC, the flow decreased during the spring period by 6%, while it increased in the summer by 2% and in autumn by 4%.

In temporal and spatial profile, after the DHC construction, the hydrological characteristics have slightly increased during the cold period of the year. The flows at Zalischyky and Mogilev-Podolsky stations are 167 m^3/s (1311 mil. m^3) and 211 m^3/s (1657 mil. m^3) for the autumn period, and 161 m^3/s (1248 mil. m^3) and 181 m^3/s (1406 mil. m^3) for the winter period. After commissioning the DHC, low decreases in flow and volume were noticed at both hydrological stations in summer. For the spring period, upstream of the DHC, flows and volumes have been reduced insignificantly from 325 m^3/s to 316 m^3/s. However, downstream, decreases of streamflow by about 100 m^3/s (from 413 m^3/s to 312 m^3/s), and of

the volume by about 0.8 km³ of water, compared to the values recorded before the DHC construction were found (the decreases being equal to 24%). For the spring season, at Zalischyky, the flow is 316 m³/s (2507 mil. m³), and for Mogilev-Podolsky is 312 m³/s (2474 mil. m³). Thus, on one hand, it can be assumed that the water resources from tributaries flowing into the DHC in the Zalischyky - Mogilev-Podolsky sector, for this season are accumulated in the DHC and do not participate in the increase of water volume of the Dniester River. On the other hand, it can be supposed that there is a change in the spring phenomena under the DHC impact, which leads to a reduction in water resources during this period (Figures 6, 7 and 8).

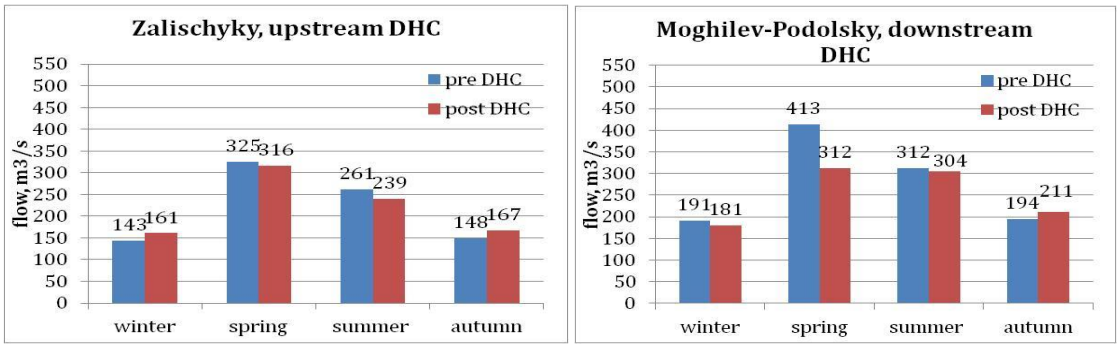

Figure 6. Seasonal water flow.

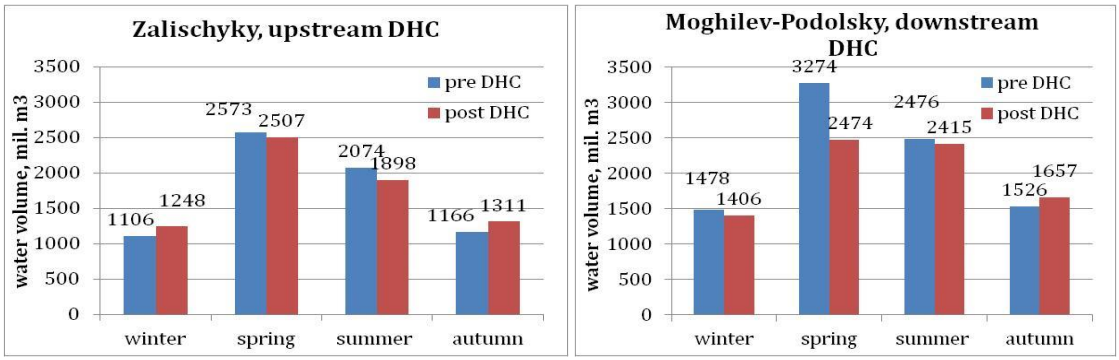

Figure 7. Seasonal water volumes.

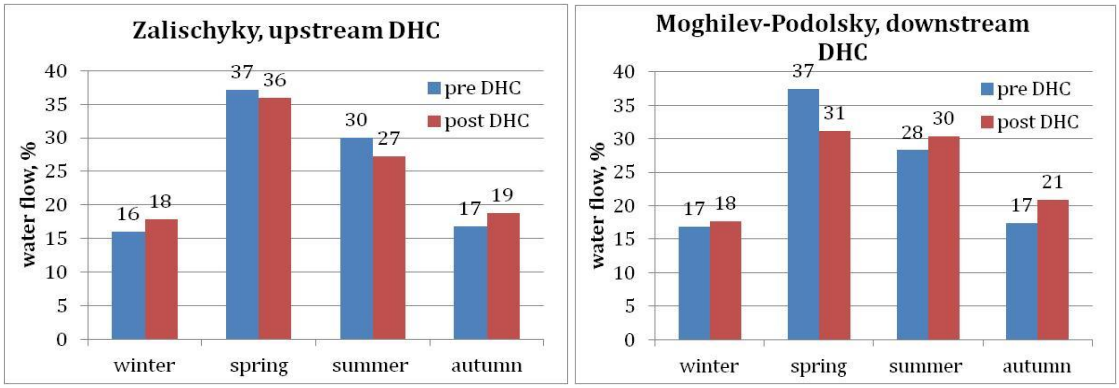

Figure 8. Seasonal distribution of the water flow.

4.1.3. The dynamic of monthly flow and volume

For a more detailed assessment of the DHC impact on the hydrological regime, the monthly flows were also analyzed using the same principle presented above. In natural flow regime, monthly flows hydrograph at Zalischyky station shows that the highest flows are in April (428 m³/s), followed by the other two spring months (approx. 280 m³/s), June (315 m³/s) and July (272 m³/s). In autumn and winter months the flow varies between 110 and 170 m³/s. After the DHC construction, upstream of the DHC, the flows increased by approx. 40% in January, 13-14% in October, November, and decreased by 11-15% in April, July, August.

At the Mogilev - Podolsky station, in natural regime, the highest flows are also observed in the spring and summer months, but the values are higher than those from Zalischyky: 523 m³/sin April, 387 m³/s in March, and 320-350 m³/s in May-July. In autumn and winter months the flows are close to 200 m³/s. In flow regulated regime, downstream the DHC, in autumn months the situation is similar with the upstream

station, in the summer months the changes are minor, but in February-April significant decreases in flows were noticed: 40% in March, 27% in April, and 18% in February. The same tendencies were observed at the stations located towards the mouth (Figures 9 and 10). Thus, a general decreasing trend of average monthly flow of the Dniester River for spring (significant) and summer is attested, on the whole sector downstream of the DHC. The slight flow increase is generally observed for the seasons characterized by lower flow (autumn and winter).

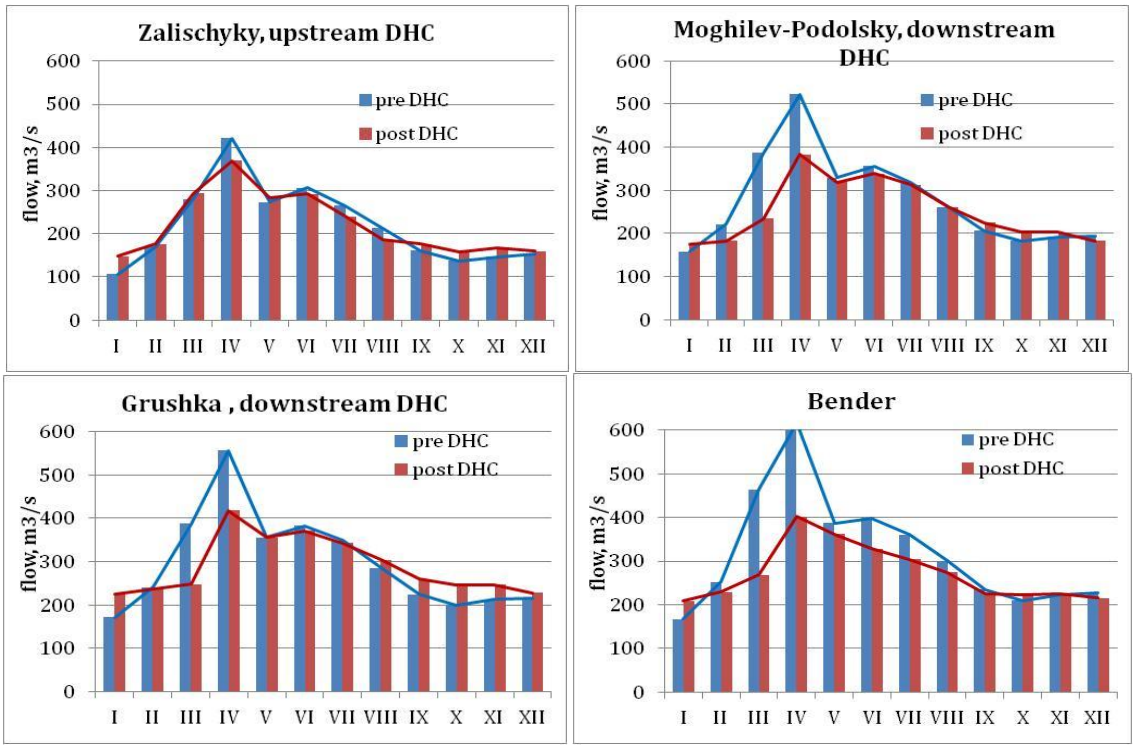

Figure 9. Distribution of monthly flow.

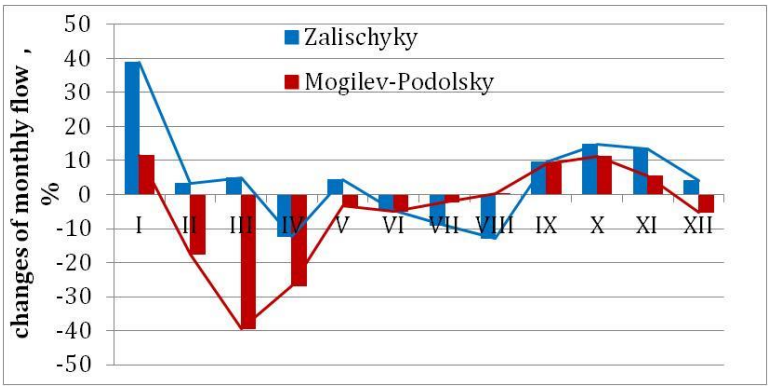

Figure 10. Changes of monthly flow between two time periods.

4.1.4. Low water season and low flow

The hydrological regime of the rivers situated in temperate zone, including those from Ukraine and Moldova, is characterized by several phases: spring floods - caused by melting snow (sometimes rain and melting snow), pluvial floods - formed as a result of summer heavy rains, low water season - caused by precipitation reduction, especially in summer–autumn as well as in winter time.

Low water is a component part of the hydrological regime of the rivers. It is a seasonal phenomenon. Main factors influencing the formation of minimal flow are the climatic and hydrogeological ones. On one hand, precipitation absence causes reduction of rivers rainwater supply, on the other hand, the groundwater supply is the main water source for rivers during this season. Within the Dniester River basin, the low water is manifested in the summer - autumn and winter periods. During the warm season, the minimum flows are lower compared to those in the cold season, due to high evaporation processes. The winter low water coincides with the winter phenomena. The periods with minimum flows are observed annually and, in some years, they can be extended even for 4-5 months (Figure 11).

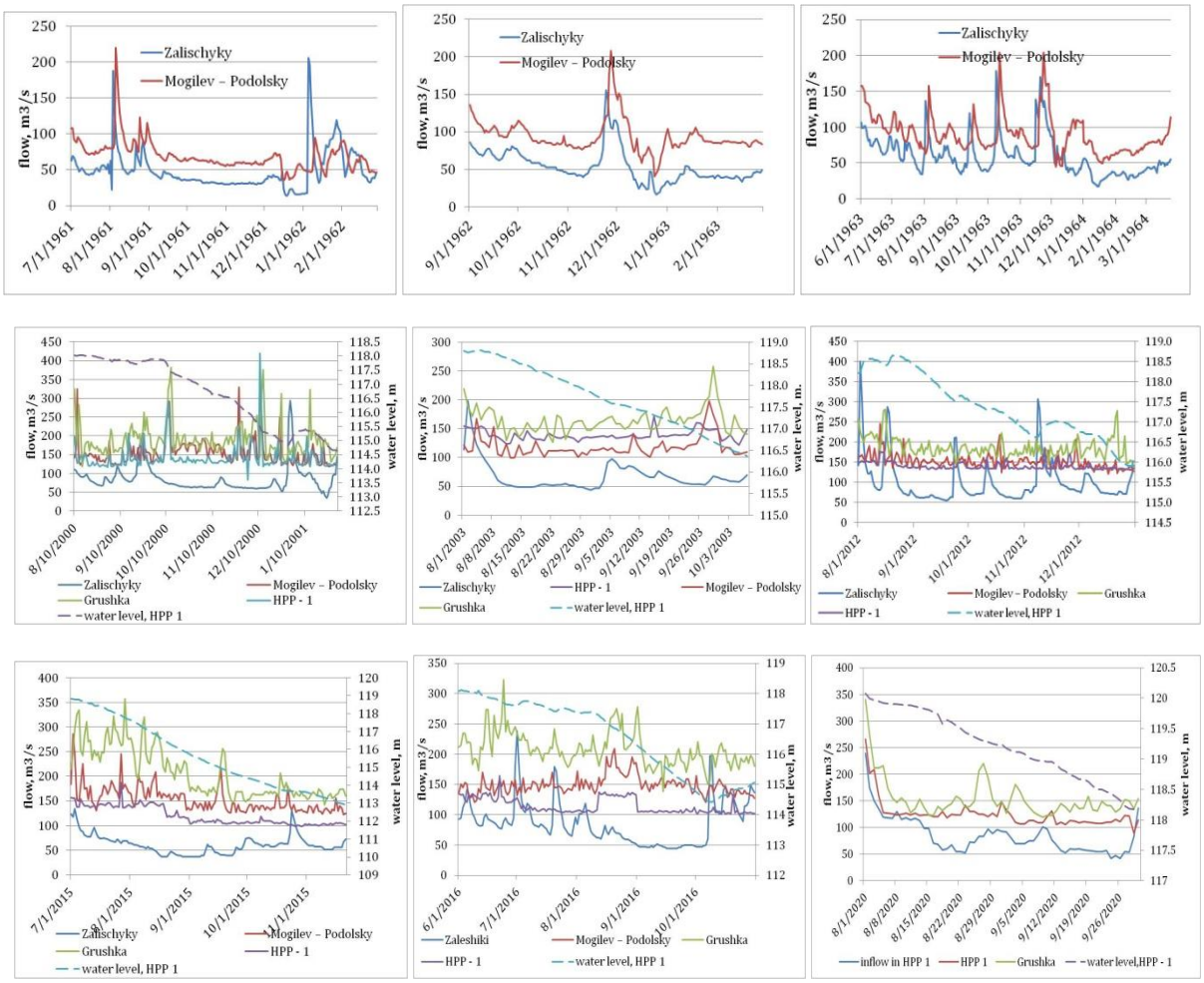

Figure 11. Low water phase.

In order to evaluate certain events of low water, data with values below 100 m^3/s were extracted from the time series of Zalischyky (as reference station), HPP-1, Mogilev – Podolsky, Grushka hydrological stations. 100 m^3/s is the minimum flow that must be discharged from DHC according to Operation Rules [34-36]. Examples of low water periods are shown in the figure above. In the pre-DHC period, low waters are highlighted in the years 1961, 1962, 1963 and 1967 with long periods of flows below 100 m^3/s. In the years 1961-1963, the flows below 100 m^3/s continue from July 1961 until February 1962, then from September 1962 until February 1963, after that from June to March 1964. Another long period with flows below 100 m^3/s is August 1967- January 1968. After the DHC construction, low flows seasons are observed especially in the early 2000s (2000, 2003) and in the last 10 years: 2011, 2012, 2015, 2016, 2020, 2022. The period of occurrence of minimum flows continues to either July – January.

Finally, the low water is a natural phase of the hydrological regime of the Dniester River. This is largely formed between July and February. Its duration is significant, in some years it can last 1-1.5 months, but there are many years in which the duration is extended to 8 months - a significant period that has an impact on both biodiversity and economical activities. During the low water season before the DHC construction, the flows in the Zalischyky - Mogilev-Podolsky sector were even around 50 m^3/s for a long time. Under the DHC impact, during this phase the minimum flows are characterized by an increase, and are not reduced below the value of 100 m^3/s in the downstream (with some exceptions). The DHC maintains the water flow within the reference value even if in upper part of the basin the natural flow is reduced to 50 m^3/s for a long period. In this sense, in order to maintain the minimum reference flow, the volume from the HPP-1 reservoir is reduced in order to compensate the flow for the downstream. The water level at HPP-1 decreases on average by 3.2 m. in comparison to the initial one. Thus, the DHC has a positive effect on maintaining the minimum flow and reduction of the risk of extreme hydrological droughts in the downstream sector.

4.1.5. Minimum (low) flow

For assessment of changes in minimum flow, a couple of indicators were analyzed: minimum flow, annual minimum flow for 7, 30, 90 days. As a result of the analysis, at the station upstream the DHC, the

minimum average flows for the pre-DHC and post-DHC periods are equal to 34 m³/s and 52 m³/s respectively, the increase being of 52% (Figure 12). At the downstream stations, the minimum flows also have been doubled in the second period. At Mogilev-Podolsky the minimum average flow was evaluated to 107 m³/s post DHC, compared to 51 m³/s, pre-DHC, and at Grushka - 115 m³/s, compared to 63 m³/s for the pre-DHC period.

The general trend of minimum annual flows for the whole period is increasing at the Zalischyky station (Figure 13). Extreme minimum flows are recorded in 1953 - 14.4 m³/s, 1956 - 13.3 m³/s, 1957 - 17 m³/s, 1959 - 7.18 m³/s, 1961 - 14.2 m³/s, 1993 - 15 m³/s. The highest values of the minimum flows were recorded in 1971, 1975, 1980 - 70 m³/s in each year, 1997, 1998 - 80-84 m³/s, 2008 - 76.3 m³/s. At Mogilev- Podolsky, the extreme minimum flows were observed in 1953 - 18.9 m³/s, 1960 - 21.2 m³/s, 1973 - 25.7 m³/s. After the DHC construction the lowest flows were approx. 95-99 m³/s, registered in the years 2003-2006. The highest values of the minimum flows of approx. 120-133 m³/s were recorded in 1993, 1997-1999, 2008, 2009.

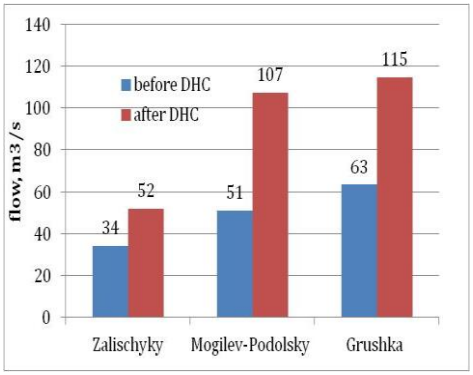

Figure 12. Minimum average.

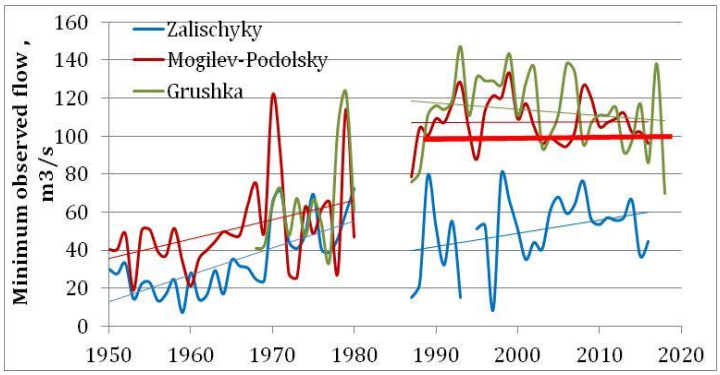

Figure 13. Minimum observed flow.

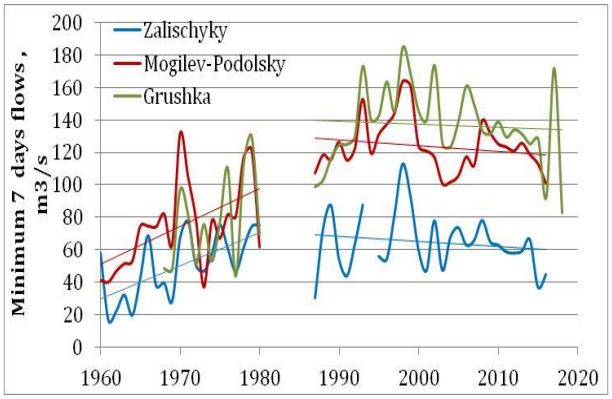

Figure 14. Minimum 7 days flows.

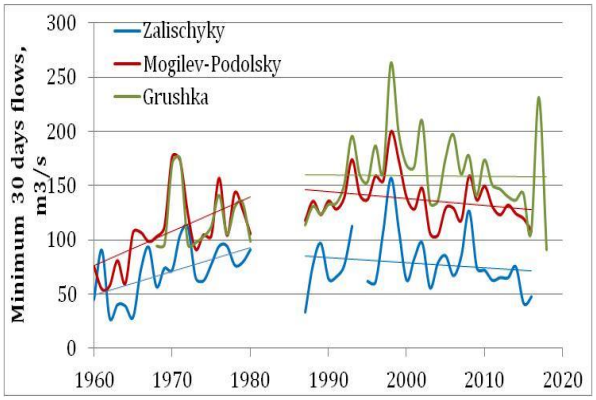

Figure 15. Minimum 30 days flows.

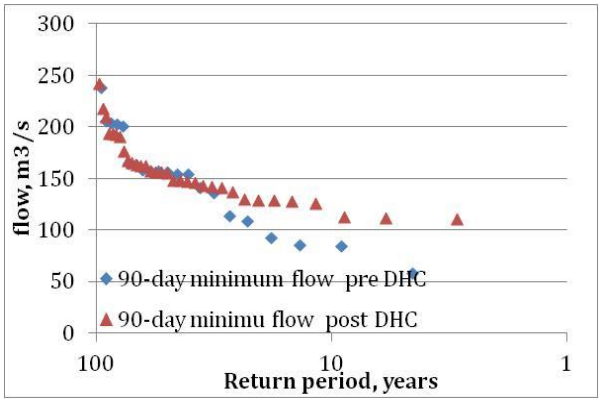

Figure 16. Frequency of 90 days flows at Mogilev-Podolsky.

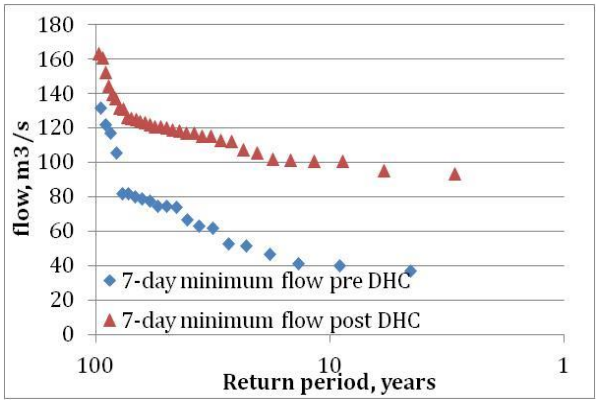

Figure 17. Frequency of 7 days flows at Mogilev-Podolsky.

Trends of minimum flows for 7 and 30-days are shown in the Figures 14 and15. Broadly speaking, they coincide with the conclusions regarding the minimum flows. In Figures 16 and 17, it can be seen that the magnitude of the curves for 90 and 7-days minimum flow probabilities knows major shifts. Such phenomena are observed in the downstream parts of the DHC, generally due to discharges of minimum flow which is established by Operation Rules of DHC being equal to 100 m^3/s.

As a conclusion, the assessments show that, for all the periods, the minimum flow has increased significantly. This means, in practice, that, for example, hydrological droughts with low probabilities that occurred in the past, in the DHC downstream, at present would be much rarer events. In general, the periods with minimum flow were changed downstream of the DHC and more water is now present in the river during the low water period. However, for the last decades it was observed that the low flow frequency has increased, fact that has a disastrous impact on aquatic ecosystems as well as on economy. In this regard, reevaluation of minimum flow discharged from DHC in order to improve the state of ecosystems and population is considered important.

4.1.6. Low flow and the DHC Operation Rules

A special analysis was performed in order to assess the compliance with the Operation Rules [34-36] in term of assurance of the minimum flow discharged from the DHC (100 m^3/s). Initially, the number of days with water flows lower than 100 m^3/s was calculated for all stations and periods. Thus, at Zalischyky, before the DHC construction, the duration of flows below 100 m^3/s is, on average, 118 days per year, which is about 32% of the year, the trend being downward. During the decade 1950-1960 the duration of the mentioned flow was, on average, 160 days/year or 44%. Over the next 15 years, by the '80, the share of days decreased to an average of 77 days/year or 21%. At present, after the DHC construction, flows below the value of 100 m^3/s appear, on average, in 91 days/year or 25%, the trend being ascendant. Between 2011-2016 the number of days increased on average to 146 days/years or 40%. At the Mogilev-Podolsky and Grushka, in the pre-DHC period, the flows with values below 100 m^3/s occurred on average 62 days/year and 19 days/years, which constitute 17% and 5%, respectively. In the post-DHC period, the number of days is reduced to 6 days and 13 days/year, respectively, the share being 2-4% (Figures 18, 19 and 21).

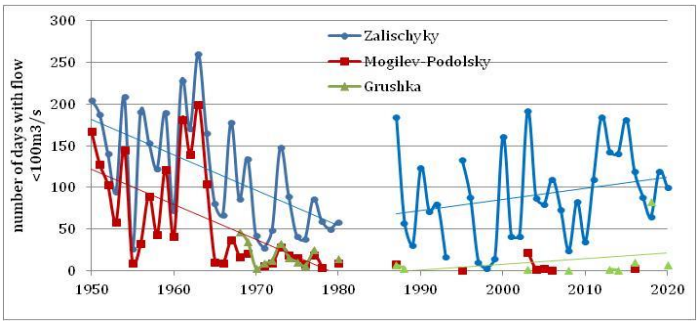

Figure 18. Duration of flow less than 100 m^3/s.

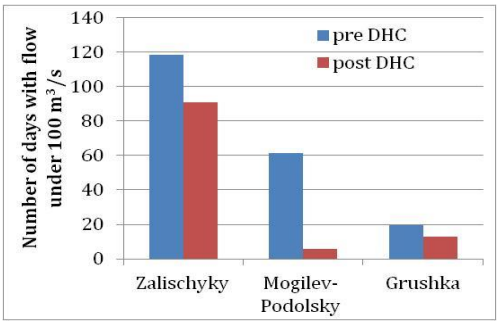

Figure 19. Number of days with flow less than100 m^3/s.

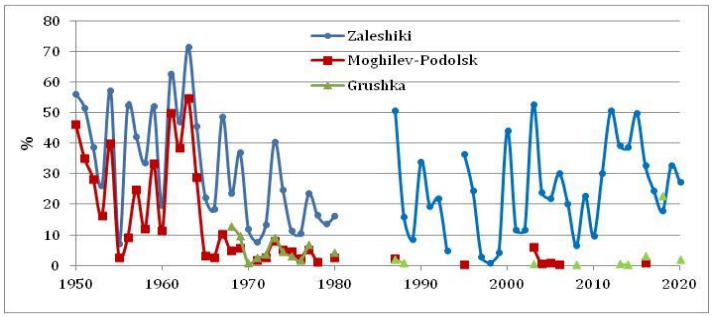

Figure 20. Share of annual days with flow less than 100 m^3/s.

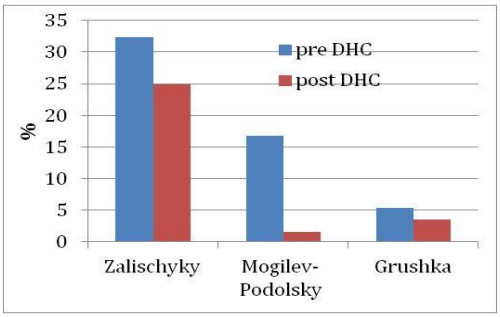

Figure 21. Average share of days with flow less than 100 m^3/s.

At Zalischyky, the average values of flows below 100 m^3/s are 72.4 m^3/s before the DHC and 80 m^3/s post DHC. At the downstream stations the values are, on average, 78 m^3/s at Mogilev-Podolsky and 76 m^3/s at Grushka in the pre-DHC period, practically 20-30 m^3/s less than the reference value. After the commissioning of the hydropower complex, the values increased to 95 m^3/s. The flows below 100 m^3/s downstream of the DHC occurred occasionally, and do not decrease much compared to the reference (Figures 22 and 23).

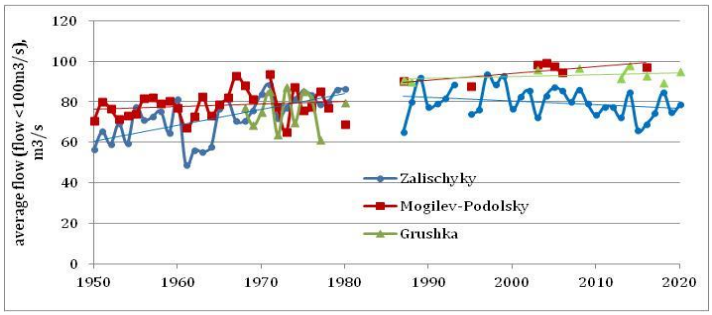

Figure 22. Average flow less than 100 m³/s.

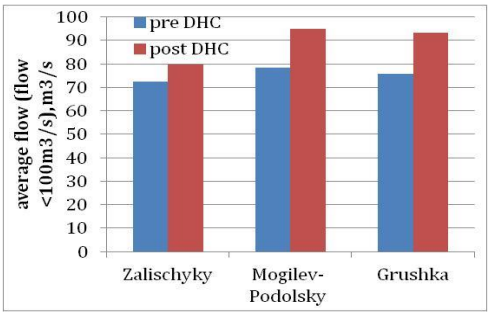

Figure 23. Average flow less than 100 m³/s

4.1.7. Spring floods

Spring floods are the phase of the hydrological regime formed as a result of snow melting or rain associated with snow melting, characterized by rising river levels and flow, quite long duration and large volumes. Sometimes, as a result of this phenomenon, the floodplains are flooded. The period of this phase occurrence is spring, in some years the beginning being registered in February, and the end in early June. The main natural factors that determine spring floods generation are: water reserves stored in snow, especially in the upper part of the basin, melting intensity and duration, water retention processes (infiltration, forest cover, etc.), climatic conditions (e.g. temperatures, precipitation and their character, etc.), etc. Water propagation process through the riverbed is determined by winter phenomena (ice formation/melting, etc.), reservoirs and dams' operation etc.

In order to assess the changes of the spring floods characteristics due to the DHC impact, the hydrological data from the Zalischyky, Grushka and Bender stations were analyzed for the pre-DHC and post-DHC periods. The statistics on spring floods were recalculated on the basis of daily data, synchronously for all stations, and certain calculation errors were excluded.

In natural flow regime, before the DHC construction, spring floods occurred on average on March 1, the earliest this phase began in the first decade of February (1957-1961, 1967, 1974), and the latest - in the last decade of March or even April (1952, 1956, 1964, 1980). The maximum flow is formed in 2-3 weeks from the beginning of the phase: at Zalischyky its date of occurrence is March 16, and at Bender March 22, with the 5 days propagation. The end of the phase is estimated for April 23 at Zalischyky and after 6 days, on April 29, at Bender. The latest the phase ended in the first days of June (1951, 1952, 1964), and the earliest, in the second decade of March (1955, 1956, 1966, 1977) (Figure 24). The duration of spring floods is 54 days at Zalischyky and 60 days at Bender. The duration of the phase has a decreasing trend: in the first period it is 51 days at Zalischyky and 69 days at Bender and in the second one, 50 days at both stations.

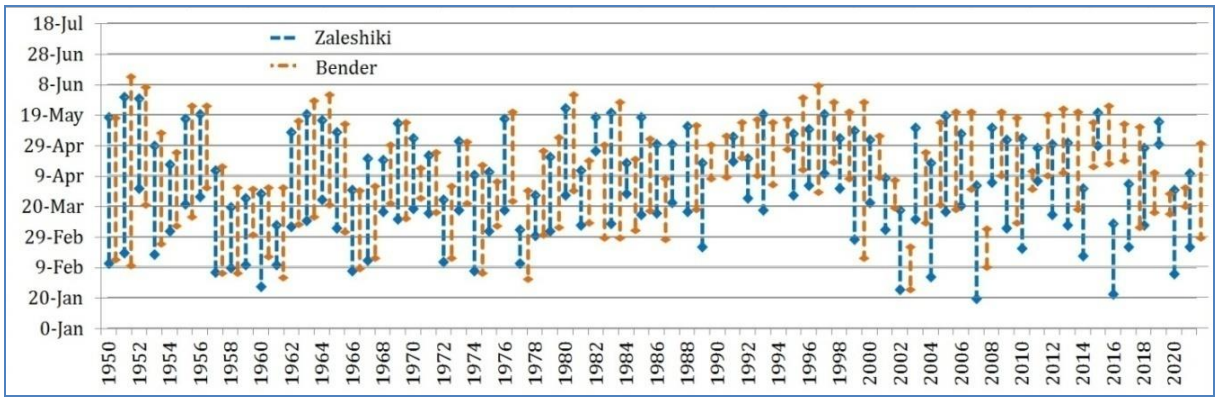

Figure 24. Spring flood occurrence at Zalischyky and Bender stations.

In the post-DHC period, spring floods dynamics change in the Zalischyky-Bender sector. In the first 10 years there is a significant delay but also a short duration of spring floods at all hydrological stations: it is approx. 40 days at Zalischyky and 44 days at Bender. Over the last 20 years, spring floods occurrence is characterized by a large variation. In some years, at Zalischyky, there is also a significantly delay, the beginning being in the last decade of March and end in the first decade of May, duration being on average 1.5 months. However, during this period, the number of years with early occurrence (the last decade of January - the first decade of February) increased (2002, 2004, 2007, 2016 and 2021). The duration of these phases in the mentioned years is on average 2 months. At Bender, the phase occurrence in the last

20 years, in general, maintains its trends from the '90s, and only in 2002, 2007, 2021 the spring floods started at the end of winter and last on average 1.5 months. In the last decade, the period of phase occurrence at Bender differs substantially from that at Zalischyky. At Bender, the phase begins in the second half of April and ends in the second decade of May. Duration of spring floods is characterized by a slight decreasing trend at all hydrological stations (Figures 25-28).

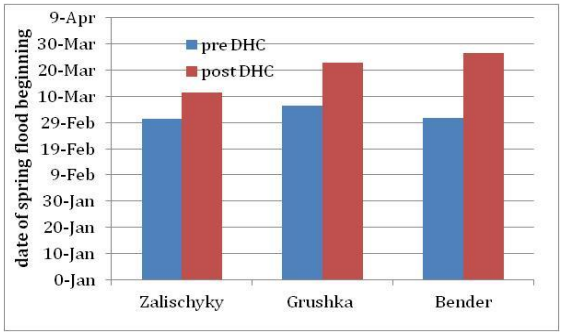

Figure 25. Average date of spring flood beginning.

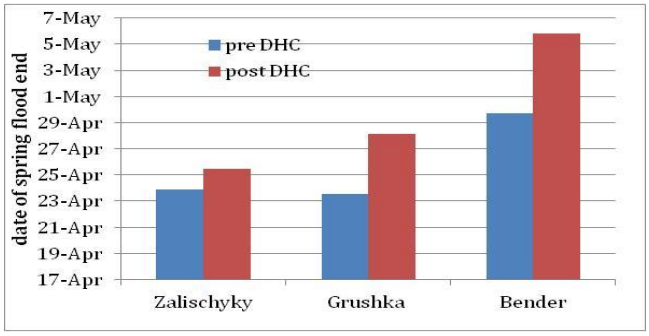

Figure 26. Average date of spring flood end.

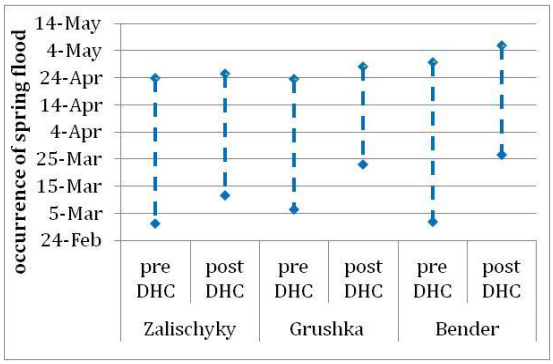

Figure 27. Average occurrence of spring flood.

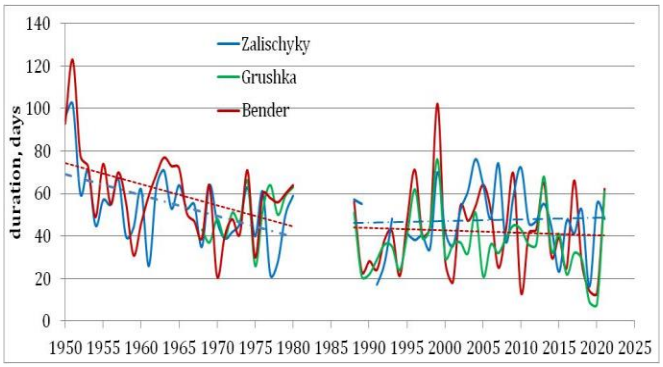

Figure 28. Spring flood duration.

Finally, for the two periods, at Zalischyky and Bender, the beginning of the phase is March 1, pre DHC, March 11 and March 26 - post DHC, respectively, the delay is 10 days in natural regime and 25 days in regulated regime. At Grushka this delay is 17 days (Figure 25). Occurrence of maximum flow, pre DHC, at Zalischyky is March 16, Grushka and Bender March 22, and post DHC, at the same posts it is March 27, April 5, April 11 or a change of 11, 13 and 21 days compared to previous period. The end of spring flood period is in the limits of April 23-29 before the DHC and April 25-May 5 after the DHC construction at the 3 analyzed stations (Figure 26), the changes being minor, 2-6 days. The duration of the natural phase is 54 days at Zalischyky and 60 at Bender and decreases in the post DHC period, to 46 days at Zalischyky, 36 days at Grushka and 42 days in Bender (Figure 29), being a decrease of the period by 8 days (14%) upstream of the DHC, and 13 days (26%) at Grushka and 18 days (30%) at Bender.

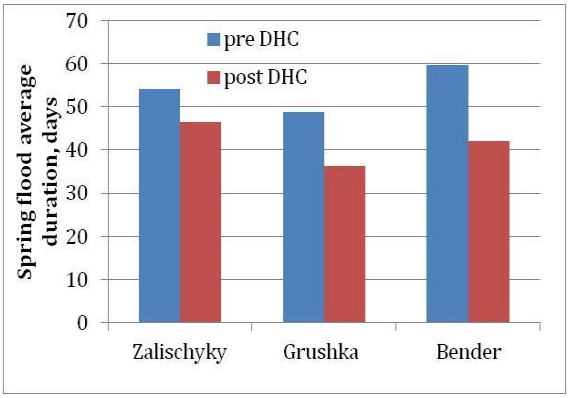

Figure 29. Spring flood average duration.

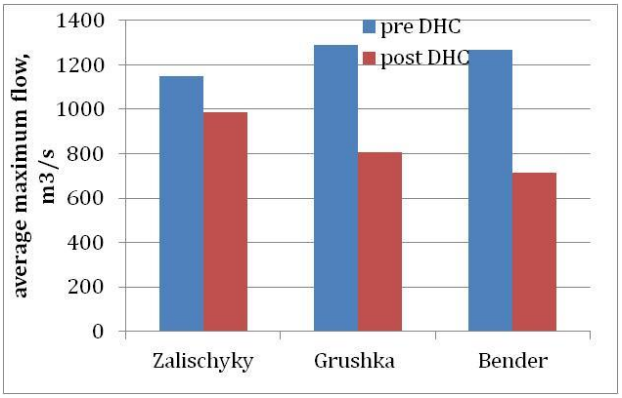

Figure 30. Maximum flow of spring flood.

The maximum flow of spring floods tends to decrease at the Zalischyky station and increase at the Bender station during the pre-DHC period. After the DHC construction, the flow decrease is observed at all hydrological stations (Figure 30). During the pre-DHC period at the Zalischyky, Grushka and Bender hydrological stations, the average maximum flows are equal to 1150 m^3/s, 1289 m^3/s, 1265 m^3/s, spatial

increase being 115-140 m³/s. During the post-DHC period, the maximum average flow is characterized by spatial decrease. Thus, at Zalischyky it is 988 m³/s or 14% lower than in the previous period, at Grushka the value is 805 m³/s or by 38% lower than before DHC, and at Bender the flow is 716 m³/s or 43% less. Spatially, the value of the maximum flow no longer increases as in pre-DHC period but decreases by 180-270 m³/s (Figures 30 and 31).

The spring flood average volume for the two periods is generally decreasing. At Zalischyky, its value is 1805 mil. m³ before the DHC construction and 1616 mil. m³ after DHC, the decrease being by 10%. At Grushka station, the average volume is within the limit of 2282 mil. m³ before the DHC and 1480 mil. m³ after the DHC, the decrease being by 35% or 800 mil. m³. At Bender, the values are 2802 mil. m³ before the DHC and 1707 mil. m³ in the period after the construction of the DHC, the decrease being by 39% or 1.1 km³. In terms of space, pre-DHC, the increase of spring floods volume was practically by 0.5 km³ on Zalischyky - Grushka sector and 1 km³ on Zalischyky - Bender sector, while after DHC it practically does not change on the same sectors, being similar to that of Zalischyky (Figures 32 and 33).

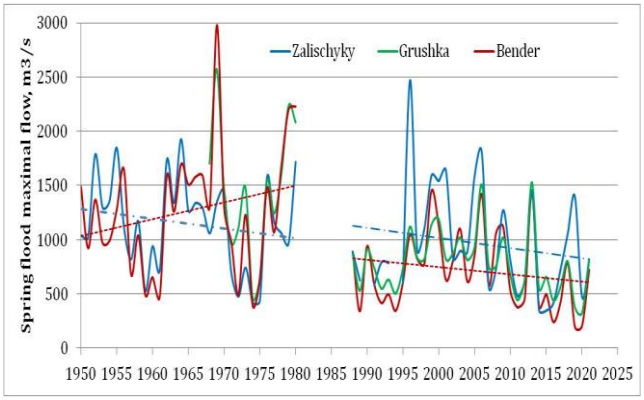

Figure 31. Spring flood maximal flow.

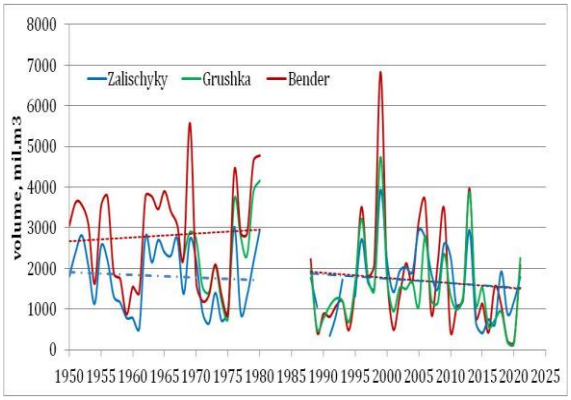

Figure 32. Spring flood volume.

Spring floods form important water resources of the Dniester River. Their share from the total annual water volume was on average 27-29% in the pre-DHC period, in the post-DHC period this value decreases significantly: upstream, at Zalischyky, the share is already 23%, downstream, at Grushka it is 16%, and at Bender -19%. The general trend is of significant decrease in the pre-DHC period and a slight decrease after DHC at all hydrological stations (Figure 34).

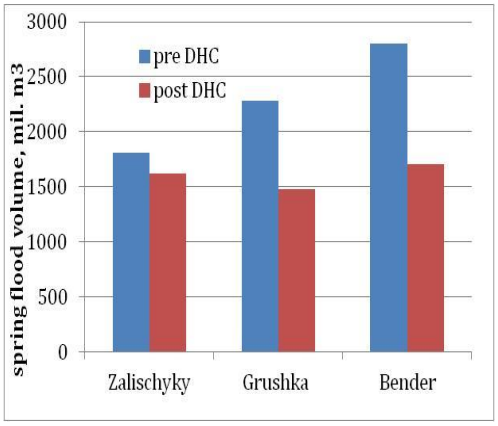

Figure 33. Average spring flood volume.

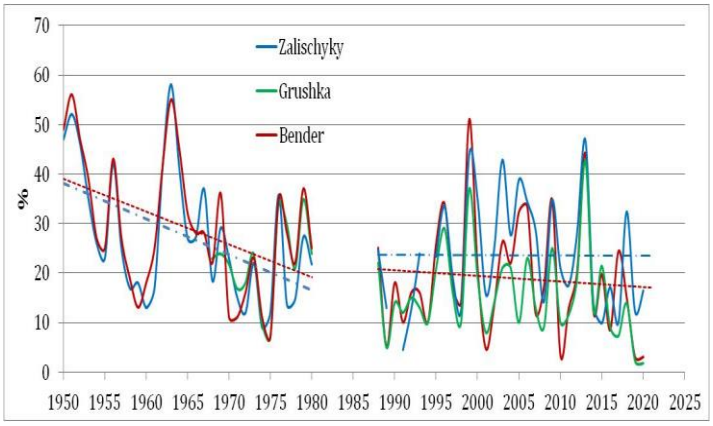

Figure 34. Share of spring floods from annual water volume.

The dynamics of spring floods in natural regime depends on the processes of water propagation in the riverbed and floodplain system and after DHC construction – it is regulated by hydrotechnical structures. The change in spring flood occurrence is significantly influenced by the planning processes of the so-called spring ecological flood. Its purpose is to provide sufficient water volumes for the Dniester riverbed to ensure reproduction of fish and stability of the Dniester ecosystems. Since the 1990s, experts from Moldova and Ukraine have been making efforts to plan and carry out this type of ecological flood. Thus, according to analyzed information four situation of spring ecological flood releases were identified:

- spring ecological flood coincides with natural spring flood;
- spring ecological flood is realized after generation of spring flood;
- spring ecological flood coincides with the beginning or end of spring flood - it is a component of it;
- spring ecological flood is released in the absence of spring flood occurrence.

Several elements are important to consider in order to discharge an efficient ecological flood: water temperature, water volume, duration, shape of hydrograph etc. All these should be studied in more details in order to plan and release from DHC an efficient spring ecological flood. Also, parameters for spring ecological flood efficiency should be developed and applied for ecosystems and fish benefit.

4.1.8. Pluvial floods

Pluvial floods are a phase of hydrological regime characterized by rapid increase of river flow and level and volume as a result of heavy rains. These are formed in the warm period of the year, on average, in the summer months: June and July. Main factor that determines generation of pluvial flood on the Dniester River are heavy rains formed in the upper part of the basin. In natural conditions (before reservoirs and dykes' construction), spatial reduction of the maximal flow of pluvial floods was determined by basin surface and floodplain width increase. As an example, the flood hydrograph of 1948 (Figure 35) shows the flood wave attenuation in natural regime, in particular, the change in hydrograph shape, as well as the decrease in maximum flow values due to water accumulation in the floodplain in the downstream part of the Dniester River.

In regulated regime, the flood wave dynamics has changed. In particular, it should be mentioned that a certain threshold for flood maximal flow is considered. Thus, according to the DHC Operation Rules, its value is 2600 m^3/s in case of flood inflow of 1-10% probability. During the DHC operation, this value was exceeded only once, in case of 2008 flood event when maximal flow discharged from the DHC was 3500 m^3/s. Thus, reservoirs operation during floods plays a significant role in flood protection of the downstream part from potential damages. However, in certain conditions, operation mistakes can create dangerous situation for population and industries from the floodplain.

Last flood event was the one from 2020, when the maximal flow at Zalischyky was 3740 m^3/s which was reduced to 2020 m^3/s at Grushka, and at Bender it was of approx. 1800 m^3/s (Figure. 36). The total volume was 2 km^3 at all stations. In general, the flood hydrograph, under the DHC impact, was changed from triangle to trapezoid thus causing a delay in the occurrence of the maximum flow by increasing the rising limb and slightly decreasing the recession limb of the flood wave.

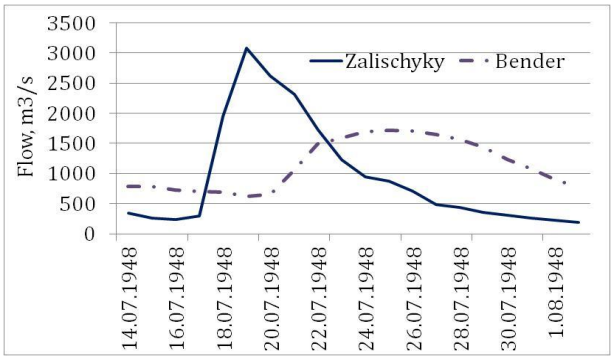

Figure 35. Flood hydrographs of 1948.

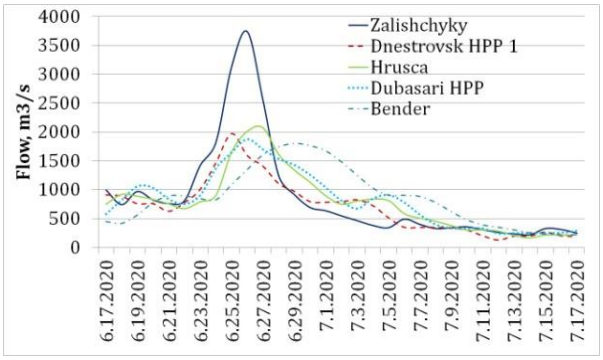

Figure 36. Flood hydrographs of 2020.

For the assessment of the DHC impact on pluvial flood phase, statistical analysis of different characteristics was performed for the mentioned periods. For the pre-DHC period, maximum daily flows are characterized by upward trends at all hydrological stations, and for the post-DHC, the trends are characterized by stability at Zalischyky and a slight decrease at downstream stations (Figure 37).

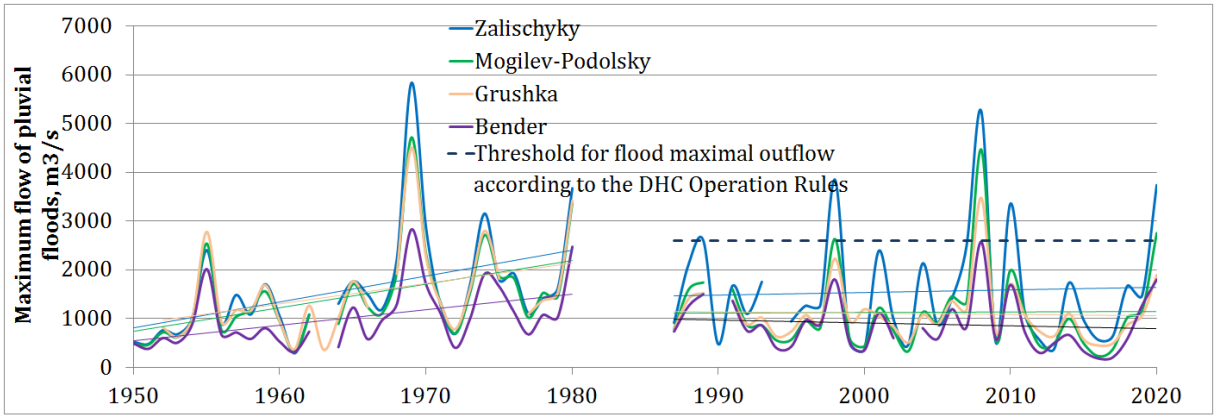

Figure 37. Maximum flow of pluvial floods.

The average values of maximum daily flows at Zalischyky station have slightly decreased in the post-DHC period, from 1609 m³/s to 1558 m³/s or by 3.2%. At DHC downstream stations, maximum flow has decreased by 25-30%. At Mogilev-Podolsky station, it decreases from 1500 m³/s to 1130 m³/s, by 370 m³/s or 25%. At Grushka, maximum instantaneous and daily flow decrease is approx. 30%: first characteristic diminishes from 1598 m³/s to 1095 m³/s or by 31.5% and the second one from 1477 m³/s to 1041 m³/s or by 29.5%. At Bender station, before the DHC construction, maximum flow, on average, is a little over 1000 m³/s and after the DHC, itis a little below 900 m³/s, the decrease being approx. by 14% (Figure 38).

Spatially, from the upper to lower part of the river, in natural regime, the maximum flow is reduced from 1609 m³/s to 1477 m³/s or by 8% on the Zalischyky - Grushka sector, however, in regulated regime, this decrease is 33%, from 1558 m³/s to 1041 m³/s. At the Bender station, during Dubasari HPP operation, the maximum flow decreased by 36% compared to Zalischyky, and after DHC construction the share is already 43%, thus, maximum flow regulation by the entire cascade of reservoirs being significant. However, the occurrence of maximum flows that exceeds 2600 m³/s increased in the last decades. Thus, for pre-DHC period, the flow over mentioned value at Zalischyky was recorded in 1969, 1970, 1980. After the DHC construction so far flows of over 2600 m³/s at the same station were manifested more often: in 1989, 1998, 2008, 2010, 2020 (Figure 37). Respectively, increasing the frequency of major floods also requires special attention for catastrophic floods management.

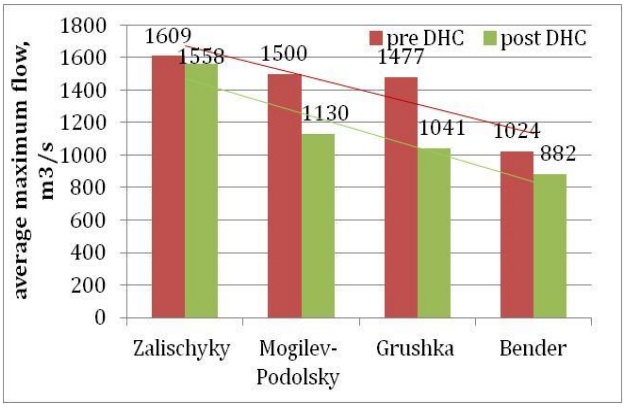

Figure 38. Average maximum flow of pluvial floods.

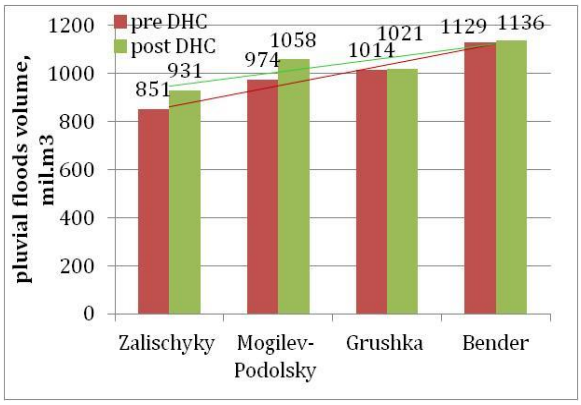

Figure 39. Pluvial floods volume.

Average flood volumes, for two considered periods, are: in the DHC upstream - 851 mil. m³ and 931 mil. m³ and in the downstream - 974 mil. m³ and 1058 mil. m³, the increase for the second period being about 9%. At Bender station, the pluvial flood volume increased to 1.1 km³ (Figure 39). The increase of this indicator together with basin surface, on the Zalischyky - Bender sector, is, on average, of 20%. For the period pre-DHC the share is 25%, and post-DHC - 18%, thus, a larger part of the flood volume being formed in the upper part of the river basin in the current period compared to the previous one.

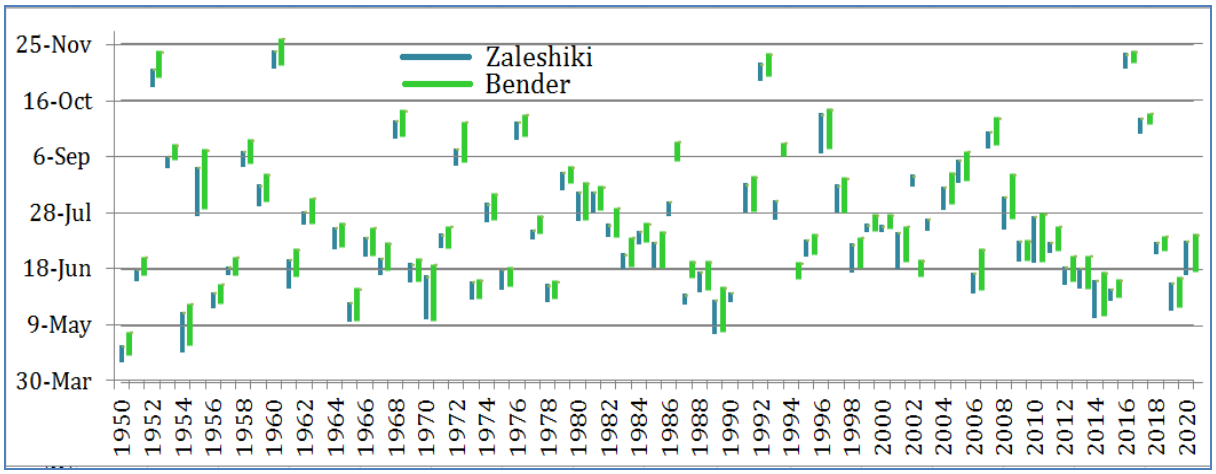

Figure 40. Pluvial floods occurrence.

In general, pluvial floods occurrence is considered to be the summer season, June and July, but there are years when the maximum flow is observed in both spring and autumn months. Figure 40 shows the pluvial floods appearance and duration. Thus, in comparison with spring floods, this phenomenon is quite short, and the occurrence differs from year to year and may include the period from April to November.

The manifestation of pluvial floods is synchronous for upstream and downstream stations, which shows that DHC does not cause a significant temporal and spatial shift of the analyzed phase. On average, for the two periods, pluvial floods occurrence is at Zalischyky July 9 - July 24, July 9 - July 25, at Mogilev – Podolsky, July 10 - July 27, July 9 - July 26, and at Bender, July 12 - July 31, July 12 - August 1 (Figure 41).

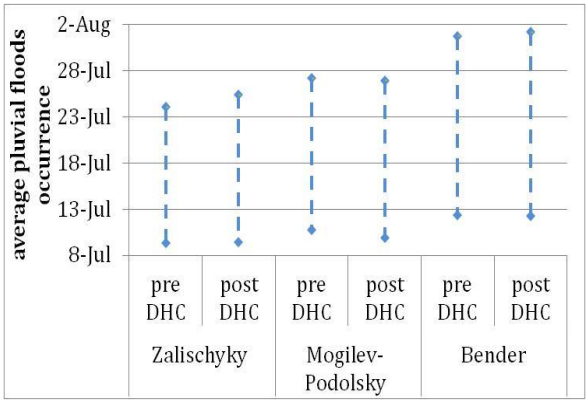

Figure 41. Average pluvial floods occurrence.

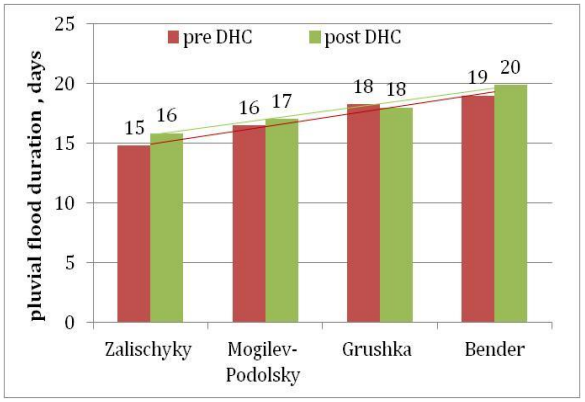

Figure 42. Pluvial flood duration.

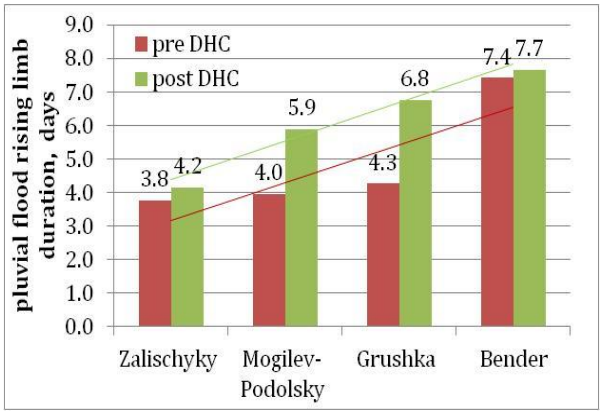

Figure 43. Pluvial flood rising limb duration.

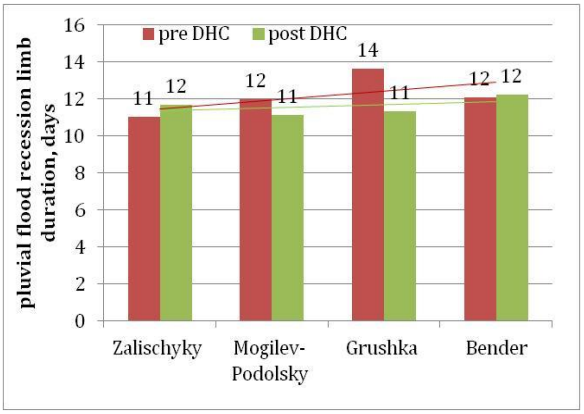

Figure 44. Pluvial flood recession limb duration.

Total duration of pluvial floods is 15-16 days at Zalischyky and Mogilev-Podolsky and 19-20 days at Bender, large differences between pre-DHC and post-DHC periods were not identified (Figure 42). However, division of flood hydrographs into two parts: rising and recession limbs, shows that changes are observed mainly for the first one. Thus, rising limb average duration, at Zalischyky, is 4 days for both periods. In the downstream, at Mogilev-Podolsky and Grushka, the number of days increased from 4 days pre-DHC to 6-7 days post- DHC (Figure 43). Flood wave recession limb is maintained within 11-12 days in the upper part of the DHC, while downstream of the DHC, it has a slight decreasing tendency, at Grushka the decrease being from 14, in natural regime to 11 days, in regulated regime (Figure 44).

Thus, the DHC impact on pluvial floods is manifested by changes of maximum flow, it decreased by about 30% in the downstream part, modification of flood wave hydrograph from triangle to trapezoid, thus causing a delay in the maximum flow by increasing the rising limb and decreasing the recession limb of the flood wave. Pluvial flood total duration does not change, and no major shift of the flood wave in space profile is observed. However, the increase in the frequency of natural floods must lead to a serious preparation of the DHC for the management of these phenomena and protection of areas in the lower part against major floods.

4.2. Hydropeaking effect

One of the direct effects of the DHC operation is the hydropeaking effect that is felt in the downstream part. It is determined by operation of HPP-2 turbines and is characterized by major intraday variations in level and flow. For analyzing this effect, we used the intraday data recorded at the automatic level stations situated downstream of HPP-2: Naslavcea (5 km downstream), Unguri (30 km downstream), Soroca (100 km downstream) and Sanatauca (180 km downstream). Time series for the first two stations consist of levels data for every 15 minutes for 2013-2020, and those from Soroca and Sanatauca consist of water levels measured hourly for the period 2017-2020. Data series contain many gaps.

For evaluation of hydropeaking effect, following characteristics were analyzed: level variation, daily level amplitudes, increasing and decreasing rate. It should be noted that actual Operation Rules do not contains information regarding any threshold for evaluation of hydropeaking effect. However, in the draft of Operation Rules, 2017 [36], it is mentioned that the water level variation in the downstream part (June – November) must not exceed 20-25 cm. In spring and summer, water level fluctuations downstream of the HHP-2 must not exceed 5cm/h or 20cm/day. Also, according to [44], one of the criteria for identification of heavily modified water bodies is water level fluctuations downstream HPP dam of over 50 cm during the day for most of the year. Thus, as threshold values, for water level fluctuation, 20 cm/day and 50 cm/day were considered, and for increasing and decreasing rate - 5cm/h or 0,08 cm/min. It should be noted that increasing and decreasing rates are changes in water level over a certain threshold in a certain period of time and are important to be estimated for evaluation of the risk of death of aquatic organisms due to turbine shutdown and discontinuity and water discharge from the HPP-2. The increasing and decreasing rates describe the rates at which water levels rise or fall during an event and are considered to have a significant effect on aquatic organisms [15-17].

4.2.1. The amplitude of the intraday water level

The first analyzed parameter to evaluate the hydropeaking effect is the water level amplitude: the daily difference between the maximum level and the minimum level (intraday level difference). As a result of performed analysis, it was found out that at Naslavcea station, the water level amplitude far exceeds the reference values. The exceedance of the 50 cm is on average 37%, being higher in 2013, 2014 - 46-58%, and lower in 2016-25%. The exceedance of the 20 cm was significant, on average - 70%, in the years 2013, 2014 being highlighted by higher values (93-99%), and in 2016, 2018 and 2019 by lower values (55-62%). At Unguri, there is an insignificant decrease in the share of values that exceed the reference. The level amplitude of over 50 cm is 33%, over 20 cm (70%). The lowest share of value that exceed 50 cm was estimated for 2016 and 2017 (14-25%), and the highest for 2013, 2014, 2020 (37-47%). Significant exceedance of the water level amplitude over 20 cm was observed in 2013, 2014 (90-96%), and less obvious in 2016 (44%). At Soroca and Sanatauca stations, the parameters of the hydropeaking effect are significantly reduced. Exceedance of the reference value of 50 cm are few (8% and 3%), and of the value of 20 cm, 33% and 14% respectively.

Based on the intraday data, the average daily water level amplitude was calculated for the entire monitoring period for all station (Figure 45). The largest fluctuations are recorded between April-July, November-January at Naslavcea and Unguri stations. At Soroca and Sanatauca such periods are in the first part of the year, and the months of June, July, the hydropeaking effect being diminished towards the sectors concerned (Figure 45).

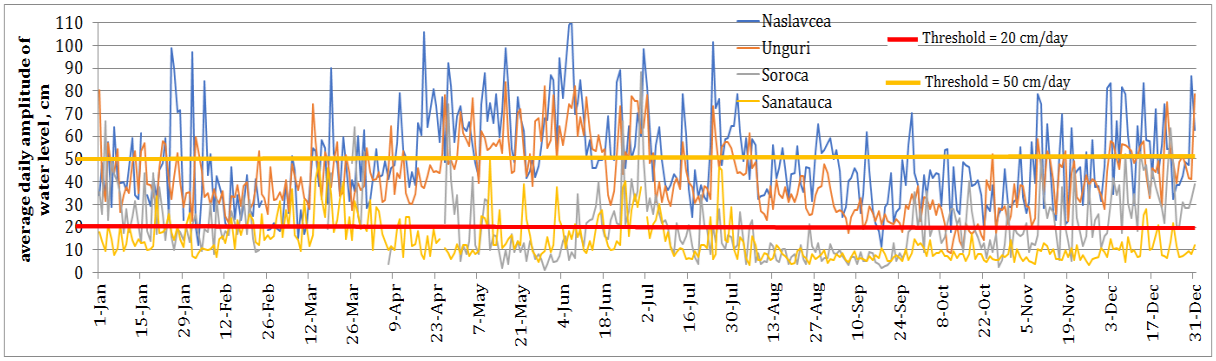

Figure 45. The average daily amplitude of the water level at all hydrological stations for the entire monitoring period.

At the monthly level, the highest values were found in April, May, June, July and December, when the averages at the stations near the HPP-2 were equal or exceeded 50 cm. The lowest values of the level's amplitude (30-35 cm), were observed in February, September and October. There are no months in which averages smaller than 20 cm were recorded at the mentioned stations. At Soroca and Sanatauca, monthly average values are below the value of 20 cm in February, May, July, August, September, October. In the other months, the averages exceed to a certain extent the reference value but not much (Figure 46).

At annual level, the largest water level variations are estimated for the first years of monitoring, 2013 and 2014, the values decreasing from 2015, and increasing towards 2020. At stations near the HPP-2, the average annual values are approx. 30 cm in 2016, approx. 40 cm in 2015, 2017, 2019, and over 50 cm in 2013, 2014, 2020 (Figure 47). At Soroca and Sanatauca stations, the amplitude values are close to 20 cm and 13 cm.

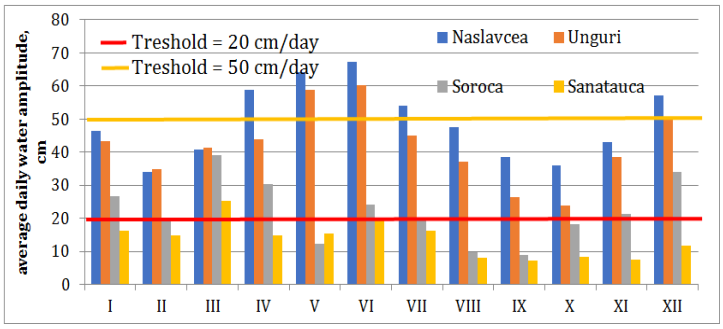

Figure 46. Average daily water amplitude at monthly level.

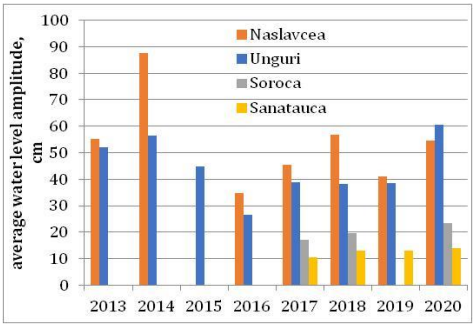

Figure 47. Average water level amplitude.

On average, the intraday amplitude of the level rises to 52 cm near the DHC (at Naslavcea), decreases to 42 cm to 30 km downstream (Unguri station), is doubly reduced to 100 km at Soroca, and decreases to 14 cm at Sanatauca. Thus, the sector that is significantly influenced by hydropeaking effect is over 100 km (HPP-2 - Soroca).

The hourly analysis of water levels shows that, in general, these increase in the afternoon and in the evening, when the demand for electricity is high. During these periods, water level values increase significantly in comparison to those between 0:00 and 6:00.

4.2.1. Increasing and decreasing rate

Increasing and decreasing rates were calculated for the 4 mentioned above hydrological stations, the averages being calculated for days, months and years. Based on performed analysis of the monthly averages of both types of rates, it can be concluded that the values at Naslavcea far exceed the threshold value, being over 0.25 cm/min and -0.15cm/min in all months of the year. At Unguri, the situation is changing, the rates being close to the reference value in autumn, and exceeding it in other months even twice. At Soroca and Sanatauca stations, the rates do not exceed 0.05 cm/min and -0.04 cm/min (Figures 48 and 49).

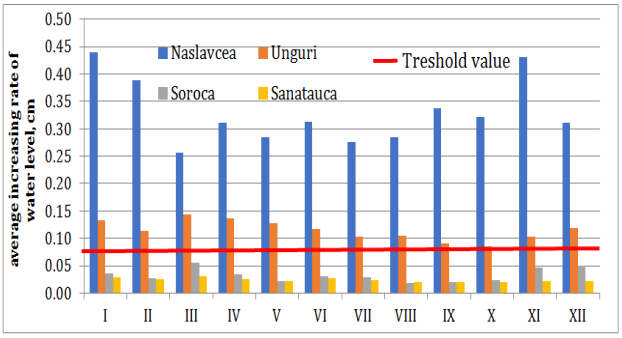

Figure 48. Average increasing rate of water level caused by hydropeaking effect at monthly level.

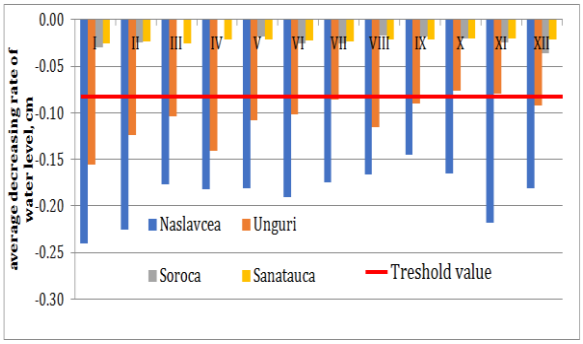

Figure 49. Average decreasing rate of water level caused by hydropeaking effect at monthly level.

At annual level, the averages of increasing and decreasing rates at Naslavcea are 0.25-0.45 cm/min and -0.14 – -0.25 cm/min, at Unguri the values are between 0.09-0.18 cm/min and -0.08 – -0.18 cm/min. At Soroca and Sanatauca stations, the rates are below 0.04 cm/min and -0.03 cm/min (Figures 50 and 51, Table 2).

Table 2. Dynamics of hydropeaking effect indicators.

Indicators	Hydrologic station			
	Naslavcea	Unguri	Soroca	Sanatauca
Water level amplitude (cm)	52	42	20	14
Increasing rate (cm/min)	0.35	0.14	0.04	0.03
Decreasing rate (cm/min)	- 0.19	- 0.12	- 0.03	- 0.03

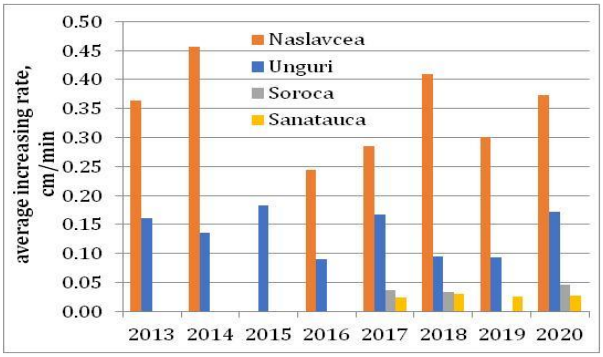

Figure 50. Average increasing rate.

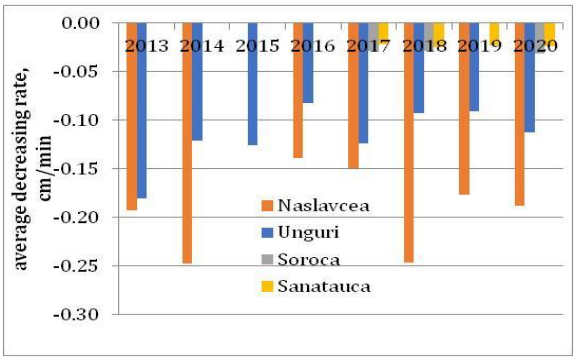

Figure 51. Average decreasing rate.

On average, increasing and decreasing rates is 0.35 cm/min and –0.19 cm/min near the DHC, the values being reduced 2 times downstream (30 km) and 5 times towards Soroca and Sanatauca.

4.3. Water temperature

The major impact of reservoir with HPP-1 on the thermal regime of the Dniester River is caused by the fact that water is discharged from the lower layers of the reservoir. The water temperature from the surface layer changes under the impact of climatic factor, but with the depth, the so-called thermal jump occurs which is characterized by a sudden drop in temperature followed by the thermocline layer characterized by constant low temperature throughout the year. Thus, flow discharged from the bottom of reservoir brings low temperatures downstream during warm period and warm waters during cold one.

For the analysis of the water temperature changes, data recorded before and after the DHC construction at the Zalischyky, Mogilev-Podolsky, Grushka, Camenca, Dubasari and Bender stations were used. Annual average values show that pre-DHC, the general trend of water temperature is constant, while in the post-DHC period the linear trend is ascending at all stations (Figure 52).

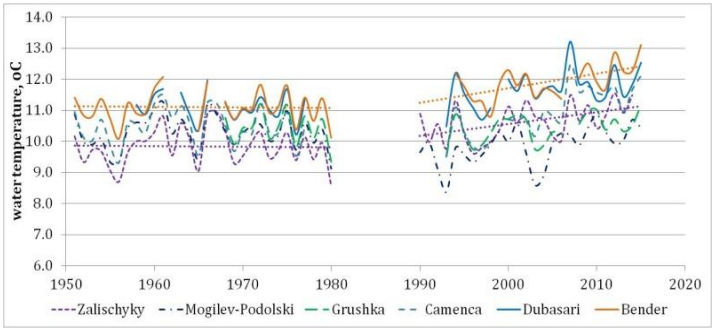

Figure 52. Dniester River water temperature dynamics.

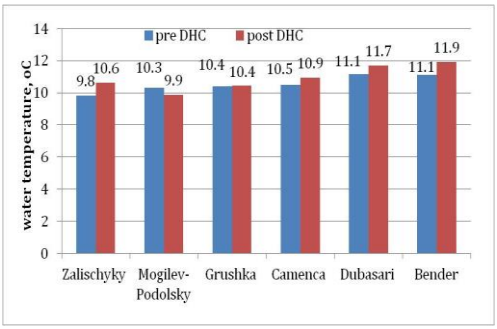

Figure 53. Average water temperature of the Dniester River pre- and post-DHC.

However, if during those 2 periods, upstream of the DHC (at Zalischyky), the average water temperature is 9.84°C and 10.64°C, the increase being 0.8°C, at Mogilev-Podolsky it is observed a decrease in average temperature by 0.43°C, from 10.29°C to 9.86°C. At Grushka, the average temperature for both periods is 10.4°C. Spatially, the temperature rise starts from Camenca, where before the DHC construction was 10.5°C, and after the DHC commissioning was 10.93°C. At Dubasari HPP these temperatures were 11.14°C and 11.7°C, the increase being 0.56°C, and at Bender 11.1°C and 11.92°C, the increase being 0.82°C, similar to that at Zalischyky. Respectively, on the DHC downstream sector, despite increasing temperature trends, the data analysis shows that the average temperature decreases downstream of the DHC, remains unchanged near Grushka sector, and begins to rise from Camenca to river mouth, the increase at Bender being similar to that at Zalischyky. In this sense, if we consider that the water temperature throughout the sector should increase by 0.8°C, then at Mogilev-Podolsky, the current temperature should be 11.1°C, at the moment it is 9.86°C, i.e.by 1.24°C lower (Figure 53).

In spatial profile, pre DHC, the water temperature rises proportionally from 9.84 °C at Zalischyky to 11.1°C at Bender (by 1.26°C). After the DHC construction, the water temperature decreased from 10.64 ° C at Zalischyky to 9.86°C at Mogilev-Podolsky or by 0.8°C, the increase being highlighted from Camenca proportionally to river mouth. After the DHC commissioning, the difference of temperature from Zalischyky and Bender is 1.3°C.

In the monthly profile, at Zalischyky, maximum temperatures are observed in the summer months (19-20°C), and minimum - in winter (0.5-1.17°C). In post-DHC period, the increase of water temperature is from 0.4 °C, in the winter months to 1.3-1.4 °C in the spring-summer period (Figure 54).

At Mogilev-Podolsky, in winter time, in pre-DHC period, the temperatures were 0.1-0.86°C and after the DHC construction, these are already 2.14-5.83°C or by 2-5°C higher than in the previous one (Figure 54). In spring, the temperatures are between 2-16.15°C in pre DHC and post DHC these are already 3-10°C. In March the water temperature increases by 1 °C, and in April and May it decreases by 3.6 and 6°C. During summer time the temperature changes are the highest: if, pre DHC, the temperatures were on average 20-21°C, post DHC these are already by 3.9-7.2°C lower (13.1 °C in June, 15.6 °C in July and17.5 °C in August). During autumn, there is an increase in water temperature by 0.9-5.56 °C, in September the modifications are minor, in October the increase is from 10.3 to 14.4 °C, and in November from 4.68 to 10.25 °C. It is observed that post-DHC, the maximum temperatures shift from July-August to August-September, with values rising only to 17.5 °C, or by 3.6 °C lower than pre-DHC.

At Grushka and Camenca, the average monthly water temperature has the same trends as at Mogilev-Podolsky, but the changes are smaller. The differences in the sense of decreasing temperatures are observed between April and August: before the DHC construction, the temperatures are in the limits of 10-21°C and post DHC these decreased by up to 3.5°C (especially between April-June). In other months, the water temperatures increase by up to 3.4 °C; in the autumn months: in September, the temperatures are in the limits of 17-18°C in both periods, in November 4-5 °C before DHC and 8°C post DHC, and, in winter, temperatures rise from 0-0.5°C to 2.7°C. At Dubasari and Bender stations the water temperature is generally increasing by 0.5-0.7°C, in March the increase being 1.8°C (Figure 54).

Finally, it is observed that the sector most affected by the change in water temperature caused by the DHC operation extends to Camenca; it is observed a decrease in water temperature in warm period and an increase in the cold period, as well as shifting of the maximum temperature by 1 month.

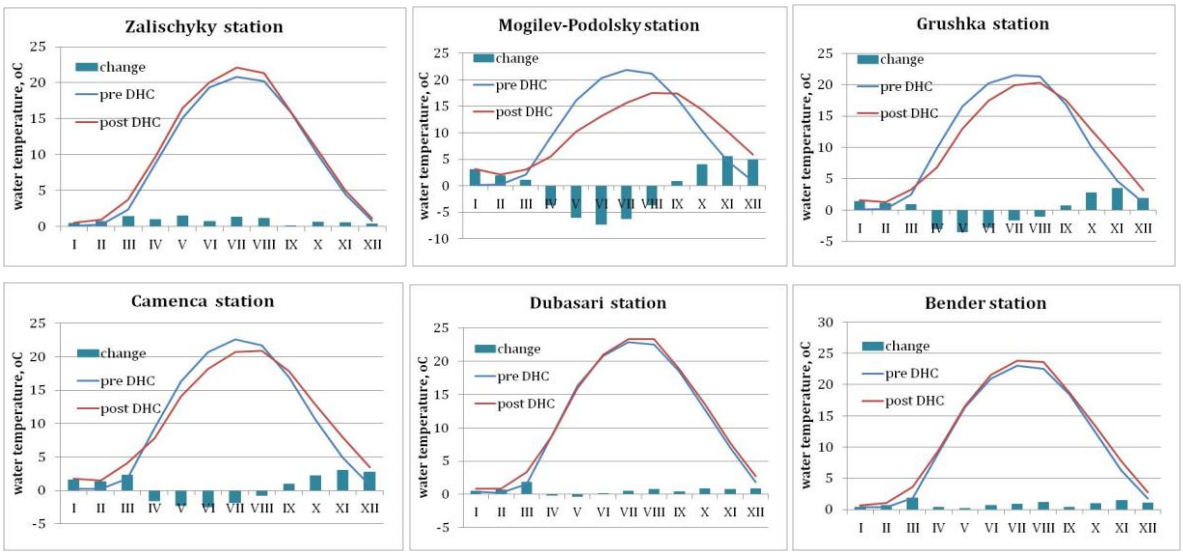

Figure 54. Monthly water temperature dynamics.

4.4. Suspended sediments

One of the main characteristics of river water dynamics is erosion, transport and accumulation of sediments. As usual, main erosion processes are specific for upper part of the basin, while sediment accumulation – for lower part. From all types of sediments (dissolved, suspended, and bed sediments), present assessment is limited to the analysis of suspended sediments transport in the Dniester River (other types are not monitored). The assessment was performed, as usual, for 2 representative periods. For Dubasari and Bender, the reference year for which the two periods were divided is 1954, when the exploitation of the Dubasari HPP has begun.

The average values of suspended sediments are shown in figures 55 and 56. The highest values at all hydrological stations are observed in the pre-DHC period. The average of this feature is approx. 100 kg/s at Zalischyky, 160 kg/s at Mogilev-Podolsky and 230 kg/s at Grushka. Thus, in the Zalischyky-Grushka sector, suspended sediments double. During the time, '70s and' 80s are highlighted when values of this characteristic were much higher compared to other years, due to floods occurrence, as well as the '60s when droughts were monitored, with suspended sediments characterized by minimum values. In the post-DHC period, suspended sediments are estimated at 59 kg/s at Zalischyky, being lower compared to

the previous period by 40%, the change being caused by natural factors. At the stations downstream of the DHC, the values are significantly lower compared to previous period, thus, at Mogilev-Podolsky the average value of suspended sediments is 2.8 kg/s and at Grushka 19.6 kg/s, the decrease being 92-98% (Figure 55).

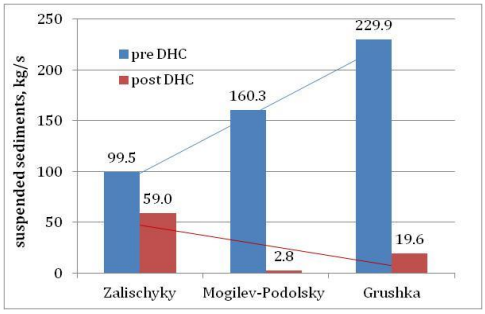

Figure 55. Suspended sediments.

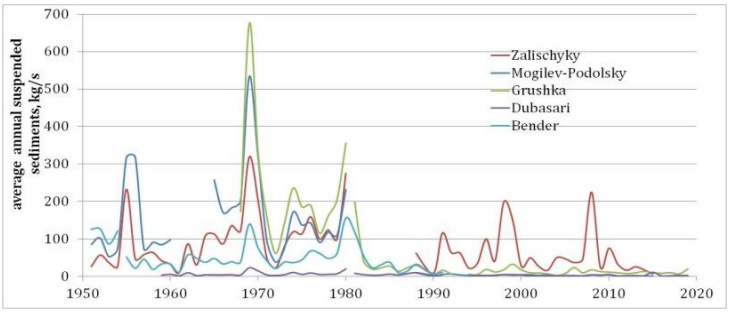

Figure 56. Average annual suspended sediments.

On monthly level, in river natural regime (at Zalischyky), most of the sediments volume is formed during spring and pluvial floods occurrence (Figure 57). Thus, the biggest amounts of sediments are observed in March-April and June-July, respectively, when large volumes of water are generated and propagated through the floodplain. Post-DHC, at Zalischyky, suspended sediment decreased by approx. 40-50% in the spring-summer months, the largest decrease being specific to February. Small increases of this element are observed for autumn months. This is caused by natural conditions of flow generation, without any reservoirs influence.

Spatially, during the pre-DHC period, there is a continuous increase of suspended sediments in the Zalischyky - Grushka sector, being by 2 - 2.8 times higher for April, June, July, November, and by 3-4 times higher for September and October, in the other months the increases being smaller (Figure 57).

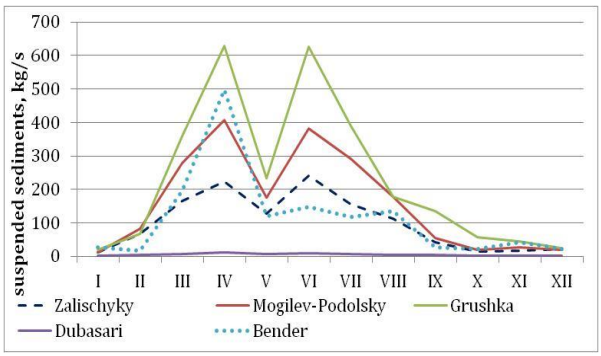

Figure 57. Monthly suspended sediments before the construction of HPP-1.

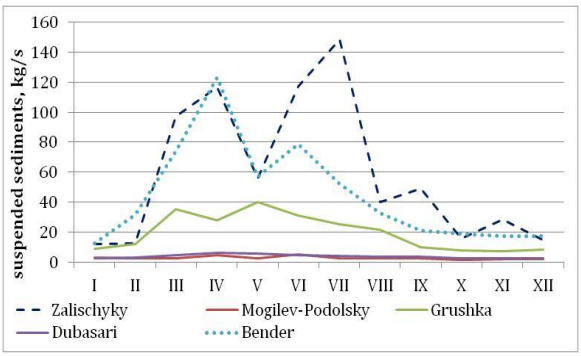

Figure 58. Monthly suspended sediments after the construction of HPP-1 and Dubasari HPP.

Post-DHC, there is a decrease of suspended sediments, due to their retention in reservoir with HPP-1. Significant decrease in sediment volumes is specific for all months of the year, so the average monthly values greater than 5 kg/s are not recorded at Mogilev-Podolsky. At Grushka, suspended sediments increase slightly, values being in limits of 7-10 kg/s in cold period and of 20-40 kg/s in warm period (Figure 58). However, these values are tens of times lower than those before the DHC construction. An increase in the suspended sediments load downstream of Mogilev-Podolsky can be observed, but the values are insignificant compared to sediments retained by reservoirs. Therefore, there is a high impact of the DHC on suspended sediments formed in the Dniester River. Also, high amounts of sediments are accumulated in the Dubasari reservoir, as seen from figure 58. Although a cumulative impact of the dams is observed, it can be noted that at the Bender station there is a certain reappearance of suspended sediments. It should be noted that analyzed data at Bender are those before 1954 (before Dubasari HPP), the length of time series being only for 1951-1954 and those for the post Dubasari reservoir construction until 1991, so the length of time series can influence the evaluation results.

5. CONCLUSIONS

Operation of the Dniester Hydropower Complex, constructed in the middle course of the Dniester River, on the territory of Ukraine, causes modification of river flow characteristics in its downstream part, region which mainly is positioned in the limits of the Republic of Moldova. This study provides detailed

investigations and arguments in order to prove the statement. As a result of performed analysis of the hydrological time series for two representative periods (before and after construction of the DHC) for the upstream and downstream stations, several conclusions were drawn and shown below.

The main impact caused by the DHC and its reservoirs construction is considered the **interruption of the longitudinal connectivity of the river**, which in turn limits the river upstream-downstream connection and modifies hydrological characteristics and other vital river components. Some of river flow elements are subject to major changes, while the others are less modified. In this regard, the main hydrological characteristics that are of great importance are **water flow and volumes**. **Annually**, for the two analyzed periods (before and after the DHC construction), these are approximately equal in the upstream part of the DHC, while in the downstream of the DHC, they decrease from 278 m^3/s to 252 m^3/s, and from 8.7 km^3 to 7.9 km^3 or by 0.8 km^3, which represents 9.2%. This tendency continues towards the Dniester River mouth where water volumes decrease by 1.5 km^3, i.e. by 15%. In terms of monthly flow, downstream the DHC, in conditions of controlled flow regime, it was noted **significant decrease** in February-April (February - 18%, March - 40%, April - 27%), and **increase** during the autumn months, by 10-14%. Thus, a decrease of flow is estimated for seasons with higher flows and an increase for the seasons characterized by lower flow (autumn and winter).

One of the main and very sensitive hydrological parameters for economy and society is **minimum flow**. Its analysis for the two time periods shows that in the second period in the upstream part of the DHC, the minimum flow increased by 52%, and in downstream has doubled reaching 107 m^3/s (compared to 51 m^3/s, before the DHC). Thus, the hydrotechnical complex has a positive impact on minimum flow and provide more water during droughts to the downstream part. With regard to the DHC Operation Rules and release of the minimum flow of 100 m^3/s as a threshold, it should be mentioned that the rule is respected: the share of days with lower flow values are 2%, minimum daily flows below mentioned value being occasionally observed. However, it was not proven that the rule is maintained with regard to instantaneous intraday flow.

In terms of maximum flow, which also represents a hazard for the population of the Dniester River basin, it is also subject to change in the downstream part due to DHC. In general, **maximum annual flows**, upstream the DHC, in the second period, has slightly increased compared to the first period, while in the downstream part, there is a reduction of this parameter by about 30% because of the DHC impact. This fact shows a reduction of flood risk, but in condition of climate change and increasing frequency and magnitude of natural hazards, flood regulation under DHC operation must be performed with high attention.

From the two flood phases of **spring flood** and **fluvial flood**, the first one is changed more under the impact of DHC operation. One of the aspects subject to change is the spring flood occurrence. In the downstream, DHC caused a delay of spring flood starting date by over 2 weeks in comparison with natural regime, while no major changes are observed in case of end date. Thus, spring flood duration is affected in terms of its decreasing in regulated regime by about 30% (in the upstream part the decrease is only 14%). Another important remark is the change of maximum flow. While in natural regime, this flow tended to increase in space by about 115-140 m^3/s, (pre DHC maximum average flow at the Zalischyky, Grushka, Bender was 1150 m^3/s, 1289 m^3/s, 1265 m^3/s), in post DHC time it decreases by 180-270 m^3/s (post DHC maximum average flow for three mentioned stations is already 988 m^3/s, 805 m^3/s and 716 m^3/s). The spring flood average volume for the two periods is generally decreasing. In the upstream part of the basin, it decreases by 10% to second studied time period, while in the downstream at Grushka station the decrease is 35% or 800 mil. m^3, and at Bender is 39% or 1.1 km^3. It should be mentioned that, in the downstream of DHC, an important role in spring flood dynamics plays so-called spring ecological flood, organized by water experts and released by DHC operators every year after its construction in order to provide sufficient water volumes for the Dniester riverbed to ensure reproduction of fish and stability of the Dniester ecosystems. Even if the spring ecological flood has noble purposes, its effectiveness is not yet clear, so in-depth studies are needed to optimize the process of evacuation and propagation of spring ecological flood through the Dniester River bed.

In conditions of **pluvial floods**, DHC operation mainly leads to modification of maximum flow by decreasing it by about 30% in the downstream part. Pluvial flood hydrograph is changed from triangle to trapezoid, thus causing a delay in the maximum flow by increasing the rising limb and decreasing the recession limb of the flood wave. No major shifts are observed in pluvial flood total duration as well as in flood wave propagation in longitudinal profile. However, the increase in the frequency of natural floods must lead to a serious preparation of the DHC for the management of these phenomena and protection of areas in the lower part against major floods.

One of the direct impacts of DHC operation is **hydropeaking effect**. Intraday level amplitude downstream of the DHC amounts to 52 cm (5 km downstream, Naslavcea post), the pulsating effect being

reduced by increasing distance form DHC. Thus, near Soroca, water level fluctuation reaches the values of 20 cm and near Sanatauca of 14 cm, the sector influenced by this effect being over 100 km. Thus, considered the described impact, the operation of HPP-2 turbines must be changed in a way as to significantly reduce hydropeaking effect to the downstream part;

Due to DHC operation along river sector is subject to **water thermal modifications.** While in the upstream part of the hydrotechnical complex, average annual water temperature has increased by 0.8°C, from 9.8°C to 10.6 °C in the second period, it has diminished by 0.43°C (from 10.29°C to 9.86 °C), in the downstream, in the close proximity of the DHC. In the lower sectors, water temperature is unchanged and only closer to river mouth, it increases with the same 0.8°C, like in the upstream, from 11.1°C to 11.92°C (Bender station). In these conditions, close to the DHC, at present, water temperature should be 11.1°C, but is 9.86°C, i.e. by 1.24°C lower. At monthly time scale, there is a decrease in the water temperature in the spring-summer time, and an increase in the autumn-winter time downstream of the DHC. Also, in the post-DHC time period, close to these hydrotechnical constructions, it is noted a maximum temperature shift from July-August to August-September, with values rising only to 17.5°C, or by 3.6°C lower than pre-DHC. In this regard, reconstruction of HPP-1 is absolutely needed in order to reduce the impact of water thermal fluctuations on the development of ecosystems and the local economy.

Other obvious impact of the DHC is the significant alteration of **sediment transport process.** Thus, suspended sediment loads decreased by 92-98% after DHC constructions. The significant decrease in sediment volumes is specific to all months of the year. The reduction of sediment transport led to the increase of the water transparency, favoring the development of the aquatic ecosystems.

In order to improve the hydrological state of the Dniester River, provide water supply to people and economy, optimize hydrological hazards regulation and mitigate the impact of the DHC on the downstream part of the river, it is of great importance to ensure integrated cooperative Moldovan-Ukrainian management of the basin, as well as a clear and transparent management and operation of the DHC.

ACKNOWLEDGMENT

The study on assessment of the impact of the Dniester Hydropower Complex on hydrological state of the Dniester River was performed within the project "The Dniester Hydro Power Complex Social and Environmental Impact Study" project that was implemented between September 2018 and December 2021 by the United Nations Development Programme in Moldova (UNDP Moldova), at the request of the Ministry of Environment of the Republic of Moldova, with the financial support of the Embassy of Sweden in the Republic of Moldova. Special acknowledgments refer to data providers: the State Hydrometeorological Service and State Water Agency from Moldova and Ukraine, Ministry of Environment of the Republic of Moldova, the Dniester Commission.

REFERENCES

1. International Hydropower Association. *Hydropower Status Report. Sector trends and insights. 2021* (2022), 27. P Retrieved from https://assets-global.website-files.com/5f749e4b9399c80b5e421384/60c2207c71746c499c0cd297_2021%20Hydropower%20Status%20Report%20-%20International%20Hydropower%20Association%20Reduced%20file%20size.pdf
2. Ritchie, H., Roser M., & Rosado P. (2020), *Energy.* Retrieved from https://ourworldindata.org/energy https://ourworldindata.org/renewable-energy#how-much-of-our-primary-energy-comes-from-renewables
3. Schwarz, U. (2019). *Hydropower pressure on European Rivers. The story in numbers*. Retrieved from https://wwfeu.awsassets.panda.org/downloads/hydropower_pressure_on_european_rivers_the_story_in_numbers_web.pdf
4. Grill, G., Lehner, B., Lumsdon, A. E., MacDonald, G. K., Zarfl, C., & Reidy Liermann, C. (2015). An index-based framework for assessing patterns and trends in river fragmentation and flow regulation by global dams at multiple scales. *Environmental Research Letters,* 10, 015001,
5. Hunt, J. D., Falchetta, G., Zakeri, B., Nascimento, A., Smith Schneider, P., Weber, N. A. B., Mesquita, A. L. A., Barbosa, P. S. F., de Castro, N. J. (2020). Hydropower impact on the river flow of a humid regional climate. *Climatic Change* 163, pp. 379–393, Retrieved from https://doi.org/10.1007/s10584-020-02828-w
6. Wang, Y., Zhang, N., Wang, D., Wu, J., & Zhang, X. (2018), Investigating the impacts of cascade hydropower development on the natural flow regime in the Yangtze River, China. *Science of the*

Total Environment, 624, pp. 1187–1194, Retrieved from https://doi.org/10.1016/j.scitotenv.2017.12.212
7. Peñas, F.J., Barquín, J., & Álvarez, C. (2016). Assessing hydrologic alteration: Evaluation of different alternatives according to data availability. *Ecological Indicators*, 60, 470–482. Retrieved from https://doi.org/10.1016/j.ecolind.2015.07.021
8. Richter, B., Baumgartner, J., Powell, J., & Braun, D. (1996). A method for assessing hydrologic alteration within ecosystems. *Conservation Biology*, *10*(4), pp. 1163–1174.
9. Richter, B., Baumgartner, J., Robert, W., & Braun, D. (1997) How much water does a river need? *Freshwater Biology, 37*(1), pp. 231–249.
10. Richter, B. D., & Thomas, G. A. (2007). Restoring environmental flows by modifying dam operations. *Ecology and Society*, *12*(1). Retrieved from http://www.ecologyandsociety.org/vol12/iss1/art12/
11. Jiang, L., Ban, X., Wang, X., & Cai, X. (2014). Assessment of Hydrologic Alterations caused by the Three Gorges dam in the middle and lower reaches of Yangtze river, China. *Water,* 6(5), pp. 1419–1434.
12. Pfeiffer, M., & Ionita, M. (2017). Assessment of Hydrologic Alterations in Elbe and Rhine Rivers, Germany, *Water,* 9(9), 684. Retrieved from https://www.mdpi.com/2073-4441/9/9/684/htm
13. Jumani, S., Deitch, M. J., Kaplan, D., Anderson, E. P., Krishnaswamy, J., Lecours, V., & Whiles, M. R. (2020). River fragmentation and flow alteration metrics: a review of methods and directions for future research. *Environmental Research Letters, 15*(12), 123009. Retrieved from https://doi.org/10.1088/1748-9326/abcb37
14. Masaki, Y., Hanasaki, N., Biemans, H., Müller Schmied, H., Tang, Q., Wada, Y., Gosling, S. N., Takahashi, K., & Hijioka, Y. (2017). Intercomparison of global river discharge simulations focusing on dam operation-multiple models analysis in two case-study river basins, Missouri–Mississippi and Green–Colorado, *Environmental Research Letters, 12*(5), 055002. Retrieved from https://doi.org/10.1088/1748-9326/aa57a8
15. Auer, S., Zeiringer, B., Führer, S., Tonolla, D., & Schmutz, S. (2017). Effects of river bank heterogeneity and time of day on drift and stranding of juvenile European grayling (Thymallus thymallus L.) caused by hydropeaking. *Science of the Total Environment, 575*, pp. 1515–1521. Retrieved from https://doi.org/10.1016/j.scitotenv.2016.10.029
16. Halleraker, J.H., Salveit, S.J., Harby, A, Arnekleiv, J.V., Fjeldstad, H.-P., & Kohler, B. (2003). Factors influencing stranding of wild juvenile brown trout (Salmo trutta) during rapid and frequent flow decreases in an artificial stream. *River Research and Application*, *19*(5-6), pp. 589–603. Retrieved from https://doi.org/10.1002/rra.752
17. Greimel, F., Schülting, L., Graf, W., Bondar-Kunze, E., Auer, S., Zeiringer, B., & Hauer, C. (2018). Hydropeaking Impacts and Mitigation. In Schmutz, S., Sendzimir, J. (eds) *Riverine Ecosystem Management.* Aquatic Ecology Series, 8, pp. 91–110. Springer, Cham. Retrieved from https://doi.org/10.1007/978-3-319-73250-3_5
18. Šilinis, L., Punys, P., Radzevičius, A., Kasiulis, E., Dumbrauskas, A., & Jurevičius, L. (2020). An Assessment of Hydropeaking Metrics of a Large-Sized Hydropower Plant Operating in a Lowland River, Lithuania. *Water, 12*(5), 1404. Retrieved from http://dx.doi.org/10.3390/w12051404
19. Bacal, P., Burduja, D., Cazanteva, O., Cojocari, A, Corobov, R., Donica, A., Filipenco, S., Jeleapov, A., Lozan, A., Melian, R., Miron, V., Purcic, V., Railean, V., Sirodoev, G., Talpa, N., Trombitsky, I., Zaharia, F., Zlate-Podani, & I., Chilaru, N. (2021). *Dniester Hydro Power complex social and environmental impact study. Non-technical summary*, Ministry of Environment, United Nations Development Program in Moldova, Chisinau. Retrieved from https://www.undp.org/moldova/publications/dniester-hydropower-complex-social-and-environmental-impact-study-non-technical-summary
20. UNDP - OSCE - UNECE (2019). *Analysis of the effects of Dniester reservoirs on the state of the Dniester river*. Vienna – Geneva – Kyiv – Chisinau. Retrieved from https://zoinet.org/wp-content/uploads/2019/12/Dniester-hydropower-effects-EN.pdf
21. Directive 2000/60/EC of the European Parliament and of the Council establishing a framework for the Community action in the field of water policy. *Official Journal of the European Communities* L327, 22.12.2000.
22. Zubcov, E. (2007). Influence of hydroconstruction on the ecological state of the Dniester River. *Akademos*, *2-3* (7), pp. 23-29 (in Russian)
23. Zubcov, E., Bagrin, N., Andreeva, N., Zubcov, N., & Borodin, N. (2019). Impact of hydropower construction on the Dniester flow of suspended solids. In *Hydropower impact on river ecosystem functioning. Proceedings of the International Conference,* Moldova, pp. 135–139. (in Russian)
24. Lebedenco, L., Nabokyn, M., Andreev, N., & Kovalyshyna, S. (2021). The state of zooplankton communities in the lower Dniester area under the conditions of river regulation and actual climatic

changes. In *Proceedings of the 10th International Conference of Zoologists "Sustainable use and protection of animal world in the context of climate change",* pp. 57–66.
25. Zubcov, E., Zubcov, N., Ene, A., Bagrin, N., & Biletchi, L.. (2010). The dynamics of trace elements in Dniester river ecosystems. *Journal of Science and Arts, 2*(13), pp. 281–286.
26. Kovalyshyna, S., Chuzhekova, T., Grandova, M., Onishchenko, E., Zubcov, E., Ukrainskyy, V., Goncharov, O., et al. (2021). Ecological Conditions of the Lower Dniester and Some Indicators for Assessment of the Hydropower Impact. *Applied Sciences, 11*(21), 9900. Retrieved from http://dx.doi.org/10.3390/app11219900
27. Corobov, R., Trombitsky, I., Matygin, A., & Onishchenko, E. (2021). Hydropower impact on the Dniester river streamflow. *Environmental Earth Sciences,* 80: 153. Retrieved from https://doi.org/10.1007/s12665-021-09431-x
28. Jeleapov, A.. (2019) Effect of reservoirs operation on the Dniester river flow regime. In *The 14th Edition of Present Environment and Sustainable Development International Symposium. Book of abstracts*, pp. 22–23.
29. Jeleapov, A. (2020). *Study of pluvial floods in the context of anthropogenic impact on the environment*. Chisinau: Impressum. (in Romanian)
30. Cazac, V., Mihailescu, C., Bejenaru, G., & Gilca G. (2007). *Water Resources of the Republic of Moldova. Surface waters.* Chişinău: Stiinta. (in Romanian)
31. Jeleapov, A., Melniciuc, O., & Bejan, I. (2014). Assessment of flood risk areas in the Dniester River basin (in the limits of the Republic of Moldova*)*. In Gh. Duca (Ed.), *Management of water quality in Moldova* (pp. 157–173). Cham, Switzerland: Springer International Publishing. Retrieved from https://www.springerprofessional.de/assessment-of-flood-risk-areas-in-the-dniester-river-basin-in-th/2043896
32. USGS, *SRTM, Sentinel* (2020) Retrieved from https://earthexplorer.usgs.gov
33. Google Earth (2019). Retrieved from https://earth.google.com/web/@23.74017362,12.61497184,-2609.32370094a,10919547.26230502d,35y,0h,0t,0r
34. *Operation rules of the Dniester hydropower complex* (1987). GIDROPROEKT. (in Russian)
35. *Operation rules of the Dniester reservoirs* (first redaction) (2011). UNIIVEP. (in Russian)
36. *Regulations to operate water reservoirs of the HPP and PSPP Dniester cascade with buffer storage reservoir normal headwater level 77.10 m*. Draft (2017). UKRGIDROENERGO.
37. *On approval of the Program of hydropower development for the period till 2026.* (2016). Order of the Cabinet of Ministers of Ukraine dated 13 July 2016 No. 552-p. Retrieved from http://d2ouvy59p0dg6k.cloudfront.net/downloads/program_of_hydropower_development_in_ua_till_2026.pdf
38. *List of pumped-storage hydroelectric power stations*. (2022). Retrieved from https://en.wikipedia.org/wiki/List_of_pumped-storage_hydroelectric_power_stations
39. *Operation rules of the Dubasari reservoir*, Chisinau, Republic of Moldova (1983). (in Russian)
40. The Nature Conservancy. (2009). *Indicators of Hydrologic Alteration Version 7.1 User's Manual*. Retrieved from https://www.conservationgateway.org/Documents/IHAV7.pdf
41. Actual observation network stream gauge. (2022). Retrieved from http://nistru.meteo.gov.ua/en/autoposts_operational_data/
42. Hydrological database of the State Hydrometeorological Service of Moldova and Ukraine (2020).
43. Organization for Security and Co-operation in Europe. (2015). *Strategic Framework for Adaptation to Climate Change in the Dniester River Basin*. Retrieved from https://dniester-commission.com/wp-content/uploads/2019/09/Dniester_English_web-1-1.pdf
44. Organization for Security and Co-operation in Europe. (2019). *Transboundary diagnostic analysis of the Dniester river basin*. Retrieved from https://dniester-commission.com/en/news/the-transboundary-diagnostic-analysis-for-the-dniester-river-basin-issued/

Central European Journal of Geography and Sustainable Development
ISSN 2668-4322, ISSN-L 2668-4322
2022, Volume 4, Issue 2, Pages: 50-63
https://doi.org/10.47246/CEJGSD.2022.4.2.3

Does flooding undermine the management capacities of the COVID-19 pandemic? A study of Lagos State, Nigeria

Christopher Ihinegbu [1,*], Bashiru Turay [1], Sampson Akwafuo[2]

[1] United Nations University – Institute for Environment and Human Security; University of Bonn, Department of Geography, 53115 Bonn, Germany;
[2] Department of Computer Science, California State University, Fullerton, United States;
ihinegbu@gmail.com (C.I.); bashiruturay19@gmail.com (B.T.); sakwafuo@fullerton.edu (S.A.)

Received: 18 July 2022; Revised: 20 October 2022; Accepted: 24 October 2022; Published online: 31 October 2022

Abstract: Given the dynamics of climate events (hazards) and their linkages to human health, it is imperative to continuallly check the impacts of these events on the public health system. While efforts have been made to understand fluvial flood and COVID-19 vulnerability and impacts, substantial gaps about impacts of their simultaneous occurrence on densely-populated communities abound. This paper presents an assessement of the occurrence of fluvial flooding and its potential to undermine the management of the COVID-19 pandemic in Lagos State, Nigeria. This study applied the indicator-based risk assessment method to determine the pattern of COVID-19 risk in the study area. Flood hazard and health facilities datasets of Lagos State were also used to determine the flood extent and pattern of flood-exposed health facilities in ArcGIS 10.7.1. Results revealed that Apapa, Eti Osa, Ibeju Lekki, Mushin, and Lagos Mainland local government areas (LGAs) were at a very high risk of COVID-19. Results also highlight six LGAs that should be prioritized in managing COVID-19 due to the exposure of the majority of its health facilities to flood. Far-reaching recommendations on the need to prioritize these flood-exposed health facilities for COVID-19 risk reduction, humanitarian aid and prevention strategies is made. Also, future research in the study area should explore sustainable strategies to adapt to COVID-19 and flood events from an interdisciplinary perspective.

Key words: COVID-19 risk, fluvial flood, hazard, health infrastructures, Lagos State.

Citation: Ihinegbu, C., Turay, B., & Akwafuo, S. (2022). Does flooding undermine the management capacities of the COVID-19 pandemic? A study of Lagos State, Nigeria. *Central European Journal of Geography and Sustainable Development, 4*(2), 50–63. https://doi.org/10.47246/CEJGSD.2022.4.2.3

1. INTRODUCTION

In today's world of increasing unprecedented and extreme events, humans and the world remain connected as our actions continue to generate global impacts. These impacts range from triggering natural hazards, biodiversity degradation, pandemics, heatwaves, and the like [1]. These hazards, events, and disasters are not just connected, they can also compound or undermine the management capacities of the other, thus generating cascading impacts [1,2]. In this study, fluvial flooding (a climatic event) and its implication for COVID-19 pandemic management has been explored in Lagos State, Nigeria.

A fluvial flood happens when the water level in a body of water (such as a river, lake, and the like) rises and spills onto the banks, coasts, and nearby land. The rise in water levels could be caused by excessive rain, tectonic activity, or snowmelt [3]. Flood exposure refers to people and assets in floodplains. The average monthly rainfall in Lagos State (hereinafter called "Lagos"), Nigeria, exceeds 200 mm during the rainy season, often more extensive than the soil's infiltration capacity [4] and therefore, a leading cause making flooding the most popular and frequent hazard [5,6]. Fluvial floods (hereinafter called "flood or flooding") occur every year in Lagos [7], resulting in the loss of lives, livelihoods, and

* Corresponding author: ihinegbu@gmail.com

infrastructure costing millions of dollars [8,9]. Because of its coastal location and status as the country's commercial and most populated state, it is especially exposed to flood [10,11].

Events of flooding have had a significant direct impact on residents of Lagos due to the lack of pre-flood preparedness. Many Lagos inhabitants live in flood-prone areas because they are uninformed of the risk at the time, proximity to their workplace, or its inexpensiveness [12,13]. This is making the vulnerability to floods increase with the rate of urbanization [6] and [14]. Some of the devasting recent flood events in Lagos are that of July 2011, which killed roughly 25 people and forced 5393 people to flee their homes, resulting in a total loss of NGN 30 billion (USD 200 million) value of properties. The June 2012 flood, which poured 216 mm of rain in a single storm, caused havoc on infrastructure, took seven lives, and impacted locals' livelihoods [8]. The flooding on July 16, 2021, affected the entire Lagos, with a flood height that submerged cars and houses on the coastlines. The full account of the damage of this recent flood event is still being estimated [15].

On the other hand, Coronavirus disease (COVID-19), a global pandemic, recorded its first case in Nigeria on February 27, 2020, and this was recorded in Lagos [16–18]. As of April 8, 2022, the state has recorded 99,226 lab-confirmed cases, which is 41.3% of the total lab-confirmed cases in the 36 States of Nigeria [19]. Since the discovery of the deadly virus in the State, the State's government has been utilizing a combination of public health and social measures to prevent the spread of the virus [20,21]. These include the closure of schools, businesses, offices, and other public facilities [17,20]. Irany et al [22] modelled the impacts and outcomes of these closures. This disease and its control measures have worsened institutional adversities and underlying and persistent economic challenges [23]. Thus, the continuing COVID-19 outbreak primarily affecting Lagos [24,25] has combined with the existing consequences of floods, resulting in severe impacts.

Floods and COVID-19's catastrophic combined effects are not new or unique to Lagos. Researchers have revealed that many other places are also struggling to manage these two dangers. For instance, on July 4, 2020, flooding caused the deaths of 65 people in Kumamoto, Japan; 217 homes were damaged, and 458 were partially destroyed, resulting in a spike of 188 COVID-19 cases by the end of the month [26]. In July 2020, as the COVID-19 cases were slowing down, serious flood incidents in 27 provinces across central and southern China threatened people's lives and homes [27]. Despite being confronted with the two dangers between May and September 2020, residents in New York, U.S.A. were more worried about and adhered to the COVID-19 measures, but were less prepared and worried about flooding during that time, which caused different exposures and casualties between the pandemic and floods [28]. Like in Lagos, floods are wreaking havoc on most of Africa's coastal areas. Due to the people's lower economic and technological capabilities to adapt, combined with the COVID-19 repercussions, puts the population in these places in a dangerous situation [29].

From the foregoing, and at the time of this research, no study had investigated the double hazards of flood and COVID-19 in Lagos State. Studies investigating either of the two hazards did so without considering the implications flood may have for the coping and management capacities of COVID-19. In addition, the Intergovernmental Panel on Climate Change characterization of risks [30,31] has not been considered in studies exploring COVID-19 risk in Lagos. Such understanding is relevant and required for a comprehensive understanding of the underlying problems for better informed local policies and actions. To address this knowledge gap, this study assesses flood hazards amid the COVID-19 pandemic in Lagos State, Nigeria from a geospatial perspective. The guiding research questions are: (a) What is the spatial pattern of COVID-19 risk in Lagos? (b) What is the pattern of flood hazards in Lagos? and (c) what implication(s) does flooding have for the management capacity of COVID-19 in Lagos? This paper is organized as follows. The next session detailed the conceptual framework and the methods employed. They are followed by a presentation of key results. Following the results is a discussion of result implications. The last session concludes the paper with a take-home message and recommendations.

2. METHODS AND DATA

2.1. Study area

The study area is Lagos State in Nigeria (Figure 1). It is a coastal state, the former capital of Nigeria, and is located between Latitude 6.520 N and Longitude 3.370 E. In terms of administration, the state has 20 Local Government Areas (LGAs), which are subsequently divided into 377 wards. It is Africa's most

populous city with an estimated population of 20 million people [32]. It is also the most industrialized of the 36 states in Nigeria and houses 60% of industries in the country [33,34]. The climate is tropical wet and dry with peak rainfall between April and November [34], and annual flood events between July and November [10,35]. Lagos State is the hub of COVID-19 cases in Nigeria. Figure 1 shows the administrative map of Lagos State.

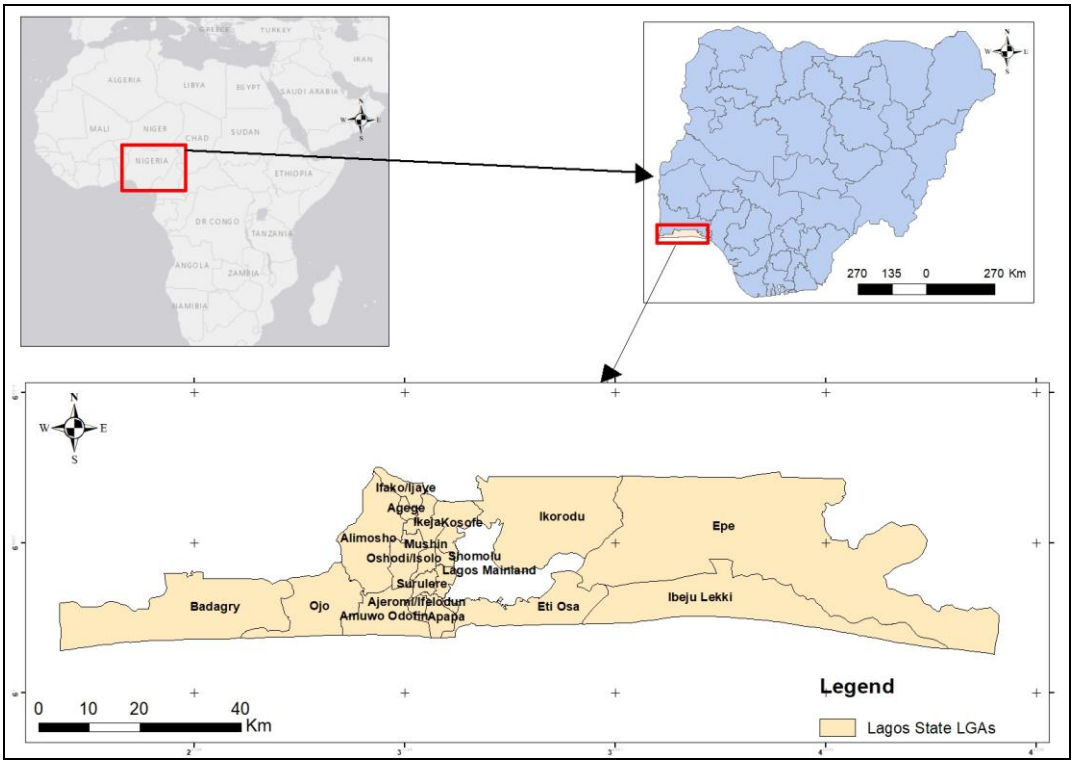

Figure 1. Showing Lagos state and its LGAs.
Source: The authors.

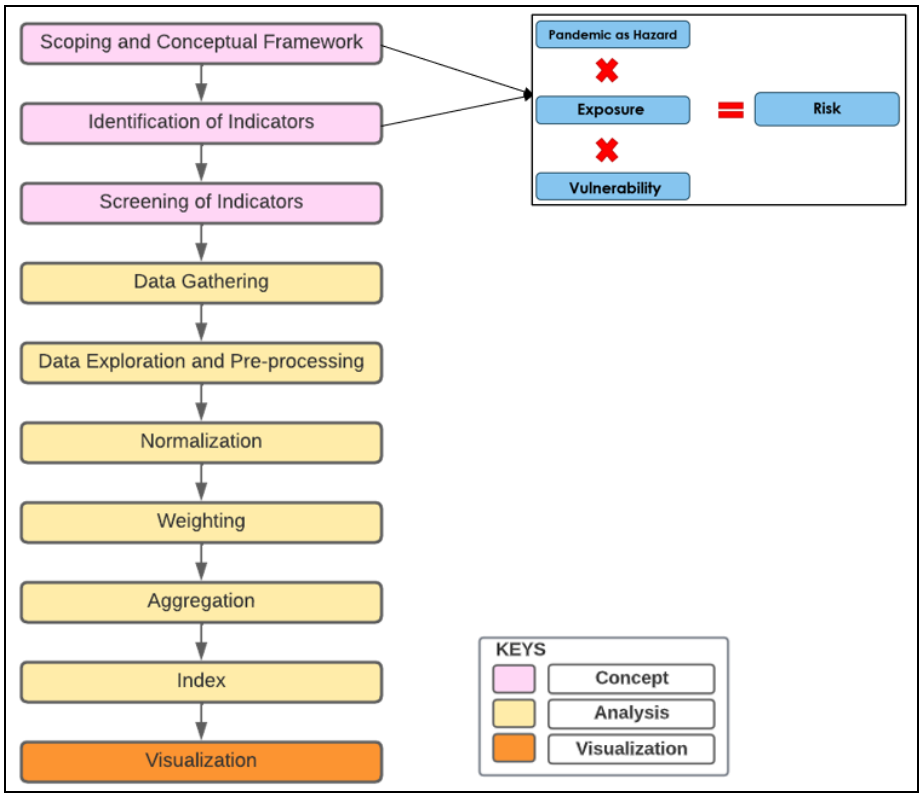

Figure 2. Workflow of methodology and conceptual framework for the COVID-19 risk index construction.
Source: Adapted from GIZ, 2017, OECD, 2008 and IPCC, 2014, 2019.

2.2.1. COVID-19 risk index construction

The first phase, which relates to the first research question (to assess the spatial pattern of COVID-19 risk), employed the indicator-based risk assessment workflow as adapted from [36] and [37] (Figure 2).

Scoping

This involves taking an exploratory lens from the literature on COVID-19 risk. A literature search on the Web of Science database yielded 25 relevant articles. The objective of this scoping was to narrow the topic of investigation to a manageable level that aligns with the existing body of knowledge. The scoping process was guided by the Intergovernmental Panel on Climate Change framing of risk, as explained in section 2.3 below [31] and the guiding questions were: (a) what are the exposed elements to COVID-19 risk? (b) what drives vulnerability and exposure to COVID-19 risk? and (c) what are the consequences of the COVID-19 risk? These guiding questions were also applied to fluvial floods; however, the focus was on COVID-19 risk. The answers to these questions as derived from the 25 reviewed articles gives first-hand information on the kinds of datasets explored in this study.

Table 1. Initial datasets for COVID-19 risk (from drivers to indicators).

S/N	Risk components	Drivers	Indicators	Definition	Format	Source
1	**Vulnerability**	Economic/ financial status	Socioeconomic vulnerability	This shows household socioeconomic status, income, and housing type	Shapefile	GRID3 Nigeria Geoportal (2021)
		Healthcare capacity/ access	Health facilities access	This shows accessibility to and usage of health facilities	Shapefile	GRID3 Nigeria Geoportal (2021)
		Pre-existing disease burden	Co-morbidities	This shows the general health condition of inhabitants	Shapefile	GRID3 Nigeria Geoportal (2021)
		Literacy	Literacy	This raster shows the number of literate people per cell grid	Raster (1 km)	WorldPop (2017)
		Awareness and negligence	Communication access	This shows the households accessibility to Television, radio and other media	Shapefile	GRID3 Nigeria Geoportal (2021)
		Aged population	Proportion of population ≥ 65	Proportion of the population ≥ 65 years per 1,000 inhabitants	Raster (1 km)	WorldPop (2020)
2	**Exposure**	Population, sanitation, housing condition	COVID-19 exposure	This shows population density, proximity to others in the household and access to water, sanitation, and hygiene	Shapefile	GRID3 Nigeria Geoportal (2021)
3	**Hazard**	COVID-19 cases as hazard	Proportion of COVID-19 cases per 1000 population	This shows the number of COVID-19 cases per 1000 population	Excel	Nigeria Center for Disease Control (2021)

Data (gathering, screening, and pre-processing)

The initial datasets for this study (COVID-19 risk) were suggested by the scoping process. That is, from drivers (emanating from literature review) to indicators (real datasets). This process yielded eight initial datasets for COVID-19 risk (Table 1). The scale of analysis of this study is the LGA level as all the datasets were available at this level for Lagos State. Tables 1 show the datasets emanating from the scoping process.

The above datasets in Table 1 were explored and pre-processed. Strikingly, none of the datasets had missing data. Also, to avoid data redundancy and show exceptional vulnerabilities, no outlier was treated. To avoid double-counting of the COVID-19 vulnerability indicators, a Pearson correlation was conducted to test for multicollinearities (Table 2). This process led to the exclusion of communication access data from the COVID-19 vulnerability datasets. This is because access to television, radio, and other communication media (as depicted by communication access data) is strongly dependent on people's financial status.

Table 2. Multicollinearity test (Pearson Correlation) for COVID-19 vulnerability datasets.

Correlations		nga_commun	HFA	SocecoV	Commorb	ABV65prop	LITERACY
nga_commun	Pearson Correlation	1	.179	.857**	-.046	.568**	-.499*
	Sig. (2-tailed)		.450	.000	.846	.009	.025
	N	20	20	20	20	20	20
HFA	Pearson Correlation	.179	1	.309	.263	.106	-.034
	Sig. (2-tailed)	.450		.185	.263	.655	.888
	N	20	20	20	20	20	20
SocecoV	Pearson Correlation	.857**	.309	1	-.020	.392	-.706**
	Sig. (2-tailed)	.000	.185		.933	.088	.001
	N	20	20	20	20	20	20
Commorb	Pearson Correlation	-.046	.263	-.020	1	-.372	-.069
	Sig. (2-tailed)	.846	.263	.933		.107	.773
	N	20	20	20	20	20	20
ABV65prop	Pearson Correlation	.568**	.106	.392	-.372	1	.198
	Sig. (2-tailed)	.009	.655	.088	.107		.402
	N	20	20	20	20	20	20
LITERACY	Pearson Correlation	-.499*	-.034	-.706**	-.069	.198	1
	Sig. (2-tailed)	.025	.888	.001	.773	.402	
	N	20	20	20	20	20	20

**. Correlation is significant at the 0.01 level (2-tailed).

*. Correlation is significant at the 0.05 level (2-tailed).

Index construction

This sub-section explains the steps involved in constructing the COVID-19 risk index. This includes data normalization, weighting, and aggregation.

Normalization

This was done by applying the [37] and [38] Linear min-max methods. This method transforms the variables into a range of 0 – 1 and is useful in showing exceptional vulnerabilities among the 20 LGAs. Mathematically, it is represented as:

$$V_n = \frac{(v_i - v_{min})}{(v_{max} - v_{\min})} \quad (1)$$

where v_i is the individual data point to be transformed, v_{min} is the lowest value of that indicator, v_{max} is the highest value for that indicator and v_n is the transformed value (new value). All datasets for COVID-19 risk were normalized using this method.

Weighting

Weighting assigns coefficients to the score of the indicators, thus rebalancing their importance to the final index. There are no universal rules for assigning weight [39]. While authors like [40] applied equal weighting, others like [39] applied a weighting system that suited their needs. For this paper, weighting was employed to aggregate the five COVID-19 normalized vulnerability indicators into one COVID-19 vulnerability index. For this purpose, the average weights from literature and experts (participatory weights) were employed. The literature scores (which ranges from 1-5) was assigned by the authors and they represent the importance of the various indicators in contributing to COVID-19 vulnerability (with 1 representing the least important and 5 implying the most important) as was deduced from the reviewed literature. As seen in Table 3, socioeconomic vulnerability is considered by various authors to be most important while other indicators were more or less seen to be of equal importance. The expert scores (ranging from 1-5) emanate from the conducted expert consultation and they represent the importance of the various indicators in contributing to the COVID-19 vulnerability. Three experts, which were accessible and relevant to this study were consulted: a public health professional, an Assistant Professor of medical geography and a development professional. They ranked the indicators in this order: socioeconomic vulnerability, health facility access, comorbidities, literacy and aged population (depicting the most important to least important indicator) (Table 3). The method is justified because the reviewed literature did not consider local peculiarities and the expert list is not very comprehensive. Hence, the average weight emanating from both complement each other. Table 3 shows the weights assigned to the COVID-19 vulnerability indicators.

Table 3. Weighting process applied to aggregate the COVID-19 vulnerability datasets.

Indicators	Literature scores	Expert scores	Literature weight	Expert weight	Average weight
Socioeconomic vulnerability	5	5	0.29	0.33	0.31
Health Facility access	3	4	0.17	0.26	0.22
Comorbodities	3	3	0.17	0.20	0.19
Aged population	3	1	0.17	0.07	0.13
Literacy	3	2	0.17	0.13	0.15
Total	**17**	**15**	**1**	**1**	**1**

Aggregation

Here, the normalized risk components of COVID-19 datasets (hazard, exposure and vulnerability) were combined into one metric, using [38] weighted linear aggregation method:

$$\sum_{i=1}^{n}(w_i * x_i) \quad (2)$$

where w_i is the weight of the index (i) and x_i is the value of the index (i). For the COVID-19 risk index construction, equal weights were assigned to the three risk components. This was done to reflect the IPCC [30,31] risk framework.

Index visualization

The COVID-19 vulnerability, exposure, hazard (representing COVID-19 cases) and risk of Lagos was visualized on maps designed in ArcGIS 10.7.1 environment.

2.2.2. Pattern of Flood Hazard and Flood-Exposed Health Facilities

The phase (second phase) relates to the second and third research questions: to assess the pattern of flood hazards and the implication for flood hazards on the management capacity of COVID-19. Here, flood hazard extent data, obtained from the UNEP Global Risk Data Platform, was entered and mapped in ArcGIS 10.7.1 environment. The description of the flood hazard data is presented in Table 4.

Also, the exposure of healthcare facilities to floods was examined from a geospatial perspective (by overlaying health facilities' shapefile on the flood hazard extent in ArcGIS 10.7.1 environment).

Thereafter, the proportion of flood-exposed health facilities in each LGA was compared with their COVID-19 risk levels, and their implications were discussed. Table 4 shows the description of the flood hazard and health facilities datasets.

Table 4. Datasets for flood hazards and health facilities.

S/N	Datasets	Indicators	Definition	Format	Source
1	Health facilities	Health infrastructures in the study area	This shows the locations of health facilities	Shapefile	GRID3 Nigeria Geoportal (2021)
2	Flood hazard	Flood hazard extent (100 years return period)	This shows the extent and depth of flood	Raster (1 km)	UNEP Global Risk Data Platform (2015)

2.3. Conceptual framework

This paper employed the Intergovernmental Panel on Climate Change – IPCC [30,31] risk framework, which conceptualized risk as a composite of hazard, vulnerability and exposure. The IPCC framework gave equal importance to the three risk components (hazards, vulnerability and exposure) and this is lacking in previous studies [41,42]. In the same vein, the IPCC allows for a more nuanced approach to risk by employing a multiple-lens perspective and deconstructing the natural disaster notion by giving equal importance to the risk components [31,43].

Risk, according to the [30,31] framework (Figure 2), is the potential of harmful consequences resulting from the combined interaction of hazards, exposure, and vulnerability. The hazard here is seen as the possibility of a natural or human-induced event to occur, that may cause loss of life, injury, health impacts, as well as other socioeconomic and environmental losses and damages [30]. Vulnerability is conceptualized as the attributes of a person or group of persons and their situation that influence their capacity to anticipate, cope with, resist and recover from the impacts of a hazard of natural, socio-natural, or anthropogenic origin (adapted from [44]). Exposure, a spatial concept, as adapted from [31], is the presence of people, ecosystem services and functions, livelihoods, and social, environmental, economic, and cultural assets and infrastructures in places that could be adversely affected by hazards of natural, socio-natural or anthropogenic origins.

This framework has been appraised by several authors. For example, [45] appraised this framework for its better contextualization of risk assessments. [46] argued that applying the framework reduces the predisposition of adverse impacts by reducing a system's sensitivity while building its capacity (vulnerability) to adjust from exposure to external stressors (hazards). However, [45] argued that the framework does not individually account for sensitivity and adaptive capacity and this might be a limiting factor for studies emphasizing differential vulnerability.

This framework (Figure 2) guided the scoping and theoretical framing.

3. RESULTS

This section presents the results of this paper.

3.1. COVID-19 risk pattern in Lagos State

This section presents the COVID-19 vulnerability, exposure, hazard, and overall risk in Lagos. This was visualized in four classes (representing low, moderate, high and very high conditions of what they depict) using the quantile classification method in ArcGIS 10.7.1.

Figure 4(b) shows that Badagry, Ibeju Lekki, Epe, Mushin, and Ajeromi LGAs are the most vulnerable (very high) to COVID-19. Ikorodu, Agege, Oshodi, Ojo, and Surulere LGAs are highly vulnerable (high); Amuwo Odofin, Apapa, Lagos Mainland, Shomolu, and Ifako are moderately vulnerable (moderate); while Alimosho, Ikeja, Kosofe, Eti Osa and Lagos Island are the least vulnerable (low) to COVID-19 in Lagos. As visualized in Figure 4(c), Apapa, Lagos Island, Eti Osa, Ibeju Lekki, and Ikorodu LGAs show very high exposure to COVID-19; Badagry, Ojo, Amuwo Odofin, Ajeromi, and Lagos Mainland LGAs shows high exposure; Oshodi, Ikeja, Shomolu, Kosofe, Mushin and Surulere LGAs shows moderate exposure; while Epe, Agege, Ifako, and Alimosho LGAs shows low exposure to COVID-19. As presented in Figure 4(d), Apapa, Eti Osa, Ibeju Lekki, Lagos Mainland, and Mushin have very high COVID-19 cases (or hazard); Ikeja, Kosofe, Shomolu, Amuwo Odofin, and Lagos Island have high COVID-19 cases; Epe, Ikorodu, Alimosho,

Oshodi, and Surulere have moderate cases; while Ojo, Badagry, Ifako, Agege, and Ajeromi have low COVID-19 cases.

Applying the IPCC framework [22,24], the result shows very high COVID-19 risk in Apapa, Eti Osa, Ibeju Lekki, Mushin, and Lagos Mainland LGAs; high COVID-19 risk in Ikorodu, Ikeja, Shomolu, Amuwo Odofin and Lagos Island LGAs; moderate COVID-19 risk in Oshodi, Surulere, Ajeromi, Kosofe and Badagry LGAs; and low COVID-19 risk in Ojo, Alimosho, Ifako, Agege and Epe LGAs. This is visualized in Figure 4 (a). Figures 4a-d show the pattern of COVID-19 risk, vulnerability, exposure, and hazard respectively in Lagos.

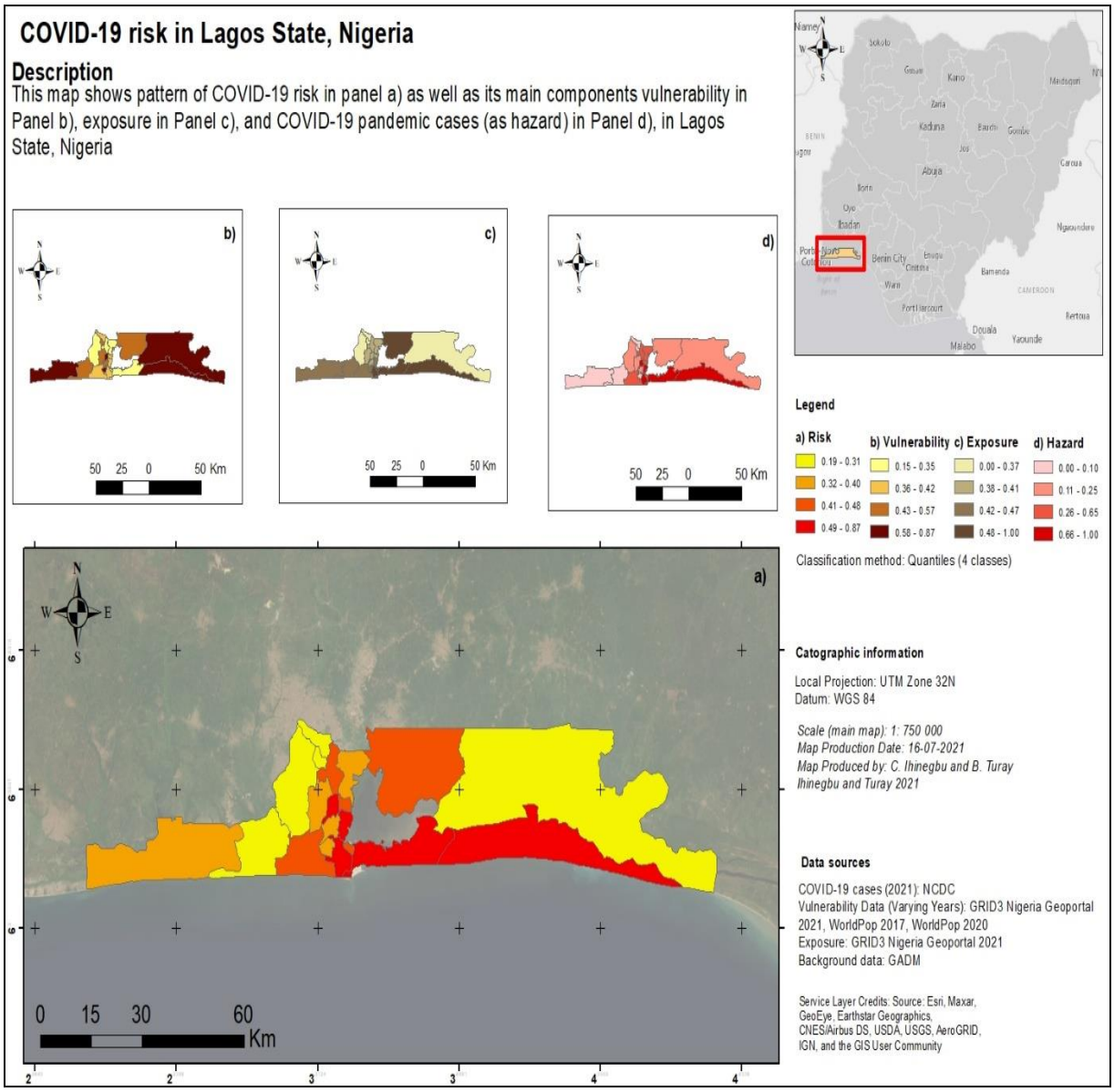

Figure 3. COVID-19 risk, vulnerability, exposure and hazard (cases) pattern in Lagos.
Source: Own processing.

3.2. Flood hazard, flood-exposed health facilities and COVID-19 risk in Lagos State

This section presents the pattern of flood hazards (Figure 5) and the exposure of health facilities to floods in Lagos. It also compares this pattern of flood exposure (of health facilities) with the COVID-19 risk in the state to identify LGAs whose healthcare systems may be overwhelmed or need emergency intervention during the flood peaks in Lagos. Figures 6(a) and 6(b) shows the distribution of health facilities and health facilities exposed to flood in Lagos respectively.

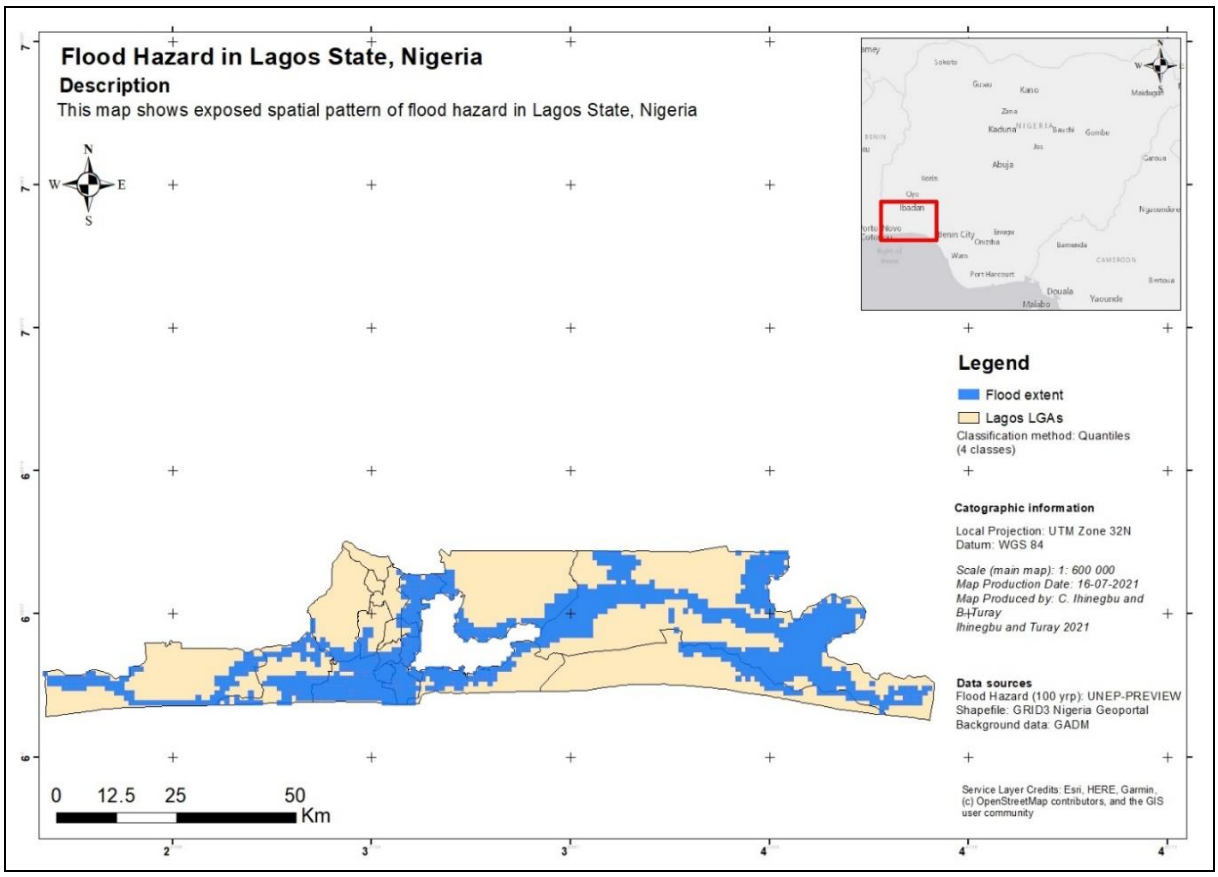

Figure 4. Pattern of Flood Hazard in Lagos State.
Source: Own processing.

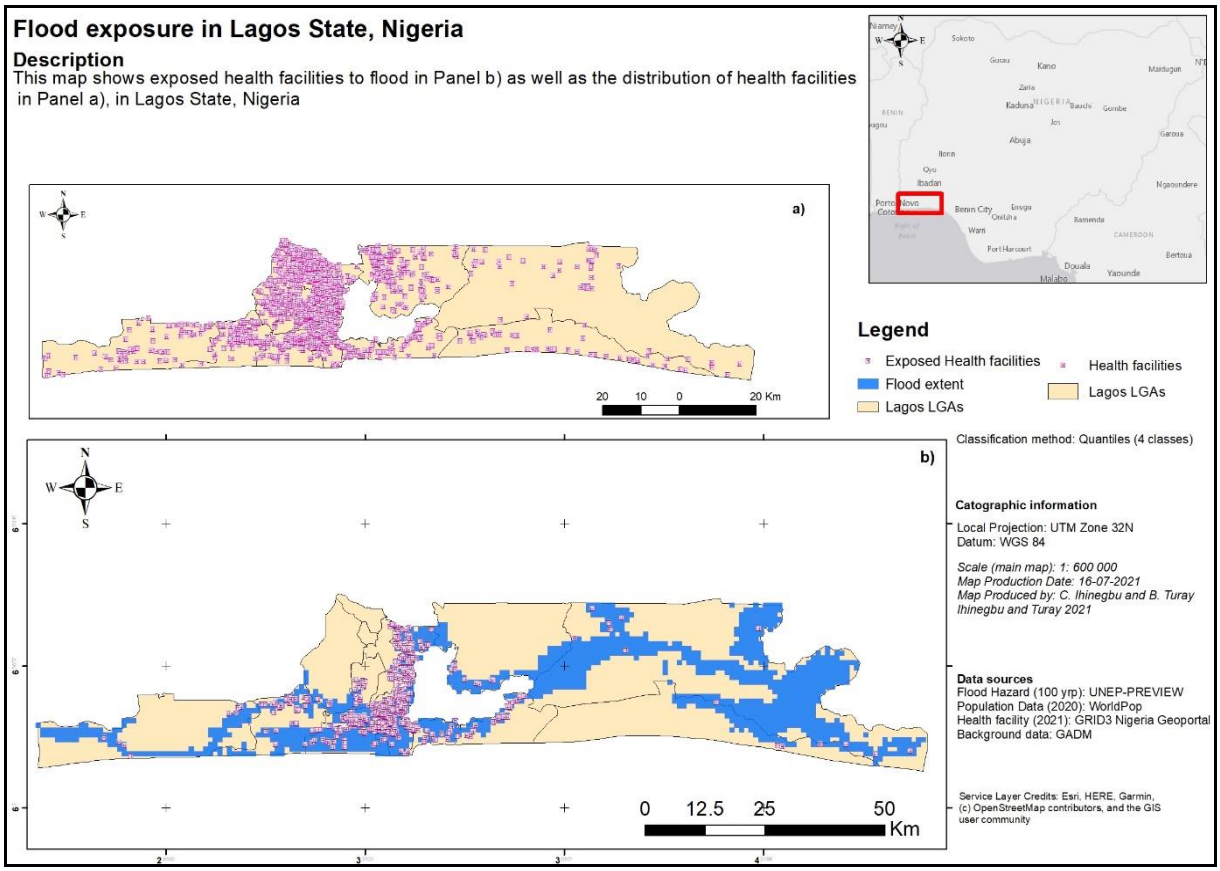

Figure 5. Pattern of health facilities and flood exposed health facilities in Lagos State.
Source: Own processing.

Table 5 compares COVID-19 risk and the pattern of flood-exposed health facilities (HF) in the LGAs and shows the LGAs whose health system may be overwhelmed due to flood exposure. This is important in managing COVID-19 risk in the state as it accounts for coping capacity (in this case, HF is a coping mechanism to fight COVID-19). Also, among the five LGAs with the highest COVID-19 risk index (Table 5), two (Apapa and Lagos mainland) LGAs are relatively at a higher risk because a high percentage of their health facilities are exposed to flood. The implication of this is that these LGAs should be prioritized in COVID-19 management decisions. Six LGAs that should be prioritized (among the 20 LGAs in Lagos) in managing COVID-19 include Apapa, Lagos Mainland, Amuwo Odofin, Lagos Island, Ajeromi and Kosofe. On the other hand, table 5 also revealed that some LGAs with very high COVID-19 risk levels (for example, Eti Osa, Ibeju Lekki and Mushin), may not be overwhelmed. This is because only a few proportions of their HF are exposed to flood.

Table 2. COVID-19 risk and flood-exposed health facilities in Lagos State.

S/N	LGAs	COVID-19 risk level	Total Health Facilities (HF)	Flood exposed HF	Percentage of flood exposed HF
1	Apapa	Very high	58	58	100
2	Eti Osa	Very high	92	53	58
3	Ibeju Lekki	Very high	51	4	8
4	Lagos Mainland	Very high	95	88	93
5	Mushin	Very high	121	15	12
6	Amuwo Odofin	High	102	90	88
7	Ikeja	High	163	6	4
8	Ikorodu	High	188	11	6
9	Lagos Island	High	61	58	95
10	Shomolu	High	79	61	77
11	Ajeromi	Moderate	80	80	100
12	Badagry	Moderate	85	8	9
13	Kosofe	Moderate	163	147	90
14	Oshodi	Moderate	189	23	12
15	Surulere	Moderate	176	92	52
16	Alimosho	Low	215	4	2
17	Agege	Low	80	-	-
18	Epe	Low	47	10	21
19	Ifako	Low	122	-	-
20	Ojo	Low	153	42	27

Key	
	LGAs with high exposure of HF to flood and should be prioritized in managing COVID-19

4. DISCUSSION

This study assessed fluvial flooding amid the COVID-19 pandemic in Lagos and revealed the hotspots of COVID-19 risk using the IPCC [30,31] lens. Our findings agree with scholars [44,47] that called for the shift from the hazard-focused narrative to a holistic one that accounts for vulnerability, exposure and hazard. The study went further to reveal LGAs whose health facilities may be overwhelmed due to their exposure to floods amid a pandemic. We argue that disaster risk reduction or assessment efforts should go beyond the hazard-exposure-vulnerability spectrum to include coping capacity (in our case study, health facilities) as people have differential shock-absorbing capacities [48,49].

Having a higher number of lab-confirmed COVID-19 cases is not immediately interpreted as being at risk unless this higher number of cases coincides with a socio-economic, medically vulnerable, and exposed population [31,50]. In this sense, the relatively higher population densities in Apapa, Osa, Ibeju Lekki, Mushin, and Lagos Mainland explain the higher possibility of person-to-person contact. Such a condition determines the exposure of individuals to the virus. When combined with the relatively higher number of over-60-year-old people, higher comorbidity, lower household income, poorer housing conditions, and other socioeconomic features, they put the population of the named LGAs at a very high risk of COVID-19, compared to the population of the other LGAs in the state [51,52]. These results are in agreement with our findings, as shown in Figures 3a-d.

The Lagos State Emergency Management Agency in 2021 identified Agege, Ifako Ijaye, Ikeja, Mushin, Oshodi, Ikorodu, and Epe LGAs to be at a relatively lower risk and exposure to flooding [53] and

this aligns with the findings of this study. The flood circumstances in Apapa, Lagos Mainland, Amuwo Odofin, Lagos Island, Ajeromi, and Kosofe, mainly due to their low-lying topographies and unplanned spaces, are exposing and endangering the inadequate healthcare equipment and buildings to harm, subjecting health personnel working in such facilities to increasing difficulties in managing the rising spread of the virus [53–57]. Similar to our findings, studies on flooding and health implications have previously shown the increased complications of dealing with healthcare emergencies amid flooding in the LGAs of Ajeromi-Ifelodun and Lagos Island [58,59].

As a limitation, it is acknowledged that the experts' list used in weighting the COVID-19 vulnerability indicators was not comprehensive and may be subjective. However, the literature opinion/scores were used to adjust for this limitation. This paper is relevant to urban sustainability research in Lagos as it assessed flood hazard (a climatic hazard) and its impact on a pandemic (in this case, undermining the potential of managing COVID-19), and by so doing, agrees that indeed, risk and hazards are sometimes interconnected [1,2].

Future research on this subject should look at whether households in the areas are preparing to adapt to future flood and COVID-19 conditions, or any other combined hazards of a similar nature, make recommendations and take practical actions following such investigations. Efforts should also be made to develop an LGA-specific flood evacuation and humanitarian response plan from a multi-disciplinary perspective.

5. CONCLUSSIONS

This study, which assesses flood hazard amid a COVID-19 pandemic, has revealed how floods may potentially undermine the management capacities of COVID-19, taking into account the exposure and vulnerability to COVID-19. Such knowledge is critical in understanding how flood hazards may impede COVID-19 management, particularly at this time when the State is struggling with both catastrophes. With the revelation of the hotspots of flood-exposed health facilities and the COVID-19 cases, this paper becomes critical and timely for disaster managers and humanitarian responders.

Following the results of this analysis, it is recommended that hotspots (for both flood-exposed health facilities and COVID-19) should be the major focus of humanitarian aid and Disaster Risk Reduction (DRR) strategies. Also, government policies should be geared toward addressing socio-economic vulnerabilities. Extreme efforts should be made to address flood hazards in the State. Healthcare infrastructure should be removed from highly flood-exposed areas where possible. If relocation to a less exposed terrain is not an option, they should be renovated or rebuilt to modern standards that are designed to minimize flood damage. Universal health and property insurance which is lacking in the state should be initiated and made affordable by the government to reduce the impacts of floods and disease outbreaks in the flood and COVID-19 hotspots (Table 5). These measures would contribute to achieving sustainable health and flood resilience in Lagos.

REFERENCES

1. O'Connor, J., Eberle, C., Cotti, D., Hagenlocher, M., Hassel, J., Janzen, S., Narvaez, L., Newsom, A., Ortiz-Vargas, A., Schuetze, S., Sebesvari, Z., Sett, D., & Walz, Y. (2021). Interconnected Disaster Risks. *United Nations University – Institute for Environment and Human Security (UNU-EHS)*. Retrieved from http://collections.unu.edu/view/UNU:8288
2. Simonovic, S. P., Kundzewicz, Z. W., & Wright, N. (2021). Floods and the COVID-19 pandemic—A new double hazard problem. *Wiley Interdisciplinary Reviews: Water*, *8*(2). Retrieved from https://doi.org/10.1002/wat2.1509
3. Zurich Insurance. (2020). Four common types of flood explained. *July 22, 2020*, pp. 1–5.
4. Whitworth Malcolm, N. U. (2015). Flooding and Flood Risk Reduction in Nigeria: Cardinal Gaps. *Journal of Geography and Natural Disasters*, *5*(1). Retrieved from https://doi.org/10.4172/2167-0587.1000136
5. Bako, A., & Ojolowo, S. (2021). Spatial knowledge and flood preparedness in Victoria Island, Lagos, Nigeria. *Jàmbá: Journal of Disaster Risk Studies, 13*(1), pp. 1-11. Retrieved from https://doi.org/10.4102/jamba.v13i1.825
6. Idowu, D., & Zhou, W. (2021). Land use and land cover change assessment in the context of flood hazard in Lagos State, Nigeria. *Water (Switzerland)*, *13*(8). Retrieved from https://doi.org/10.3390/W13081105

7. The Nigeria Hydrological Services Agency (NIHSA). (2021). *Flooding in Lagos.* Retrieved from https://nihsa.gov.ng/
8. Adelekan, I. O. (2014). Flood Risk Management By Public and Private Agents in the Coastal City of Lagos. *The 6th International Conference on Flood Management (ICFM6),* pp. 1–12. Retrieved from http://eventos.abrh.org.br/icfm6/proceedings/papers/PAP014805.pdf
9. Njoku, C., Efiong, J., Uzoezie, A., Okeniyi, F., & Alagbe, A. (2018). A GIS Multi-Criteria Evaluation for Flood Risk-Vulnerability Mapping of Ikom Local Government Area, Cross River State. *Journal of Geography, Environment and Earth Science International*, *15*(2), pp. 1–17. Retrieved from https://doi.org/10.9734/JGEESI/2018/40527
10. Oyebande, L. (1978). Urban water supply planning and management in Nigeria. *GeoJournal 2*(5), pp. 403–412. Retrieved from https://doi.org/10.1007/BF00156217
11. Adelekan, I. O. (2016). Flood risk management in the coastal city of Lagos, Nigeria. *Journal of Flood Risk Management 9*(3), pp. 255–264. Retrieved from https://doi.org/10.1111/jfr3.12179
12. Atufu, C. E., & Holt, C. P. (2018). Evaluating the impacts of flooding on the residents of Lagos, Nigeria. *WIT Transactions on the Built Environment, 184*, pp. 81–90. Retrieved from https://doi.org/10.2495/FRIAR180081
13. Dada, O. T., Ojo, D. B., Popoola, A. S., Adebara, T. M., & Oladele, B. G. (2021). Variability of sense of place in Nigerian coastal communities. *Geographical Research, 59*(3), pp. 452–464. Retrieved from https://doi.org/10.1111/1745-5871.12470
14. Oscar Higuera Roa, Jack O'Connor, Taiwo Seun Ogunwumi, Christopher Ihinegbu, Josefine Reimer Lynggaard, Zita Sebesvari, Eberle, C., & Margaret Koli. (2022). *Interconnected Disaster Risks- Lagos Floods*. Retrieved from https://interconnectedrisks.org/download
15. Princewill, N. (2021). *Lagos floods: Africa's most populous city could be unlivable in a few decades, experts warn - CNN.* Retrieved from https://edition.cnn.com/2021/08/01/africa/lagos-sinking-floods-climate-change-intl-cmd/index.html
16. Akinyemi, K. O., Fakorede, C. O., Anjorin, A. A. A., Abegunrin, R. O., Adunmo, O., Ajoseh, S. O., & Akinkunmi, F. M. (2020). Intrigues and Challenges Associated with COVID-19 Pandemic in Nigeria. *Health*, *12*(08), pp. 954–971. Retrieved from https://doi.org/10.4236/health.2020.128072
17. Alasoluyi, O. E. (2021). Teachers' Awareness and Competence in the Switch from Classroom-Based to Online Teaching During COVID-19 Pandemic in Lagos, Nigeria. *Interdisciplinary Journal of Education Research*, *3*(2), pp. 23–31. Retrieved from https://doi.org/10.51986/ijer-2021.vol3.02.03
18. NCDC- Diseases Fact Sheet. (2022). Nigeria Centre for Disease Control. *NCDC weekly report*, 1–2.
19. NCDC. (2022). NCDC Coronavirus COVID-19 Microsite. *Nigeria Center For Disease Control*, 1–1.
20. Ilori, A. (2020). Self-policing COVID-19 and civic responsibilities in Lagos Metropolis, Nigeria. *medRxiv*. Retrieved from https://doi.org/10.1101/2020.05.08.20092080
21. Ufua, D. E., Osabuohien, E., Ogbari, M. E., Falola, H. O., Okoh, E. E., & Lakhani, A. (2021). Re-Strategising Government Palliative Support Systems in Tackling the Challenges of COVID-19 Lockdown in Lagos State, Nigeria. *Global Journal of Flexible Systems Management*, *22*(S1), pp. 19–32. Retrieved from https://doi.org/10.1007/s40171-021-00263-z
22. Irany, F., Akwafuo, S., Abah, T., & Mikler, A. (2020). Estimating the Transmission Risk of COVID-19 in Nigeria: A Mathematical Modelling Approach. *Journal of Health Care and Research*, *1*(3), pp. 135–143. Retrieved from https://doi.org/10.36502/2020/hcr.6171
23. Mogaji, E. (2020). Impact of COVID-19 on transportation in Lagos, Nigeria. *Transportation Research Interdisciplinary Perspectives*, *6*. Retrieved from https://doi.org/10.1016/j.trip.2020.100154
24. Osikomaiya, B., Erinoso, O., Wright, K. O., Odusola, A. O., Thomas, B., Adeyemi, O., Bowale, A., Adejumo, O., Falana, A., Abdus-Salam, I., Ogboye, O., Osibogun, A., & Abayomi, A. (2021). 'Long COVID': persistent COVID-19 symptoms in survivors managed in Lagos State, Nigeria. *BMC Infectious Diseases*, *21*(1), Retrieved from https://doi.org/10.1186/s12879-020-05716-x
25. Abayomi, A., Osibogun, A., Kanma-Okafor, O., Idris, J., Bowale, A., Wright, O., Adebayo, B., Balogun, M., Ogboye, S., Adeseun, R., Abdus-Salam, I., Mutiu, B., Saka, B., Lajide, D., Yenyi, S., Agbolagorite, R., Onasanya, O., Erinosho, E., Obasanya, J., Adejumo, O., Adesola, S., Oshodi, Y., Akase, I. E., Ogunbiyi, S., Omosun, A., Erinoso, F., Abdur-Razzaq, H., Osa, N., & Akinroye, K. (2021). Morbidity and mortality outcomes of COVID-19 patients with and without hypertension in Lagos, Nigeria: a retrospective cohort study. *Global Health Research and Policy*, *6*(1). Retrieved from https://doi.org/10.1186/s41256-021-00210-6
26. Izumi, T., & Shaw, R. (2022). A multi-country comparative analysis of the impact of COVID-19 and natural hazards in India, Japan, the Philippines, and USA. *International Journal of Disaster Risk Reduction*. *Volume 73,* 102899. Retrieved from https://doi.org/10.1016/j.ijdrr.2022.102899

27. Guo, Y., Wu, Y., Wen, B., Huang, W., Ju, K., Gao, Y., & Li, S. (2020). Floods in China, COVID-19, and climate change. *The Lancet Planetary Health*, *4*(10), e443–e444. Retrieved from https://doi.org/10.1016/S2542-5196(20)30203-5
28. Zinda, J. A., Zhang, J., Williams, L. B., Kay, D. L., Alexander, S. M., & Zemaitis, L. (2022). Different Hazards, Different Responses: Assessments of Flooding and COVID-19 Risks among Upstate New York Residents. *Socius: Sociological Research for a Dynamic World*, *8*, pp. 1-20. Assessments of Flooding and COVID-19 Risks among Upstate New York Residents. Retrieved from https://doi.org/10.1177/23780231211069215
29. Turay, B. (2022). Flood hazard management in a multiple hazard context: a systematic review of flood hazard management during the COVID-19 pandemic in Africa. *Discover Water*, *2*(6). Retrieved from https://doi.org/10.1007/s43832-022-00014-w
30. IPCC. (2014). *Climate Change 2014: Synthesis Report. Contribution of Working Groups I, II and III to the Fifth Assessment Report of the Intergovernmental Panel on Climate Change*, Geneva, Switzerland.
31. IPCC. (2019). Climate Change and Land: an IPCC special report. *Climate Change and Land: an IPCC special report on climate change, desertification, land degradation, sustainable land management, food security, and greenhouse gas fluxes in terrestrial ecosystems*, pp. 1–864.
32. Nwafor, M. E., & Onya, O. V. (2021). Road transportation service in Nigeria: Problems and prospects. *Advance Journal Of Economics And Marketing Research*, *4*(3). Retrieved from http://iiasdpub.co.uk/ajemr/wp-content/uploads/2019/04/Nwafor-Michael-Ezaka-and-Onya-Ogwu-Victoria.pdf
33. Adejompo, F. (2014). Temporal Trends in Agglomeration Economies amongst Firms in the Lagos Region, Nigeria. *Ethiopian Journal of Environmental Studies and Management*, *7*(1). Retrieved from https://doi.org/10.4314/ejesm.v7i1.3
34. Ihinegbu, C., Nwosu, I., & Nnamchi, H. (2020). Residents' perception of the consequences of industrial activities in Ilupeju, Southwestern Nigeria. *Journal of Human Behavior in the Social Environment*, *30*(8), pp. 951–970. Retrieved from https://doi.org/10.1080/10911359.2020.1767012
35. Adelekan, I. O., & Asiyanbi, A. P. (2016). Flood risk perception in flood-affected communities in Lagos, Nigeria. *Natural Hazards*, *80*(1), pp. 445–469. Retrieved from https://doi.org/10.1007/s11069-015-1977-2
36. OECD. (2008). *Handbook on Constructing Composite Indicators: Methodology and User Guide*. OECD. Retrieved from https://doi.org/10.1787/9789264043466-en
37. GIZ. (2017). The Vulnerability Sourcebook Concept and guidelines for standardised vulnerability assessments, pp. 1–180.
38. Beccari, B. (2016). A comparative analysis of disaster risk, vulnerability and resilience composite indicators. *PLoS Currents*, *8* (Disasters). Retrieved from https://doi.org/10.1371/currents.dis.453df025e34b682e9737f95070f9b970
39. Sarkar, A., & Chouhan, P. (2021). COVID-19: District level vulnerability assessment in India. *Clinical Epidemiology and Global Health*, *9*, pp. 204–215. Retrieved from https://doi.org/10.1016/j.cegh.2020.08.017
40. Macharia, P. M., Joseph, N. K., & Okiro, E. A. (2020). A vulnerability index for COVID-19: spatial analysis at the subnational level in Kenya. *British medical journal global health*, *5*(e003014). Retrieved from https://doi.org/10.1136/bmjgh-2020-003014
41. Iyanda, A. E., Boakye, K. A., Lu, Y., & Oppong, J. R. (2022). Racial/Ethnic Heterogeneity and Rural-Urban Disparity of COVID-19 Case Fatality Ratio in the USA: a Negative Binomial and GIS-Based Analysis. *Journal of Racial and Ethnic Health Disparities*, *9*(2), pp. 708–721. https://doi.org/10.1007/s40615-021-01006-7
42. Osayomi, T., Adeleke, R., Taiwo, O. J., Gbadegesin, A. S., Fatayo, O. C., Akpoterai, L. E., Ayanda, J. T., Moyin-Jesu, J., & Isioye, A. (2021). Cross-national variations in COVID-19 outbreak in West Africa: Where does Nigeria stand in the pandemic? *Spatial Information Research*, *29*(4), pp. 535-543. Retrieved from https://doi.org/10.1007/S41324-020-00371-5
43. Kumar, P., Geneletti, D., & Nagendra, H. (2016). Spatial assessment of climate change vulnerability at city scale: A study in Bangalore, India. *Land Use Policy*, *58*, pp. 514–532. Retrieved from https://doi.org/10.1016/j.landusepol.2016.08.018
44. O'Keefe, P., Westgate, K., & Wisner, B. (1976). Taking the naturalness out of natural disasters. *Nature*, *260*(5552). Retrieved from https://doi.org/10.1038/260566A0
45. Sharma, J., & Ravindranath, N. H. (2019). Applying IPCC 2014 framework for hazard-specific vulnerability assessment under climate change. *Environmental Research Communications*, *1*(5), 051004. Retrieved from https://doi.org/10.1088/2515-7620/ab24ed

46. Crane, T. A., Delaney, A., Tamás, P. A., Chesterman, S., & Ericksen, P. (2017). A systematic review of local vulnerability to climate change in developing country agriculture. *WIREs Climate Change*, *8*(e464). Retrieved from https://doi.org/10.1002/wcc.464
47. Hewitt, K. (2019). *Interpretations of calamity: From the viewpoint of human ecology*. Retrieved from https://books.google.com/books?hl=en&lr=&id=vMyxDwAAQBAJ&oi=fnd&pg=PP1&dq=Hewitt+K+(1983)+The+idea+of+calamity+in+a+technocratic+age&ots=bNI34ptYro&sig=WoT435LiLbCneCIvaE5EssDeWVo
48. Birkmann, J., Cardona, O. D., Carreño, M. L., Barbat, A. H., Pelling, M., Schneiderbauer, S., Kienberger, S., Keiler, M., Alexander, D., Zeil, P., & Welle, T. (2013). Framing vulnerability, risk and societal responses: the MOVE framework. *Natural Hazards*, *67*(2), pp. 193–211. Retrieved from https://doi.org/10.1007/s11069-013-0558-5
49. Turner, B. L., Kasperson, R. E., Matson, P. A., McCarthy, J. J., Corell, R. W., Christensen, L., Eckley, N., Kasperson, J. X., Luers, A., Martello, M. L., Polsky, C., Pulsipher, A., & Schiller, A. (2003). A framework for vulnerability analysis in sustainability science. *Proceedings of the National Academy of Sciences*, *100*(14), pp. 8074–8079. Retrieved from https://doi.org/10.1073/pnas.1231335100
50. Abayomi, A., Balogun, M. R., Bankole, M., Banke-Thomas, A., Mutiu, B., Olawepo, J., Senjobi, M., Odukoya, O., Aladetuyi, L., Ejekam, C., Folarin, A., Emmanuel, M., Amodu, F., Ologun, A., Olusanya, A., Bakare, M., Alabi, A., Abdus-Salam, I., Erinosho, E., Bowale, A., Omilabu, S., Babatunde S., Osibogun, A., Wright, O., Idris, J., & Ogunsola, F. (2021). From Ebola to COVID-19: emergency preparedness and response plans and actions in Lagos, Nigeria. *Globalization and Health*, *17*(79). Retrieved from https://doi.org/10.1186/s12992-021-00728-x
51. Nigeria GeoPortal. (2020). Nigeria GeoPortal. Retrieved from https://nigeria.africageoportal.com/search?collection=Dataset
52. Otuonye, N. M., Olumade, T. J., Ojetunde, M. M., Holdbrooke, S. A., Ayoola, J. B., Nyam, I. Y., Iwalokun, B., Onwuamah, C., Uwandu, M., Abayomi, A., Osiboun, A., Bowale, A., Osikomaiya, B., Thomas, B., Mutiu, B., & Odunukwe, N. N. (2021). Clinical and Demographic Characteristics of COVID-19 patients in Lagos, Nigeria: A Descriptive Study. *Journal of the National Medical Association*, *113*(3), pp. 301–306. Retrieved from https://doi.org/10.1016/j.jnma.2020.11.011
53. LASEMA. (2021). Flood prone areas in Lagos - Nigeria Property finder. Retrieved from https://propertyfinder.com.ng/flood-prone-areas-in-lagos/
54. NIHSA. (2020). *Annual Flood Outlook.* Vol. 1, pp. 1–2.
55. NIMET. (2022). Nigerian meteorological agency (nimet). Retrieved from http://nimet.gov.ng/
56. Okediran, J. O., Ilesanmi, O. S., Fetuga, A. A., Onoh, I., Afolabi, A. A., Ogunbode, O., Olajide, L., Kwaghe, A. V., & Balogun, M. S. (2020). The experiences of healthcare workers during the Covid-19 crisis in lLagos, Nigeria: A qualitative study. *Germs 10*(4), pp. 356–366. Retrieved from https://doi.org/10.18683/germs.2020.1228
57. ThinkHazard. (2020). Think Hazard - Lagos - Urban flood. Retrieved from https://thinkhazard.org/en/report/2230-nigeria-lagos/UF
58. Adelekan, I. O. (2010). Vulnerability of poor urban coastal communities to flooding in Lagos, Nigeria. *Environment and Urbanization*, *22*(2), pp. 433–450. Retrieved from https://doi.org/10.1177/0956247810380141
59. Chioma, O. C., Chitakira, M., Olanrewaju, O. O., & Louw, E. 2019). Impacts of flood disasters in Nigeria: A critical evaluation of health implications and management. *Jàmbá: Journal of Disaster Risk Studies*, *11*(1). Retrieved from https://doi.org/10.4102/jamba.v11i1.557

Central European Journal of Geography and Sustainable Development
ISSN 2668-4322, ISSN-L 2668-4322

2022, Volume 4, Issue 2, Pages: 64-77
https://doi.org/10.47246/CEJGSD.2022.4.2.4

The relation between digitalization and regional development in Romania

Daniela Antonescu[1,*], Ioana Cristina Florescu[1], Victor Platon[1]

[1] Institute of National Economy, Romanian Academy, no.13, 13 September Street, 050711 Bucharest, Romania; daniela.antonescu25@gmail.com (D.A.); ioanaflorescu2001@yahoo.com (I.C.F.); victor.platon54@gmail.com (V.P.)

Received: 8 November 2022; Revised: 19 December 2022; Accepted: 22 December 2022;
Published online: 27 December 2022

Abstract: Digitalization is an essential element for the development of today's society, in the context of actual geo-political challenges. Moreover, the COVID-19 pandemic has accelerated the process of digitalization, offering new perspectives on sustainable and inclusive development. From the point of view of the regional approach, digitalization can have an important impact on the level of territorial development and on the reduction of economic and social inequalities. This paper proposes to identify the relationship between a series of indicators specific to digitization and regional GDP, with the help of panel models. The objective of the research is to estimate the relationship between GDP and two indicators specific to digitalization: online commerce and broadband internet infrastructure, the level of the eight development regions in Romania. Dependency modelling, based on econometric equations, offers the possibility of highlighting the way in which the two indicators of the digital economy contribute to the growth of GDP per capita. This analysis aims to illustrate the fact that broadband technologies and the increase in the number of people using the Internet for commercial purposes can have a positive impact on the growth of the regional economy. The results of the analysis highlighted the direct relationship of the indicators between the three variables related to the digitalization process at the level of Romania's regions and the strong influence of broadband internet and online trade on GDP per capita, proving that any growth among independent variables will lead to an increase amongst the dependent variables.

Key words: Digitalization, GDP, regional inequalities, Panel model, OLS model.

Citation: Antonescu, D., Florescu, I.C., & Platon, V. (2022). The relation between digitalization and regional development in Romania. *Central European Journal of Geography and Sustainable Development*, 4(2), 64–77. https://doi.org/10.47246/CEJGSD.2022.4.2.4

1. INTRODUCTION

Digital transformation is a complex process that helps to increase the quality of life and make services more efficient without which the economy could not function. For the digital technology to remain relevant, it must be used and to create added value.

In the context of the emergence of different crises (COVID-19 pandemic, geopolitical, climate, etc.), digitalization appears as an absolute necessity, supported by an intense R&D-innovation process (R-D-I). The health crisis has made digitalization a priority for businesses, public authorities, regions, States and nations. Advanced digital technologies have been associated with survival during lockdown, with firms that have invested in this area more likely to stay afloat.

Given the increasing importance of digitalization in a global economy that puts pressure on different territorial levels, this article aims to analyze the relationship between regional GDP and a number of indicators specific to digitalization, using panel regression models, trying to provide a global picture of how it is understood and approached at Community level and in Romania.

In order to achieve the objective set out in this article, the literature on digitization was consulted and a database with specific data was set up/processed at the level of the eight development regions (NUTS 2) of Romania, taken from official EU sources (Eurostat). The data processing was carried out on

[*] Corresponding author: daniela.antonescu25@gmail.com; Tel.: +40 766 295 926

the basis of econometric modeling, with the help of Eviews 9.5 software, which offers the opportunity to highlight how the selected indicators contributed to regional economic development.

2. LITERATURE REVIEW

At present, it can be said that there is no generally accepted definition of the concept of digital transformation, and terms such as digitalization, digital age or digital transformation are often used in an interchangeable way [1].

The digital transformation process involves the skills needed in order to use innovative new digital technologies to increase economic performance and improve/simplify people's lives. At the same time, quantifying the influence of digital technologies on economic development is one of the important concerns of scientific studies and analysis.

There is a direct relationship between digitalization and economic growth, analyzed in the literature and presented in Table 1.

Table 1. Digitalization - literature review.

Auhors	Year	Results
Andrey P. Hardy	1980	He analyzed the relationship between telephone services and economic development; the role of the telephone as a contributing agent to economic development has been investigated. The time series for 60 countries over a period of over 13 years were used to quantify how the phone contributed to economic development. Analysis of dynamics and cross-correlation techniques showed that the telephone has systematically contributed to economic development.
Gary Madden and Scott Savage	1998	The impact of investments in telecommunications infrastructure on economic growth has been assessed. The study's findings suggested that telecommunications infrastructure played an important role in economic development, with the causal link between nominal investment in telecommunications and GDP growth in both directions, which concluded that there was an interdependence between the two indicators.
Leonard Waverman and Kalyan Dasgupta	2005	Mobile telephony has been shown to have had a positive and significant impact on economic growth, especially in developing countries.
Herbert G. Thompson and Christopher Garbacz	2011	The Article builds the stochastic frontier based on the Cobb-Douglas production function, obtaining results related to the efficiency of using the digital potential in the analyzed countries.
Christine Zhen-Wei Qiang, Carlo Maria Rossotto and Kuniko Kimura	2009	The impact of fixed/mobile broadband on economic development was analyzed. Thus, it had been found an association between fixed broadband access and per capita GDP growth in both developed and developing countries.
Harald Gruber and Pantelis Koutroumpis	2010	The analysis was carried out for a group of 192 countries and revealed that investments in mobile telecommunications infrastructure have made a considerable contribution to economic growth and productivity.
Nina Czernich, Oliver Falck, Tobias Kretschmer and Ludger Woessmann	2011	The conclusions showed that a 10 percentage point increase in fixed broadband penetration results in annual GDP per capita growth of 0.9-1.5 percentage points.
Herbert G. Thompson and Christopher Garbacz	2011	There was a significant impact of mobile broadband on GDP per household based on the analysis of indicators in 43 countries between 2005 and 2009.
Neil Townsend and Chris Ahlfeldt	2017	Studies have shown that fixed broadband speed affected property prices in England between 2005-2010. It was found that disconnecting a common property from a first-generation high-speed broadband connection would depreciate its value by 2.8%.

A. Hikmaturokhman, K. Ramli, M. Suryanegara, A.A.P. Ratna, I.K. Rohman and M.A. Zaber	2022	The study shows a correlation between broadband speed and variables associated with quality of life. In addition, fixed broadband speed was found to be associated with better maths and English skills.
Harald Edquist	2022	Based on panel analysis of data from 116 countries between 2014 and 2019, the paper investigates the association between broadband internet speed and labor productivity. The authors identified a significant and robust relationship when a one-year gap is introduced for the series defining mobile broadband infrastructure. The interpretation of the results shows that a 10% increase in mobile broadband infrastructure in the period t-1 is associated with a 0.2% increase in labor productivity in the period t. The results are robust only for non-OECD and low-income countries.

Source: [2–9].

Internet connectivity has enabled businesses to access global markets, and through the openness of perspective it provides it helps to improve quality of life, working conditions, especially for small businesses and rural or marginalized communities.

Connectivity also plays an important role in increasing interest in investing or innovating complementary hardware and software technologies. The World Bank's digitalization Index shows that a 10 percentage point increase in its value has a 3% increase in the GDP ratio. This aspect is also supported by an analysis of 75 countries, which, on a subsequent update, showed that a 1% increase in fixed broadband penetration results in a 0.08% increase in GDP, while for the penetration of mobile broadband connectivity, a 1% increase translates into a 0.15% increase in GDP [10–12].

The analysis of the positive economic implications of online commerce clearly shows that there are a number of economic benefits: Increased efficiency, reduced costs (costs related to the search, administration and/or distribution of goods and services), price differences, etc. [13,14].

3. STUDY AREA – A BRIF ANALYSIS

In Romania, development regions are "areas which correspond to county groups, established by their voluntary association based on agreement signed by the representatives of county councils, as well as by those of the General Council of Bucharest; regions represent the framework of design, implementation and evaluation of regional development policies, as well as collection of specific statistical data, in accordance with European regulations issued by Eurostat for the second territorial classification level, NUTS II, existing within the EU" [15].

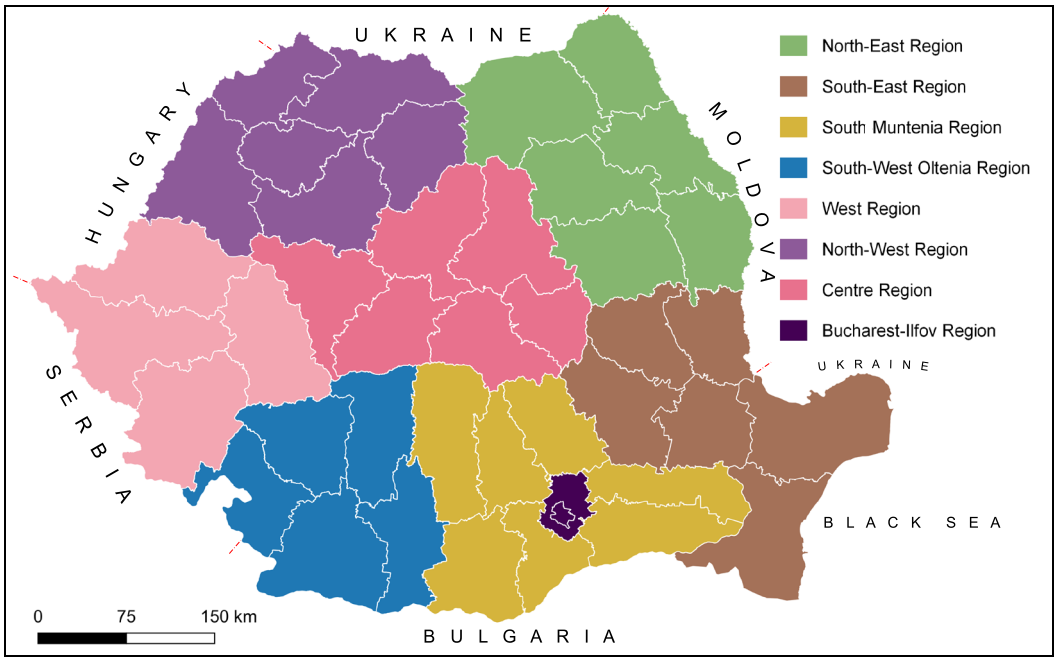

Figure 1. The development regions of Romania.
Source: Marin V.A., 2022

The regional policy in Romania is implemented by development regions, made up of counties formed by voluntary association based on a convention signed by the representatives of the county councils and of the General Council of the Bucharest Municipality, respectively.

The context of analysing is represented by the eight development regions (statistical regions) created after the accession to the European Union (in 2007) – Figure 1. These regions were established considering the potential functional integration criterion around some polarising centres (Iasi, Timisoara, Craiova, etc.), corresponding to the NUTS 2 system of the European Union. On setting-up the regions other criteria were taken into account as well, such as: resource complementarity, economic and social activities, functional links, etc. The eight development regions created in accordance with the Regional Development Law no. 151/1998 (amended by Law no. 315/2004). These regions were created taking into account the potential functional integration criterion, around some polarizing centers (Iasi, Timisoara, Craiova, etc.), having correspondence with NUTS 2 system of the European Union. When creating regions, it was also considered other criteria such as: criterion of complimentarily of resources, of economic and social activity, functional connection, etc.

The eight development regions created according to Regional Development Law no. 151/1998 (amended by Law 315/2004) are the following (Table 2).

Table 2. Development regions in Romania Eurostat Code.

Eurostate Code	Regions NUTS 2	Counties
RO11	North-West	Bihor, Bistriţa-Năsăud, Cluj, Maramureş, Sălaj, Satu-Mare
RO12	Center	Alba, Sibiu, Braşov, Covasna, Harghita, Mureş
RO21	North-East	Bacău, Botoşani, Iaşi, Neamţ, Suceava, Vaslui
RO22	South-East	Brăila, Buzău, Constanţa, Galaţi, Tulcea, Vrancea
RO31	South Muntenia	Argeş, Călăraşi, Dâmboviţa, Giurgiu, Ialomiţa, Prahova, Teleorman
RO32	Bucharest-Ilfov	Bucharest, Ilfov
RO41	South-West Oltenia	Dolj, Gorj, Mehedinţi, Olt, Vâlcea
RO42	West	Arad, Caraş-Severin, Hunedoara, Timiş

Source: Eurostat.

For next, we use the regional GDP (per capita) for the regional analysis regardin to the territorial development level. This indicator representing the basic criterion to establish both the contribution of the member-state to the community budget, and also the level of allocations from structural funds (the average GDP/capita, computed for a period of three years represents the criteria for establishing the eligible regions). In 2020, at regional level, the average value of GDP per capita were 21,937.5 euro/capita, 44.44% higher compared to 2014, but decreasing compared to 2019 (-1.07%) (Table 3).

Table 3. Dynamics of average GDP per capita at regional level, 2014-2020 (euro per capita).

	2014	2015	2016	2017	2018	2019	2020
GDP per capita	15,187.9	15,987.5	17,312.5	19,125	20,362.5	22,175	21,937.5

Source: Own processing.

The analysis by regions showed a maximum value of GDP per capita in the Bucharest-Ilfov region, of 49,200 euro per capita, and a minimum in the North-East region, of 13,600 euro per capita. In evolution, the largest increase was recorded by the South Muntenia region (+58.5%), followed by the North-West (+52.7%) and the North-East (+49.5%) (Table 4).

Table 4. Evolution of GDP per capita at regional level, 2010-2021 (euro per capita).

Regions/ Years	North-West	Center	North-East	South-East	South Muntenia	Bucharest-Ilfov	South-West Oltenia	West
2010	10,900	11,400	7,400	9,700	10,300	28,000	9,100	13,200
2011	11,000	11,800	7,500	9,900	9,900	28,800	9,300	13,700
2012	10,800	11,800	7,300	10,600	10,800	31,500	9,100	13,900
2013	12,200	13,400	8,800	12,000	10,700	32,700	10,600	14,800
2014	12,300	13,400	8,900	12,800	11,200	33,500	10,600	14,900
2015	13,100	13,700	9,100	13,300	12,500	34,200	10,600	15,000
2016	13,600	14,500	9,500	13,300	12,300	37,300	11,300	16,100

2017	15,200	16,000	10,300	14,100	13,500	39,400	12,100	17,900
2018	17,400	17,700	11,700	15,400	14,400	43,200	13,900	19,300
2019	18,300	19,000	12,500	16,500	15,500	45,300	15,400	20,400
2020	20,200	20,400	13,600	17,300	16,500	50,100	16,900	22,400
2021	20,000	20,100	*13,600*	17,200	16,400	*49,200*	16,800	22,200

Source: Own processing.

The development differences between regions are relatively large, with the coefficient of variation reaching 0.517%, when taking into account the Bucharest-Ilfov region (Table 5). In the situation without the Bucharest-Ilfov region, this coefficient is 0.160% (relatively constant in the analyzed period).

Table 5. Dynamics of Variation Coefficient - GDP per capita at regional level, 2014-2020 (%).

	2014	**2015**	**2016**	**2017**	**2018**	**2019**	**2020**
Var_Coeff_With Bucharest-Ilfov Region	0.520	0.553	0.533	0.524	0.509	0.524	0.517
Var_Coeff_Without Bucharest-Ilfov Region	0.160	0.167	0.178	0.166	0.158	0.163	0.160

Source: Own processing.

As result of analysing GDP/capita evolution a trend is given by more marked disparities between the eight regions NUTS-2, as result of increased economic concentration in areas regarded as attractive by population or investors, areas that can ensure a better living standard and activities with higher profitability.

Another important aspect analysed is the demographic one. Several times, the existence of a numerous population in a region can be an advantage, provided that it has the competences and skills necessary to an advanced society. In the period 2014–2022, the variation of the population at the level of the eight development regions registered a decreasing trend for 6 regions and increase for two regions (North-East and Bucharest-Ilfov). The region South Muntenia recorded a minimum rate (-6.47%) population, while the maximum growth was registered in the capital of country, Bucharest-Ilfov region (+6.81%) (Table 6).

Table 6. Dynamics of Variation Coefficient – Legally Resident Population at regional level, 2014-2022 (no, %).

Regions	**2014**	**2022**	**2022 vs. 2014 (%)**
North-West	2,837,677	2,807,762	-1.05
Center	2,638,500	2,602,817	-1.35
North-East	3,908,257	3,988,412	+2.05
South-East	2,892,498	2,756,531	-4.70
South Muntenia	3,289,404	3,076,503	-6.47
Bucharest-Ilfov	2,481,789	2,650,691	+6.81
South-West Oltenia	2,228,738	2,092,212	-6.13
West	2,022,867	1,967,793	-2.72

Source: Own processing.

With respect to classifying a region within the NUTS-2 category, the limits are given by the numbers of population: between 800,000 and 3 million inhabitants. These limits are not complied with and compliance failure occurred already on their set up in the year 1998 by all development regions from Romania which have values over the maximum one established by the EU. The regions with a population of over three million inhabitants (1998) were North-East (3.7 milion inhabitants) and South Muntenia (3.2 million inhabitants). Now, these regions register 3.99 milion inhabitants, respectively 3.1 milion inhabitants. Otherwise, the two regions and in particular the North-East region are on the last positions within the EU-27 in relation to GDP dimension.

Another important field taken into account on analysing of study area is the labour force employed population growth was negative for all regions (exception Bucharest-Ilfov), the maxim value was registerd in South Muntenia region (-13.5%) and minimum in Center region (-7%) (Table 7).

Table 7. Civil employment population at regional level (thous. Inhabitants).

Regions	2016	2017	2018	2019	2020	2021	2021 vs. 2016 (%)
North-West	1,168	1,179.8	1,182.6	1,193.1	1,187.4	1,065	-8.8
Center	1,036.2	1,045	1,051.8	1,055.9	1,048.4	963.9	-7.0
North-East	1,116.1	1,124.1	1,134.8	1,143.9	1,136,7	965.3	-13.5
South-East	9,45.2	949.6	949.4	956.2	947.8	837.4	-11.4
South-Muntenia	1,095.9	1,101.8	1,107.6	1,109	1,100.1	945.0	-13.8
Bucharest-Ilfov	1,360.3	1,368.7	1,373.1	1,425	1,420.9	1,416.6	4.1
South-West Oltenia	761.3	767.3	778.3	782.9	780.1	657.6	-13.6
West	834.6	830.5	829.9	826.6	819.4	749.4	-10.2

Source: Own processing.

The regional innovation degree characterized by the number of innovative enterprises is also in favour of the Bucharest-Ilfov region, which has a share of 43.03% from total 2,900 enterprise (2020), the last place being held by the region South-West Oltenia with only 2.3% from total. With respect to the regional evolutions, we presented the following conclusions: Bucharest-Ilfov region registered 10.54% on increase in 2020 as compared with the year 2014. Another regions registered decresee in number of innovative enetrprises: in South-East by about -82.32%; South Muntenia region 52.12% decrease as compared with the year 2014; the region with the lowest degree is the West region, -6.29% (Table 8).

Table 8. Innovative enterprises (no., %).

Regions	2014	2016	2018	2020	2020 vs. 2014 (%)	% of total (2020)
North-West	401	592	940	386	-3.74	13.3
Center	463	280	429	409	-11.66	14.1
North-East	444	424	436	357	-19.59	12.3
South-East	560	508	313	99	-82.32	3.4
South Muntenia	353	132	201	169	-52.12	5.8
Bucharest-Ilfov	1,129	714	1,691	1,248	10.54	43.0
South-West Oltenia	120	57	81	68	-43.33	2.3
West	175	218	107	164	-6.29	5.7
Total	3,645	2,925	4,198	2,900	-20.44	100.0

Source: Own processing.

4. DIGITALIZATION IN THE EUROPEAN UNION AND IN ROMANIA

4.1. Digitalization in EU-27

At the European Union level, digital transformation is one of the Community priorities opening up new opportunities for business and consumers, new horizons for networking with other economic areas worldwide, supporting the green transition and climate neutrality by 2050.

There is a specific policy addressed directly to digitalization, which funds actions and measures that support the acquisition of digital skills and training based on the digitization of services (public or private), while respecting the fundamental rights and values of its citizens. At the same time, the report on shaping *Europe's digital future* (2021) supports the integration of digital technologies in private companies and the implementation of digital services in public administrations, with a direct impact on quality of life [16].

Digital platforms, the Internet, cloud computing and artificial intelligence are among the technologies that influence many sectors, such as financial services, transport, energy, agri-food, telecommunications, industrial production, health, etc. Technologies can optimize production, help reduce greenhouse gas emissions and waste, increase competitive advantages and bring new services and products to the market.

Digitalization is a cross-cutting field, playing a key role in almost all EU policies, and the health crisis has emphasized its importance. Digital solutions have provided important opportunities, becoming essential in ensuring Europe's recovery and regaining a competitive position in the global economy.

Programs supporting investment, such as Horizon Europe (Research and Innovation) or the Connecting Europe Program (infrastructure), allocate considerable funds to digitization (Table 9).

Table 9. European Union Programs with a Digital component.

Program	Description
Digital Europe Program	Investments: €7.6 billion funds are allocated for: supercomputer production (€2.2 billion), artificial intelligence (€2.1 billion), cybersecurity (€1.6 billion), advanced digital skills (€577 million), use of digital technologies in society and the economy (€1.1 billion).
Online platform creation program	offers significant opportunities for markets, which are important communication channels
Cyber Security Program	Cybersecurity is becoming important for consumer online safety. In 2021, the Directive was adopted to ensure a high level of cybersecurity at EU level, and Parliament recently adopted rules for the new European Cybersecurity Center and the fight against the dissemination of terrorist content online.
Artificial Intelligence (AI)	Specific legislation must create a framework for action that inspires trust, introduces ethical standards, supports job creation, helps build competitive "AI made in Europe", and also influences the global standards.
Digital skills and Education Program	Aims to bridge the gap in IT knowledge and support the need for digital education.
Fair taxation of the digital economy	A global minimum tax rate and new tax rules are advancing to ensure fair taxation where surplus value is created through digital processes.

Source: [17].

The Recovery and Resilience Facility has been launched at EU level, which supports individual Member States' recovery plans (NRPs).

The Recovery and Resilience Mechanism is the main pillar of the NextGenerationEU program, with €723.8 billion in loans and grants available to support reforms and investments by EU countries. The aim of this mechanism is to support investments and key reforms in order to achieve sustainable recovery and to improve the economic and social resilience of EU Member States [18].

At the end of the investment period in 2027, European economies and societies will be better prepared for the challenges and opportunities resulting from green and digital transitions.

In the recovery mechanism, digitalization has an important place. In 2021, the European Commission presents the vision and prospects for Europe's digital transformation by 2030 with the so-called "compass for the digital dimension", which focuses on:

1. skills (increasing number of ICT specialists, increasing share of the population with digital skills, etc.);
2. digital transformation of enterprises (increasing the share of EU enterprises using cloud computing /AI/big data, increasing innovation, etc.);
3. digitalization of public services;
4. digital transition focused on the citizen.

In order to achieve the digital targets and objectives, the launch of large-scale multinational projects that no Member State could develop on its own will be accelerated and facilitated. These projects combine investments from the EU budget, including the Recovery and Resilience Mechanism, with those from the private sector. We mention here: Data infrastructure, low-power processors, 5G communications, high-performance computing, secure quantum communications, public administration, blockchain technology, digital innovation centers and digital skills. It is noted that for digital transformation, about 24.17% is allocated to the first pillar and 4.67% to the second [17] (Table 10).

Table 10. Analysis of digitalization in the context of the EU-27 Recovery and Resilience Facility.

Pillar	First pillar	Second pillar	Total
Green Transition	38.22%	11.67%	49.89%
Digital Transformation	24.17%	4.67%	28.84%
Smart growth, sustainable and inclusive	13.53%	35.92%	49.45%
Social and Territorial Cohesion	9.90%	33.07%	42.97%
Health	6.74%	10.61%	17.35%
Policy for the next generation	7.44%	4.06%	11.50%

Sursa: [17].

Moreover, the European Union promotes the people-centered *Digital Agenda*, guaranteeing the security and resilience of digital supply chains, based on viable solutions. The Digital Agenda will be implemented through regulatory cooperation, capacity and skills building, investments in international cooperation and research partnerships. Investments in the digital economy bring together Member States,

private companies, and other partners who share the same vision of digitalization. Potential areas of partnership are: Wi-Fi networks, 6G networks, quantum technologies, the use of technologies to combat climate change and environmental issues, etc. [17].

4.2. Digitalisation in Romania

In 2021, according to Eurostat data, Romania ranks 27 within the European Union in terms of the Digital economy and society Index (DESI) and the digitalization of public services (interaction with public authorities, obtaining information from public authorities' websites, downloading official forms, submitting completed forms, etc.) [18].

In terms of human capital in the field of digitalization, Romania ranks 26, obtaining a below average score on most indicators. Although Romania has a large number of ICT graduates (ranking 4 in this respect), the shortage of ICT specialists limits the country's ability to innovate and take advantage of the benefits of digital transformation [18].

As for the number of female ICT people, Romania ranks 3, and in terms of connectivity, some progress was made in 2021 in terms of fixed broadband coverage. However, the adoption of broadband has progressed at a slow pace. Romania ranks seventh in the EU regarding broadband internet use (at least 100 Mbps) [18]. Around 30-31% of people aged 16 to 74 have basic digital skills, below the EU average (56% in 2021) [18].

As for ICT specialists, Romania holds about half of the EU-27 average, namely 2.2% (2019), 2.3% (2020) and 2.4% (2021), compared to the EU-27 average of 4.3% (2021).

At institutional level, the Authority for the Digitalization of Romania (ADR) was established in 2020, being subordinated to the Ministry of Research, Innovation and Digitalization.

For the period 2021-2030, the Romanian Government has allocated EUR 100 [19].

The NRRP targets 64 reforms, 107 investments, 500 milestones and has an EU funding of 29.1 billion euros (14.2 billion euros in non-reimbursable funds and 14.9 billion euros in loans) [19].

The financial allocations through NRPP are as follows [19].

- 57.17% for the "green energy transition" (eliminating coal from energy production by 2032, reducing carbon emissions, subsidizing zero-emission vehicles, increasing energy efficiency in buildings).
- 20.64% for the digitalization of public administration (including id cards) and business environment, healthcare, education, improving connectivity and cyber security.

Within NRRP, the digitalization of enterprises plays an important role, being considered an important factor in increasing the competitiveness and innovation potential of both SMEs and large enterprises. The proposed investments in digitalization will support the digitalization of small and medium-sized enterprises and public administration, including citizens, subsequently contributing to increased competitiveness, fostering innovation in some areas and facilitating new working arrangements [19].

5. DIGITALIZATION AT REGIONAL LEVEL IN ROMANIA

5.1. Broadband infrastructure

Relevant data presented by a study developed by ANCOM (National Authority for Management and Regulation in Communications) shows that in Romania, there were 5.7 million fixed internet connections at the end of 2020 (+8% annual evolution), of which 4.5 million (80%) were very high-speed connections (over 100 Mbps) [18].

Driven by the health crisis, total fixed internet traffic recorded an exceptional growth in 2020 (+51%), with the average monthly fixed internet traffic per capita of 44 GB/month. Mobile internet traffic grew by 30%, lower than in previous years.

At the national level, on average, 7 in 10 households have a fixed internet connection, meaning 8 in 10 households in urban areas and 6 in 10 households in rural areas. This gap decreased during 2020, the growth rate of the number of connections in rural areas (+16%) being much higher than that in urban areas (+4%).

At the end of 2020 there were 20.4 million active mobile internet connections (+3%), two-thirds (13.6 million) being 4G or 5G connections (+13%), and the total mobile internet traffic increased by 30% compared to 2019, so the average traffic reached 4.9 GB/month/inhabitant.

Between 2010 and 2021, over three quarters of Romanian households (78.2%) had access to the home internet network (Figure 2). In urban areas, 84.8% of the households are connected to the internet, and in rural areas, 69.7% of the households.

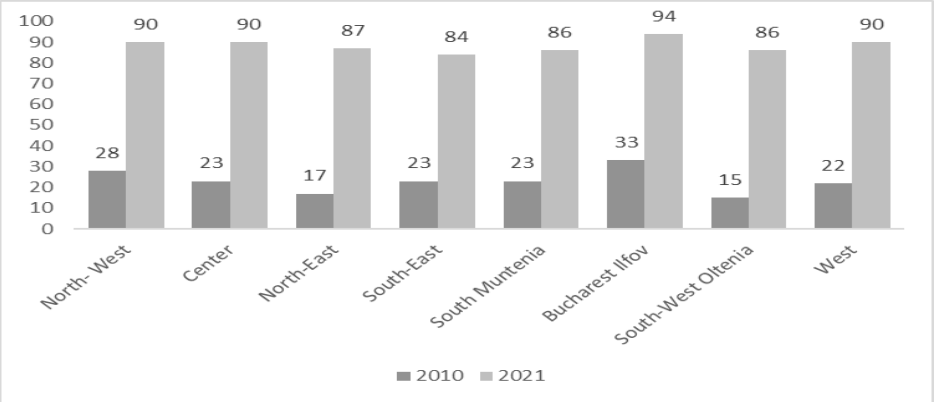

Figure 2. Comparison between the year 2010 and 2021 for the broadband infrastructure by development regions in Romania (% in total housing).
Source: Authors computations from Eurostat data.

At regional level, internet connection was more widespread among households in the Bucharest-Ilfov region (78.5% of the population), followed by the West (67.8%) and North-West (67%) regions. Regarding broadband internet connection, the situation at regional level is as follows: South-West Oltenia 61%, Center 60.8% and South Muntenia 60.3%. The lowest shares are recorded by the South-East (59.8%) and North-East (55.8%) regions.

The types of connections used to access the internet from home are 77.5% in favor of fixed broadband connections (fixed broadband connections), followed by mobile broadband connections (66.3%) and narrowband connections (13.6%).

Table 11. Broadband infrastructure by development regions in Romania in the period 2010-2021 (% in total housing).

Regions	2010	2011	2012	2013	2014	2015	2016	2017	2018	2019	2020	2021
North-West	28	31	51	61	60	70	72	80	87	85	89	90
Center	23	28	46	52	53	65	67	68	76	80	82	90
North-East	17	17	41	47	51	57	62	68	69	77	77	87
South-East	23	25	52	56	57	57	67	71	69	77	79	84
South Muntenia	23	35	48	50	51	61	65	70	74	79	82	86
Bucharest-Ilfov	33	54	71	78	79	80	88	88	94	91	92	94
South-West Oltenia	15	31	48	53	52	62	71	69	80	83	82	86
West	22	30	53	61	63	75	74	85	85	87	89	90

Source: Authors computations from Eurostat data.

The share of households in total households with access to broadband internet is shown in table 6. It can be seen that all regions have increased the value of this indicator, with a tendency to reduce territorial inequalities (Table 11, Figure 2).

5.2. E-commerce

Amid the slowdown in physical operational processes registered by companies during the COVID-19 pandemic, there has been a significant increase in online commerce [18]. Moreover, the Internet, along with advances in information technology and logistics/delivery, has allowed companies to rethink their business in a way that can continue their business efficiently.

Through online commerce, companies have been able to operate anywhere and anytime, eliminating multiple barriers. Also, many companies have implemented mixed sales systems, thus obtaining the anticipated results. During the COVID-19 pandemic period, there were changes in management approached by companies, many of them targeting distribution channels. As a result, companies have implemented their own promotional sites, thus expanding their activities to a higher level of coverage.

In 2020, Romania became the EU leader in terms of the growth rate of online commerce (45% of Romanian internet users bought online) [18].

The e-commerce market in 2020 reached EUR 5.6 billion and registered an annual growth of 30%, in the context of the COVID-19 pandemic and the previous modest performance of this sector compared to the situation of online commerce in other countries.

The e-commerce market in Romania was estimated at 6.2 billion euros in 2021, with local sales accounting for half of the total achieved in Eastern Europe [18].

The analysis of the online commerce indicator by development regions in Romania in 2021 shows that the first places are occupied by the most developed regions, namely: Bucharest-Ilfov with 58%, Center with 43%, West with 41% and North-West with 37% (Table 12).

Table 12. Online commerce in Romania's development regions during 2010-2021 period (%).

Regions	2010	2011	2012	2013	2014	2015	2016	2017	2018	2019	2020	2021
North-West	2	4	5	9	9	14	16	16	23	29	40	37
Center	5	8	6	7	7	9	11	17	18	27	39	43
North-East	3	5	7	7	7	9	9	16	17	18	32	33
South-East	3	3	4	4	8	7	10	11	16	19	30	31
South Muntenia	2	4	5	6	7	11	10	15	18	20	32	33
Bucharest-Ilfov	8	14	10	20	25	19	19	22	36	31	56	58
South-West Oltenia	3	6	1	10	8	9	12	15	14	22	36	35
West	4	3	3	7	11	8	8	17	15	23	39	41

Source: Authors computation on Eurostat data.

6. METHODOLOGY

The research methodology used in this article was mixed being used both quantitative and qualitative methods in order to to estimate the statistical impact of share of households using broadband infrastructure in total households at regional level (%) and individual persons shopping online in total population at regional level (%) on the GDP per capita (euro/inhabitant) indicator, at the level of development regions (NUTS 2) in Romania, using data available at Eurostat for the period 2010-2021.

The quantitative method involved identifying and selecting this specific indicators and running a panel analysis on them by using EViews 9.5, thus comparing the OLS method, OLS with fixed effect and OLS with random effects using AIC (Akaike information criterion measuring the quality of the econometric model), R^2 (a statistical measure representing the proportion of the dependent variable variance in our case, which is explained by independent variables in the regression model), RMSE (Average Square Error Root, a measure of differences between sample or population values predicted by a model or estimator and observed values), Hausman test in order to selecting the optimal model and discussing the results. Once the best method was established, we made an analysis of the regional heterogeneity.

7. RESULTS AND DISCUSSIONS

In order to achieve the targets proposed for the econometric analysis GDP per capita was chosen as the dependent variable, and online commerce and broadband infrastructure as the independent variables.

The term "panel data" refers to the pooling of observations on a cross-section of households, countries, firms, etc., over several time periods" [14]. This can be achieved by surveying a number of households or individuals just like in the analysis made in this article and following them over time.

The model set out below is a particular form shown in Equation 1, adapted to the objective of this article:

$$GDP\_PER\_CAPITA = a_1*BROADBAND + a_2*ONLINE\_COMMERCE + c + \varepsilon_i \quad (1)$$

where:

a_1, a_2 = coefficients of the independent variables;

c = the constant of the regression equation;

ε_i = residual variable;

i = 2010, ..., 2021.

7.1. OLS model

By applying the OLS model, we can explain the dependency of GDP per capita on important factors of the digital economy (broadband internet infrastructure and online commerce). Moreover, the validity of the model was demonstrated by the prob(f-statistic) which was 0.0000. The value of R-square was

0.421127. The attached probability of the broadband was of 0.2421 above the 5% threshold and of the online commerce of 0.0001 below it which indicates that the model does not explain the relationship between variables well, and we will explore two other methods: panel with random effects and panel with fixed effects. The attached coefficients for the OLS method can be observed in Equation 2.

$$GDP\_PER\_CAPITA = 64.00942*BROADBAND + 377.7075*ONLINE\_COMMERCE + 6485.240 + \varepsilon_i \quad (2)$$

7.2. Panel model with random effects

In the case of the ols model with random effects, the online commerce has a positive effect on the GDP per capita (t-statistic=11.24878>3 and prob=0.0000), proving a direct and positive relationship between those two variables. Thus, from the model and from equation 3 it is shown that a 1% increase in online commerce leads to an increase in GDP per capita by 247.13 euros.

The final Equation (3) of this method is:

$$GDP\_PER\_CAPITA = 32.5671650702*BROADBAND + 247.134798226*ONLINE\_COMMERCE + 10589.9047142 \quad (3)$$

The other independent variable has also a direct and positive relationship with the dependent variable (t-statistic=2.527939>2 and prob=0.0000), as shown from the equation with the increase of 1% in broadband infrastructure, the GDP per capita will increase with 32.567 euros. The constant is also significant as its attached probability is p=0.0000<0.05. R^2 is 0.761754, almost double than in the previous applied method.

But in order to see if this type of panel model with random effect is appropriate or not and that a fixed effect would be better it is needed for the Hausman test to be used. The hypothesis used in order to test are: H0: the panel model with random effects is adequate and H1: the panel model with fixed effects is adequate. According to the attached probability of the Chi-Square of 46.8740 is 0.0000 so we will accept the second hyphotesis, namely H1.

7.3. Panel model with fixed effects

According to this model there can be observed a positive and direct relationship between the online commerce and GDP per capita (a 1% increase in online commerce will lead to an increase of 192.76 euro/inhabitant) and broadband and GDP per capita (a 1% increase in the broadband infrastructure will lead to an increase of 39.04 euros/inhabitant).

As shown by the R^2, which is 0.96, the influence of the independent variables upon the dependent one is very high. The attached probabilities of all the coefficients are 0.0000, showing that they are significant for the 5% threshold. Furthermore, the Prob(F-statistic)=0.0000 proves the validity and the F-statistic test 259,2516>0, the significance of the model.

The final equation of the panel model with fixed effects is shown below:

$$GDP\_PER\_CAPITA = 39.0437564071*BROADBAND + 192.762233534*ONLINE\_COMMERCE + 11048.9379175 \quad (4)$$

This model shows a conclusive picture of the influence of indicators in the implementation of digitalization at regional level. The results of the analysis highlighted the direct relationship of the indicators between the three variables related to the digitalization process at the level of Romania's regions and the strong influence of broadband internet and online trade on GDP per capita, proving that any growth among independent variables will lead to an increase amongst the dependent variables.

7.4. The regional heterogenity

By applying the fixed effects model, we can determine the regional heterogeneity for the eight regions of Romania by computing the longitudinal effects and their regression equations taking into consideration that the slope is the same. By replacing the constant term in equation there have been obtained the following equation for every region:

GDP_PER_CAPITA (B-I) = 29594 + 39.04376*BROADBAND + 192.7622*ONLINE_COMMERCE
GDP_PER_CAPITA (W) = 11459 + 39.04376* BROADBAND + 192.7622* ONLINE_COMMERCE
GDP_PER_CAPITA (C) = 9727 + 39.04376* BROADBAND + 192.7622* ONLINE_COMMERCE
GDP_PER_CAPITA (S-E) = 8830 + 39.04376* BROADBAND + 192.7622* ONLINE_COMMERCE
GDP_PER_CAPITA (N-W) = 8.690 + 39.04376* BROADBAND + 192.7622* ONLINE_COMMERCE
GDP_PER_CAPITA (S M) = 7859 + 39.04376* BROADBAND + 192.7622* ONLINE_COMMERCE

GDP_PER_CAPITA (S-W O) = 7013 + 39.04376* BROADBAND + 192.7622* ONLINE_COMMERCE
GDP_PER_CAPITA (N-E) = 5218 + 39.04376* BROADBAND + 192.7622* ONLINE_COMMERCE

As it is shown from the equations on the first place there is situated the Bucharest-Ilfov region with a constant term of 29,594 euro/capita followed by the West region with 11,459 euro/capita, Center region with 9,727 euro/capita, South-East (8,830 euro/capita), North-West (8,690 euro/capita), South Muntenia (7,859 euro/capita), South-West Oltenia (7,013 euro/capita) and on the last the North-East region with 5,218 euro/capita.

The results are as expected especially because of the Bucharest-Ilfov region which is the most developed region of the country and also contains the capital of Romania and the West region which during 2000-2007 has registered the fastest growth amongst all the other regions.

In Equation 4 if both of the independent variables would be null, then the resulted value of GDP/capita would be 11,048.94 euro/capita. The highest value for the GDP/capita would be of Bucharest-Ilfov Region with 29,594 euro/capita and the lowest of 5,218 euro/capita would be the one of North-East region (Figure 3). Comparing the obtained results with the constant term of the fourth equation it is shown that the Bucharest-Ilfov region has a value of 2.6 higher than the average of the eight regions, followed by the West region with a value of 1.03 higher. All the other regions are below average.

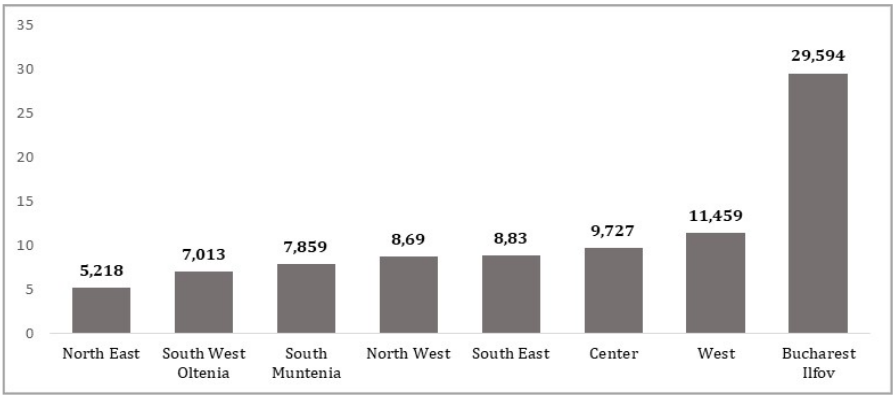

Figure 3. Free term (euro per capita)
Source: Authors computations.

The variance coefficient has a value of 69.84% showing a high etherogenity at national level but if we eliminate the Bucharest-Ilfov region this would decrease to 23.7%. This proves the fact that amongst the regions of Romania there is maintained a relatively reduced inequality, the situation changing when the Bucharest-Ilfov region is taking into consideration.

8. POLICY IMPLICATION FROM REGIONAL POLICY PERSPECTIVE

The regional development concept of Romania (adopted in the year 1999) is the basis of the National Regional Development Strategy and of the strategies at territorial level and pursues: diminishing regional disparities, stimulating balanced development, reviving disfavoured areas, correlating regional development with the sectoral one, and cooperation between regions. These objectives are found again in the Regional Operational Programme financed both by Structural Funds and national funds, and they are based on the strategic development priorities [20,21].

In accordance with these objectives, the general principles at national and local level were outlined (promoting market economy mechanisms at regional level, improving competitiveness and realising sustained economic growth, promoting harmonious development in the territory), to which we can add the principles of the EU Structural Funds and cohesion policy (subsidiarity, programming, partnership, additionality, co-financing, concentration, monitoring and evaluation) [22].

In present programming period, EU regional policy works to make a difference in 5 key areas:

- investing in people by supporting access to employment, education and social inclusion opportunities;
- supporting the development of small and medium size businesses;
- strengthening research & innovation through investment and research-related jobs;
- improving the environment through major investment projects;
- modernising transport and energy production to fight against climate change, with a focus on renewable energy and innovative transport infrastructure.

Romania will receive a total of €31.5 billion from Cohesion Policy in 2021-2027 in the framework of its Partnership Agreement with the Commission to promote the economic, social and territorial

cohesion of its regions and its green and digital transition. The EU funds will also support the development of a competitive, innovative and export-oriented Romanian economy.

For the current programming period, the European Union has allocated to the cohesion policy €4.33 billion from the European Regional and Development Fund (ERDF) that will support Romania's innovative and smart economic transformation. Funds will increase the competitiveness of small and medium-sized enterprises (SMEs), and support research and innovation, in particular through business-academia collaboration. Innovative enterprises and innovative activities in traditional SMEs will also be supported.

The EU will also invest in the digitalisation of companies and the development of innovative digital public services. The digital skills of the population, particularly students and teachers, will also be improved [23].

9. CONCLUSIONS

Digitalization is an essential element for the current structure of society, given the COVID-19 pandemic and geopolitical challenges. From the point of view of the regional approach, digitalization has an important impact on the level of territorial development and on reducing economic and social inequalities.

At European level, it can be said that the digital economy and society are in a high dynamic, which is amplified and accelerated by post-COVID-19 pandemic recovery attempts. Thus, in order to achieve the digital objectives, the EU will accelerate and facilitate the launch of national and multinational projects combining different types of funding (EU budget, recovery and resilience mechanism, private funds, etc.).

The analysis of the digital domain in Romania shows that, between 2010 and 2021, over three quarters of households (78.2%) had access to the internet at home: In urban areas, 84.8% of households are connected to the internet, and in rural areas, only 69.7% of households.

In the territorial aspect, the internet connection was more widespread among households in the Bucharest-Ilfov region (78.5% of the population), followed by the West (67.8%) and North-West (67%) regions. The regions representing the average broadband internet connection are South-West (61%), Center (60.8%) and South Muntenia (60.3%).

Also, in 2020, Romania became the EU leader in terms of the growth rate of online trade. The e-commerce market reached 5.6 billion euros and registered an annual growth of 30% in the context of the COVID-19 pandemic and the previous modest performance of the sector compared to the situation of online commerce in other countries.

As regards the econometric model used to highlight the relationship between the three proposed indicators (GDP, broadband and online trade), it demonstrates a conclusive picture of the indicators' influences on regional development. The resulting equations show the direct and positive link between broadband infrastructure and e-commerce with GDP per capita, proving that any growth among independent variables will lead to an increase among dependent variables.

From the analysis of the panel regression model, it was shown that the fixed effect model is best suited to illustrate the regional GDP dependence on the two regressors (internet infrastructure and online commerce). The values of the coefficients in the fixed effect model equation are statistically significant and have a positive influence on GDP. For example, as online commerce grows by 1%, GDP per capita will increase by 192.76 euros. In the case of broadband internet infrastructure, a significantly positive relationship with GDP per capita can also be observed. The high value of R^2 shows that the two endogenous variables explain 96% of the variation of the dependent variable.

In terms of supporting digitization in Romania, the National Recovery and Resilience Plan focuses on the digital transition and addresses challenges in all its sectors. The measures contained in the Romanian strategy cover five of the seven priority areas identified by the European Commission: connectivity, human capital, digital public services, the digitalization of the business environment and investments in digital capacities and advanced technologies.

The funded investments will contribute to increasing Romania's progress in digital competitiveness, in areas such as human capital, broadband connectivity, the integration of digital enterprise technologies and digital public services.

REFERENCES

1. Antonescu, D. (2013). *The Regional Development Policy of Romania in the Post-Accession Period*. Working Papers, Romanian Academy, National Institute of Economic Research, Bucharest. Retrieved from http://www.workingpapers.ro/2013/wpince131209.pdf

2. Hardy, A. P. (1980). The role of the telephone in economic development. *Telecommunications Policy, 4*(4), 278-286. https://doi.org/10.1016/0308-5961(80)90044-0
3. Gruber, H. & Koutroumpis, P., (2010). Mobile Communications: Diffusion Facts and Prospects. *Communications & Strategies*, 77, 133-145. Retrieved from https://www.researchgate.net/publication/228295613_Mobile_Communications_Diffusion_Facts_and_Prospects
4. Czernich, N., Falck, O., Kretschmer, T., & Woessmann, L. (2009). Broadband Infrastructure and Economic Growth. *CESIFO Working Paper,* No. 2861. Retrieved from https://papers.ssrn.com/sol3/papers.cfm?abstract_id=1516232
5. Krugman, P. (1991). *Increasing Returns and Economic Geography*. *Journal of Political Economy, 99*(3), 483-499. Retrieved from https://pr.princeton.edu/pictures/g-k/krugman/krugman-increasing_returns_1991.pdf
6. Thompson, H.G., & Garbacz, C. (2011). Economic impacts of mobile versus fixed broadband, *Telecommunication Policy*, *35*(11), 999-1009. https://doi.org/10.1016/j.telpol.2011.07.004
7. Hikmaturokhman, A., Ramli, K., Suryanegara, M., Ratna, A. A. P., Rohman, I. K., & Zaber, M. (2022). A Proposal for Formulating a Spectrum Usage Fee for 5G Private Networks in Indonesian Industrial Areas. *Informatics, 9*(2), 44. MDPI AG. Retrieved from http://dx.doi.org/10.3390/informatics9020044
8. Waverman, L., & Dasgupta, K. (2010). *Connectivity Scorecard 2010*. Retrieved from https://www.ifap.ru/pr/2010/n100212a.pdf
9. Edquist, H. (2022). The economic impact of mobile broadband speed, *Telecommunications Policy*, *46*(5), June, 102351. https://doi.org/10.1016/j.telpol.2022.102351
10. Mack, E. (2014). Businesses and the need for speed: The impact of broadband speed on business presence. *Telematics and Informatics, 31*(4), 617-627. https://doi.org/10.1016/j.tele.2013.12.001
11. Boldrin, M., & Canova, F. (2001). Inequality and convergence in Europe's regions: Reconsidering European regional policies. *Economic policy, 16*(32), 206-253. Retrieved from http://apps.eui.eu/Personal/Canova/Articles/icoeu.pdf
12. Madden, G., & Scott, S.J. (1997). CEE telecommunications investment and economic growth. *Information Economics and Policy*, *10*(2), 173-195. Retrieved from https://mpra.ub.uni-muenchen.de/11843/
13. Wei-Qiang, C. Z., & Rossotto, C. M. (2009). Economic impacts of broadband. In *Information and Communications for Development: Extending Reach and Increasing Impact* (pp. 35-50). Washington, DC: The World Bank. https://doi.org/10.1596/978-0-8213-7605-8
14. Baltagi, B. H., (2021). *Econometric Analysis of Panel Data*, sixth edition Springer. ISBN-13:978-3-030-53952-8 Retrieved from: https://link.springer.com/book/10.1007/978-3-030-53953-5
15. Eurostat. Statistical regions in the EuropeanUnion and partner countries NUTS and statistical regions 2021 Regions and cities — Overview. (2022). Retrieved from https://ec.europa.eu/eurostat/documents/3859598/15193590/KS-GQ-22-010-EN-N.pdf/82e738dc-fe63-6594-8b2c-1b131ab3f877?t=1666687530717
16. European Commission. *The Recovery and Resilience Facility*. (2022). Retrieved from https://ec.europa.eu/info/business-economy-euro/recovery-coronavirus/recovery-and-resilience-facility_en
17. European Comission. *Digital Agenda For Europe*. (2022). Retrieved from https://www.europarl.europa.eu/ftu/pdf/en/FTU_2.4.3.pdf
18. National Authority for Communications Administration and Regulation. *Piața serviciilor de comunicații din Romania*. Raport de date statistice – Semestrul I 2022. (2022). Retrieved from https://statistica.ancom.ro/sscpds/public/files/255_ro (in Romanian)
19. Ministry of European Investments and Projects. Romanian's Recovery and Resilience Plan. (2022). Retrieved from https://mfe.gov.ro/wp-content/uploads/2021/10/facada6fdd5c00de72eecd8ab49da550.pdf (in Romanian).
20. Popescu, C., Mitrică, B. &, Mocanu, I. (2016). Dezvoltarea regională înainte și după aderarea la Uniunea Europeană. In D. Bălteanu, M. Dumitrașcu, S. Geacu, B. Mitrică, M. Sima (Eds.), *Romania—Natură și Societate* (pp. 613-620). Bucharest, Romania: Publisher Romanian Academy. (in Romanian)
21. Bălteanu, D., Mitrică, B., Mocanu, I., Sima, M. & Popescu, C. (2016), Caracterizarea geografică a regiunilor de dezvoltare. In D. Bălteanu, M. Dumitrașcu, S. Geacu, B. Mitrică, M. Sima (Eds.), *Romania—Natură și Societate* (pp. 621-652). Bucharest, Romania: Publisher Romanian Academy. (in Romanian)
22. Mitrică, B., Săgeată, R., Mocanu, I., Grigorescu, I., & Dumitrașcu, M. (2021). Competitiveness and cohesion in Romania's regional development: A territorial approach. *Geodetski Vestnik*, *65*(3), 440-458. https://doi.org/10.15292/geodetski-vestnik.2021.03.440-458
23. European Commission. *EU Cohesion Policy: €31.5 billion for Romania's economic, social and territorial cohesion, competitiveness and green and digital transition in 2021-2027*. Press release, 25 July 2022, Brussels. Retrevied from https://ec.europa.eu/commission/presscorner/detail/en/IP_22_4662

Central European Journal of Geography and Sustainable Development
ISSN 2668-4322, ISSN-L 2668-4322

2022, Volume 4, Issue 2, Pages: 78-93
https://doi.org/10.47246/CEJGSD.2022.4.2.5

Identifying spatiotemporal variability of traffic accident mortality. Evidence from the City of Belgrade, Serbia

Suzana Lović Obradović[1,*], Hamidreza Rabiei-Dastjerdi[2,3], Stefana Matović[1]

[1]Geographical Institute "Jovan Cvijić" SASA, 9 Đure Jakšića, Belgrade 11000, Serbia;
[2]School of Architecture, Planning and Environmental Policy & CeADAR, University College Dublin (UCD), Belfield, Dublin 4, Ireland;
[3]Social Determinants of Health Research Center, Isfahan University of Medical Sciences, Isfahan, Iran
s.lovic@gi.sanu.ac.rs (S.L.O.); hamid.rabiei@ucd.ie (H.R.D.); s.matovic@gi.sanu.ac.rs (S.M.)

Received: 13 December 2022; Revised: 23 December 2022; Accepted: 27 December 2022;
Published online: 28 December 2022

Abstract: Traffic accident mortality (TAM) is a significant global problem and part of the sustainable development goals strategy. In Serbia, a decline in the number of deaths in traffic accidents is evident, but in certain time intervals and areas, the number of deaths is higher than in others. This paper adopted Joinpoint regression analysis and a geospatial approach to assessing spatial, temporal, and spatiotemporal mortality variability due to traffic accidents in Belgrade from 2016 to 2021. Results suggested statistically significant change during each year and spatial clustering of higher values of deaths in central Belgrade municipalities. Spatiotemporal analysis of traffic accidents data indicated a change in spatial clusters over time, pointing out two types of hotspots for traffic accident mortality–Sporadic - and New hotspots along the international highway, main, and local roads, in the broader area of the city. The main findings of this paper pointed to the areas in Belgrade where the population is more endangered in traffic compared to other areas. The results and conclusions can serve traffic managers and decision-makers as a basis for more detailed research and local-specific traffic safety strategies.

Key words: Traffic Accident Mortality, Joinpoint Regression Analysis, Optimized Hotspot Analysis, Space-Time Mining Pattern Analytics, Belgrade, Serbia.

Citation: Lović Obradović, S., Rabiei-Dastjerdi, H., & Matović, S. (2022). Identifying spatiotemporal variability of traffic accident mortality. Evidence from the City of Belgrade, Serbia. *Central European Journal of Geography and Sustainable Development*, *4*(2), 78–93. https://doi.org/10.47246/CEJGSD.2022.4.2.5

1. INTRODUCTION

Traffic accident mortality (TAM) is a significant global problem. Around 1.3 million people died from a road traffic crash, costing most countries 3% of their gross domestic product [1]. The number of deaths in traffic accidents at a global level in the period from 2000 (19,099 per 100,000 inhabitants) to 2019 (16,714 per 100,000 inhabitants) slightly decreased to more than 12% [2]. This problem is integral to the Sustainable Development Goals (SDG) strategy. By SDG Target 3.6, the number of global deaths and injuries from road traffic accidents should be halved [3]. The extent of this problem can be seen in the fact that this target still needs to be met.

Serbia and other countries of the Balkan Peninsula face the same problem. The decline in the number of deaths caused by traffic accidents began in the last decade of the 20th century due to the stabilization of the economic situation in the country, increasing living standards, tightening the penal policy for traffic violations, etc. [4]. This trend continued at the beginning of the 21st century, which was greatly influenced by the adoption of the Law on Traffic Safety on Roads [5] as well as an intensive media campaign on the behavior of road users [6]. Despite the downward trend in the number of fatalities and number of deaths, Serbia is far from achieving the SDG target.

* Corresponding author: s.lovic@gi.sanu.ac.rs; Tel.: + 381-11-2637-597

In Serbia, the City of Belgrade has the highest number of traffic accident deaths [7]. Belgrade is a crossroads of national and international roads, so it is characterized by a high degree of daily mobility of the population. A total of 766,275 vehicles were registered in Belgrade in 2021, which is slightly less than one-third (28.5%) of all registered vehicles in Serbia [8]. Given that, identifying the areas where a higher number of fatal traffic accidents occurs and monitoring the change in trend in Belgrade is required to reduce the number of deaths.

The assessment of spatial and spatiotemporal patterns is achievable using spatial analysis [9] while significant temporal trend changes can be detected using Joinpoint regression analysis [10]. The data on the number of dead in traffic accidents in Serbia are georeferenced and are grateful material for detecting micro-locations where the highest number of dead was recorded. Since data also contain a time component, it is possible to determine the nature of the temporal trend and whether statistically significant changes in the trend exist.

This study aims to assess the spatial, temporal, and spatiotemporal patterns of the TAM in the City of Belgrade from 2016 to 2021 to identify the areas where the population is the most endangered by adopting a geospatial approach. Yet, this methodological approach has not been applied to study TAM in Belgrade and Serbia. Targeting the area where most people die and when it happens is the initial step towards reducing the number of deaths. Accordingly, three main research questions are:

– What are the temporal dynamics of TAM in Belgrade? And are there statistically significant changes in the studied period, from 2016 to 2021?

– Are spatial, temporal, and spatiotemporal mortality patterns due to traffic accidents noticeable?

– Are TAM patterns constant over space and time or only characterized by temporal variability?

2. LITERATURE REVIEW

TAM is a problem equally represented in underdeveloped [11], developed [12], as well as in developing countries [13]. The change in the number of deaths can be indirectly linked to economic growth. Thus, a study conducted in Nigeria showed that economic development, observed through GDP growth, has conditioned a long-term decrease in crashes and fatalities [14]. Directly, it can be related to the consumption of alcohol [15], drugs [16], etc. TAM is a significant factor in public health problems and a society's economic and social development [17]. Therefore, identifying high-risk crash spots is vital [18].

Recent findings suggest that mortality due to traffic accidents is not random but clustered in space [19,20] and time variable [21,22]. Spatial variations of TAM are noticeable within the state; in Italy are directly associated with disparities in employment rate and alcohol use [23], and in the Netherlands, with per capita income, traffic density, and the availability of advanced trauma care [24]. In Iran, for example, the deaths caused by traffic accidents are spatially diverse and clustered, conditioned by population density differences, traffic volume, highway length, land use, etc. [25]. A study conducted in Japan showed that the spatial variability of TAM can be linked to different socioeconomic characteristics of the population [20]. Some studies indicate that the number of deaths in traffic accidents varies over time and that changes in the trend (increasing or decreasing) are conditioned by the economic crisis [22], in addition to various targeted prevention measures [26].

A review of past studies showed that the researchers successfully applied geospatial approaches to investigating traffic accident data [27] and detecting the areas with the higher concentration of events. A study by Wang et al. [28] suggests Kernel density (KD) analysis for identifying road traffic risk locations, i.e., locations with the highest concentration of incidents. Another study supports that the KD analysis is a practical approach to indicating the distribution according to a pattern; the authors also suggest that this analysis does not provide statistical significance [29]. To overcome this gap, the same study proposes the use of hotspot analysis. Given that the output of hotspot analysis can reveal statistically significant patterns, it is successfully applied for the identification of spatial grouping of traffic accidents [30] and their spatial grouping based on severity [31]. Pljakić et al. [32] employed this method to assess the high frequency of the total number of accidents and pedestrians, and Vaz et al. [33] to identify hotspots and coldspots of road traffic injuries. The study of Kang et al. [29] revealed areas with a high concentration of traffic accidents with the elderly population using hotspot analysis. Finally, numerous studies have implemented space-time mining pattern analytics for spatiotemporal analysis of traffic accidents [29,34], emphasizing their significance to the sustainable development of the studied area [35].

However, relatively few studies connect these two phenomena regarding the application of spatial analysis in TAM research Erdogan [19] investigated the degree of a spatial grouping of high road mortality rates using global and local spatial autocorrelation analyses. The same author successfully applied a geographically weighted regression model to predict death rates. For detecting spatiotemporal variability of hotspots/coldspots and trends of road traffic accident fatalities in Bangladesh between January 2013 and June 2016, Rahman, Crawford, and Schmidlin [36] utilize KD estimation, space-time cube, and emerging hotspot analysis. These methods had satisfactory results and potential for use in other case studies. Given that a significant number of deaths among motorcyclists have been reported in Iran, Saadat et al. [25] utilized the Moran's I index for assessing spatial clustering of these events, Getis-Ord G* statistics to identify hotspots, and geographically weighted regression to determine the spatially varying relationship between environmental factors (population density, level of development, traffic volume, length of highways, etc.) and the number of deaths. These spatial analyses allow identifying the most dangerous places for motorcyclists and the factors that affect their vulnerability. Yoon and Lee [34] investigated the dynamics of changes in the number of pedestrian deaths, comparing the areas where environmental enhancement projects for pedestrians were implemented with those that did not. A declining trend (different variations of coldspots) has been observed in areas where prevention measures come into force. They concluded that the space-time mining pattern is an efficient tool for assessing pedestrian safety.

Previous studies showed that Joinpoint regression analysis is a valuable tool for investigating the time trend of mortality due to traffic accidents and identifying the moment when a statistically significant change occurred. This method helps identify time trends and statistically significant changes in time-series data [9]. Thus, studies conducted in the Slovak Republic [21] and a region in Span – Comunitat Valenciana [22] showed a declining trend after adopting new road safety measures. Bandi, Silver, Mijanovich, and Macinko [37] explored the temporal trend in motor vehicle fatalities in the United States for 42 years for different age groups and genders and concluded that the declining trend followed the entry into force of policies targeting risky behaviors related to motor vehicles. Other studies have also successfully used Joinpoint regression analysis to evaluate policies aimed at increasing traffic safety and reducing mortality based on an assessment of the changing trend in the number of deaths after their adoption [38,39].

In Serbia, most previous studies on TAM were primarily focused on analyzing the gender and age structure of deaths in traffic accidents, the causes of fatal traffic accidents, and the type of vehicle that participated in the accidents [40]. The factors that influenced the fatal outcome of traffic accidents [41] and changes in the number of deaths in traffic accidents based on demographic characteristics [42] were also investigated. Simić et al. [43] have studied the impact of an economic crisis and transition on the health status of the population of Serbia based on mortality rates of various diseases, encompassing TAM. A group of authors [17] examined road traffic fatalities in Serbia from 1999 to 2014 using Joinpoint regression analysis, and they concluded that the number of fatal injuries significantly decreased, starting in 2008 when a strong media campaign was implemented and in 2009 when the new Law of the Traffic Safety in Serbia entered into force.

The evaluation of the studies to date showed that spatial, temporal, and spatiotemporal analyses are useful for detecting TAM patterns and areas where the population is most endangered. The literature examining this issue in Serbia and in its immediate surroundings is very limited. Traffic accidents and their fatal outcomes are differently distributed in space and time, depending on many factors. Therefore, it is necessary to identify their spatiotemporal patterns, especially there areas where the number of deaths increases over time. The use of open data and spatial analysis makes it possible to identify areas where the concentration of TAM is increased in space and time, creating a base for more detailed research with a focus on dangerous locations.

3. METHODS AND DATA

3.1. Study area

Belgrade is the capital of Serbia and its most populous city, with a population of 1,692,768 (523.4 inhabitants/km^2) and an area of 3,234 km^2 [44,45] (Figure 1a). It is a separate territorial unit and is administratively divided into 17 municipalities (Figure 1b). Ten municipalities, with 78.8% of the

population (1,333,486), belong to the central urban city core. Central Belgrade municipalities are Čukarica, Novi Beograd, Palilula, Rakovica, Savski Venac, Stari Grad, Voždovac, Vračar, Zemun, and Zvezdara. In comparison, seven municipalities (Barajevo, Grocka, Lazarevac, Mladenovac, Obrenovac, Sopot, and Surčin) make up the broader territory of the city. All these municipalities belong to the Belgrade Police Administration. International Corridor 10 (highway) passes through the territory of Belgrade and is also a crossroads of important state roads (Figure 1c).

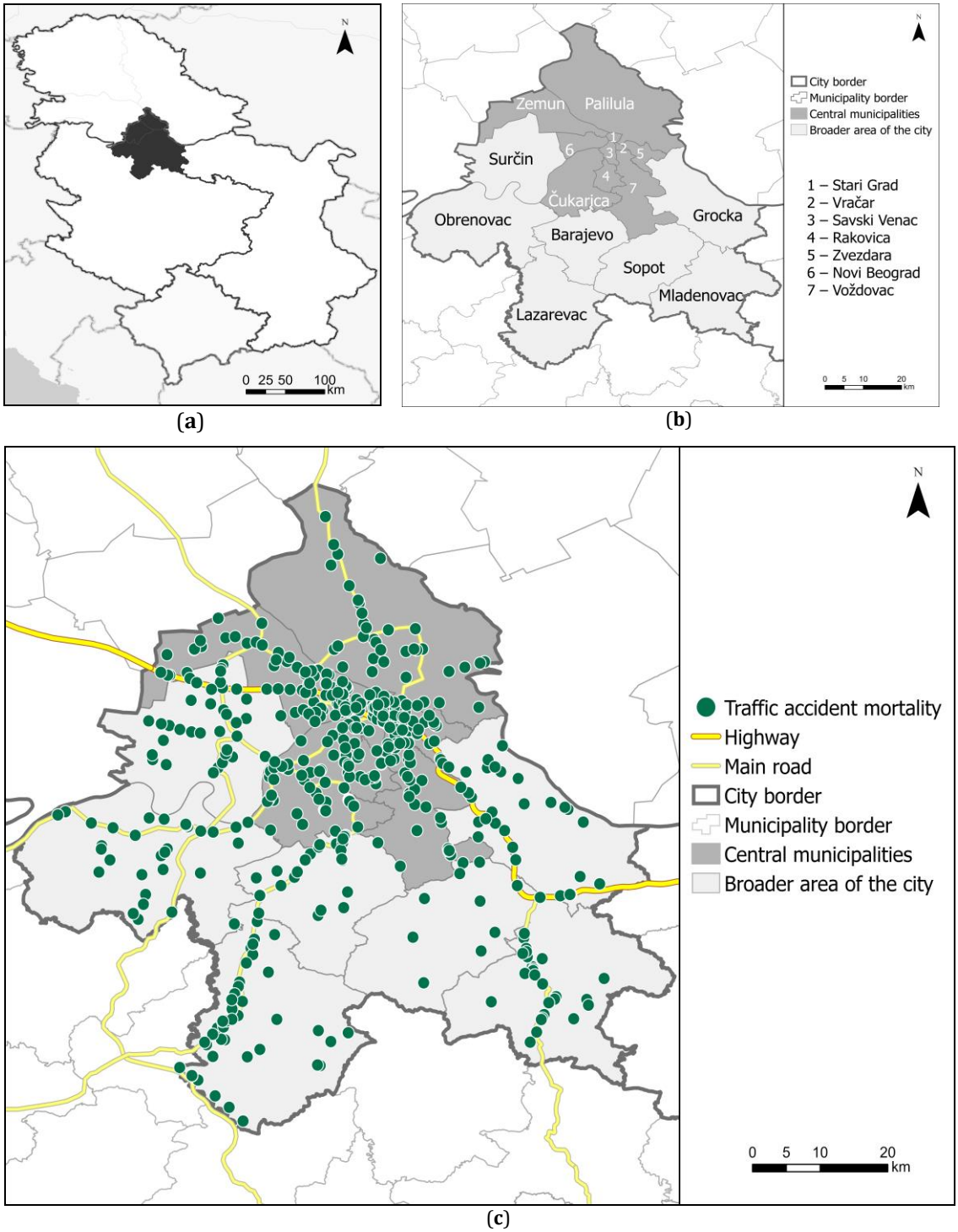

Figure 1. Study area (**a**) Position of the City of Belgrade in Serbia, (**b**) Municipalities of the City of Belgrade, (**c**) Location of traffic accidents with a fatal outcome for the period 2016–2021.

Note. The data in Figure 1 are visualized based on data obtained from Data on traffic accidents by police administrations and municipalities [Data set], by Open Data portal, 2022 (https://data.gov.rs/sr/datasets/podatsi-o-saobratshajnim-nezgodama-po-politsijskim-upravama-i-opshtinama/). In the public domain.

Belgrade is the country's administrative, health, political, educational, and cultural center. Economically, it is the most developed part of the country [46], with a high proportion of the value of the national gross domestic product [47]. A significant circulation of the population characterizes Belgrade, which records a continuously positive internal migration balance in the 21st century [48]. Slightly more than 15,000 (15,366) traffic accidents were recorded in Belgrade in 2021 (44.2%) out of a total of 34,751 in Serbia [49], Figure 1c. According to RTSA data [50], the Police Administration of Belgrade belongs to the group of administrations with a very high percentage of drivers in traffic under the influence of alcohol in the settlement in 2020 (1.3%).

3.2. Data

Data on TAM (incidents) for the Police Administration of Belgrade were obtained from the Open Data portal of the Republic of Serbia [49]. Accumulated data on traffic accidents by police administrations and municipalities from 2016 to 2021 were used (Figure 1c). The data contain a unique accident ID number, information on the police administration, municipality, and geolocation (X and Y coordinates). TAM data are also time-determined (date and time). Each recorded traffic accident was attributed to the type of traffic accident (with material damage, with the injured, and with the dead), the description of participants, and a detailed description of the traffic accident.

3.3. Methodology

After the introductory analysis of the quantification of traffic accidents, the temporal dynamics of TAM were analyzed over hours, days, months, and years within the studied period. We utilised a Joinpoint regression analysis, a widely used method for the study of temporal dynamics, to determine a certain moment, specifically a month during the year (from 2016 to 2021), when a statistically significant change in TAM in Belgrade occurs. The study is conducted in Joinpoint Trend Analysis Software, Version 4.9.0.0 [51]. A positive slope value indicates increasing while a negative slope indicates decreasing trend. A statistically significant change in trend is denoted with joinpoint, and the numerical expression of the change is determined using the Monthly Percentage Change (MPC) since monthly data were used [52].

This paper adopted Optimized hotspot analysis to assess whether mortality due to traffic accidents on the territory of Belgrade is clustered or randomly distributed in space. This analysis is suitable for incidence point data. They are aggregated into polygons using the Collect events option. Optimized hotspot analysis executes Hotspot analysis based on Getis-Ord Gi* statistic [53]. The formula can be written as follows:

$$G_i^* = \frac{\sum_{j=1}^{n} w_{i,j} x_j - \bar{X} \sum_{j=1}^{n} w_{i,j}}{S \sqrt{\frac{\left[n \sum_{j=1}^{n} w_{i,j}^2 - \left(\sum_{j=1}^{n} w_{i,j} \right)^2 \right]}{n-1}}} z \quad (1)$$

$$\bar{X} = \frac{\sum_{j=1}^{n} x_j}{n} \quad (2)$$

$$S = \sqrt{\frac{\sum_{j=1}^{n} x_j^2}{n} - \bar{X}^2} \quad (3)$$

where: x_j denotes the value of $\bar{X}$ at location j, $w_{i,j}$ is the weight between i and j, and n is the total number of TAM [54].

This analysis enables the identification of statistically significant clusters of high and low values of TAM in space. The outputs of the analysis are *Z*-score (standard deviation) and *p*-value (probability), which indicate spatial dependence. High values of *Z*-score and low *p*-value indicate a statistically significant hotspot (clustering of high values). The higher value of the positive *Z*-score, the more intense hotspot. Low negative values of *Z*-score and low *p*-value suggest coldspot (clustering of the low values). The lower value of the negative *Z*-score specifies a more intense coldspot. Three confidence levels (90%, 95%, and 99%) are possible. For values of *Z*-score near zero, no spatial clustering is detected (not significant).

The next step involved the utilization of space-time mining pattern analytics, including the space-time cube model and emerging hotspot analysis. Hotspot analysis enables the study of spatial patterns of TAM but not their temporal evolution in space. Incorporating the time dimension in spatial analysis provides insight into spatiotemporal patterns, i.e., how incident patterns of TAM in Belgrade change in space from 2016 to 2021. A space-time cube is a powerful form of three-dimensional (3D) modeling that generates spatiotemporal data in a cube. The cube consists of bins whose spatial dimension is defined by the x- and y-axis, while the z-axis determines time. Bin's position in space (x and y) and time (z) is fixed [55, 56]. Horizontal bins make time slices (the rows that share a temporal extent), while vertical makes time series (columns with the same spatial extent).

Since the data are represented with points and time-stamped for this study, we used the tool space-time cube by aggregating points. Based on their spatial and temporal determinants, the incidents are structured in bins, and summary Field statistics are calculated. In contrast, the trend for bin values over time at a given location is measured with the Mann-Kendall statistic [57]. The results are saved in a net CDF format compatible with various programs.

The results of space-time cube analysis are visualized using the 2D tool emerging hotspot analysis due to the simple presentation of the results, allowing an accurate interpretation. This analysis allows observing the temporal trends of hot and coldspots. It is also based on Getis-Ord Gi* statistic, which in this case, is calculated for each bean. The output categorizes the location of interest in one of 17 categories that describe the nature of hot-and coldspots [58]. All spatial analyses were conducted in Version 2.5 of ArcGIS Pro [59].

4. RESULTS

4.1. Temporal trend of TAM

In the past six years, from 2016 to 2021, 552 people died in traffic accidents in Belgrade. The highest number of deaths (99) was recorded in 2018, and the lowest was in 2021 (76). A deeper analysis of the time dynamics of TAM shows that the largest population died on average in September and October (56). When the hours during the day are analyzed, the highest number of deaths is recorded at 4 pm (37) when traffic frequency is increased due to employees returning from work. Observed by days of the week, the highest number of deaths occurred on Friday and Saturday (Figure 2).

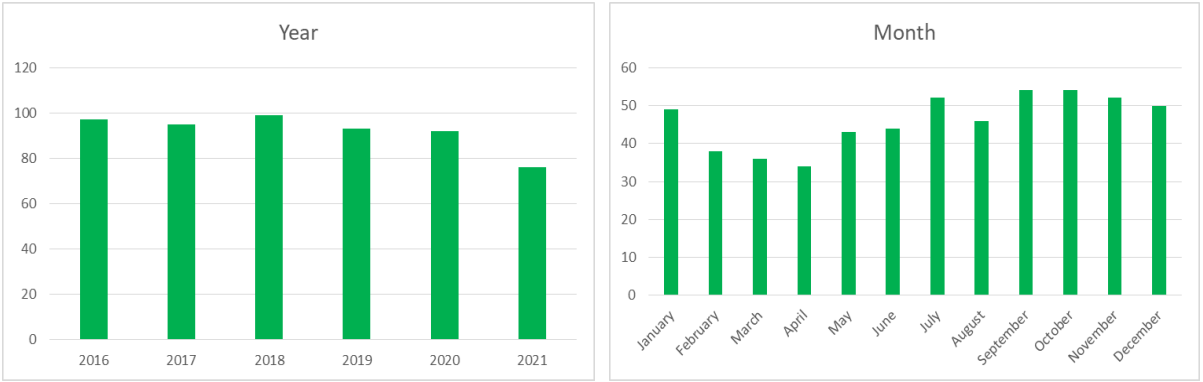

(a) **(b)**

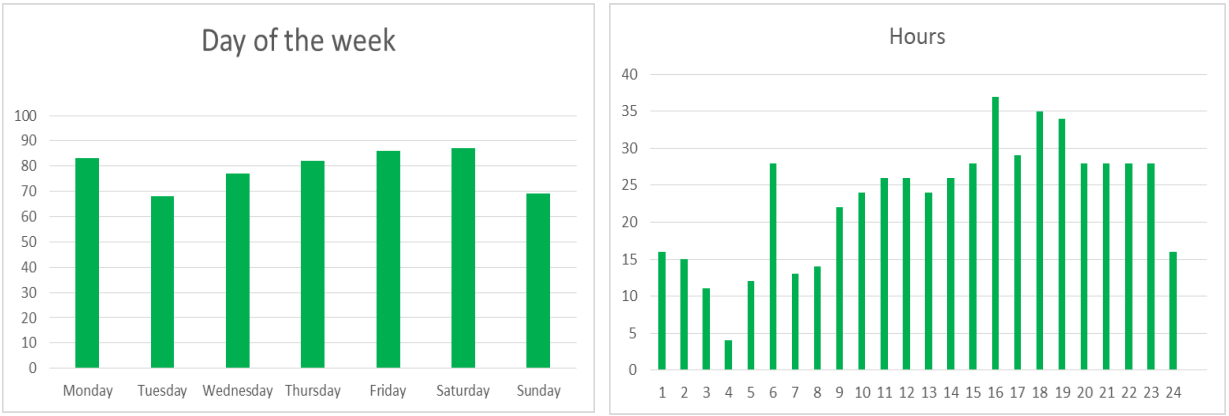

(c) **(d)**

Figure 2. Temporal distribution of TAM in Belgrade (2016–2021) by (**a**) years, (**b**) months, (**c**) days, and (**d**) hours.
Note. Data in the graph are calculated based on Traffic accidents by police administrations and municipalities [Data set], by Open Data portal, 2022 (https://data.gov.rs/sr/datasets/podatsi-o-saobratshajnim-nezgodama-po-politsijskim-upravama-i-opshtinama/). In the public domain.

The results of the Joinpoint regression analysis provided insight into the TAM trends and their statistically significant changes over the months for each of the six analyzed years. One joinpoint, i.e., the month during the year when a statistically significant difference in the number of deaths in traffic accidents was indicated, is detected for each year (Figure 3).

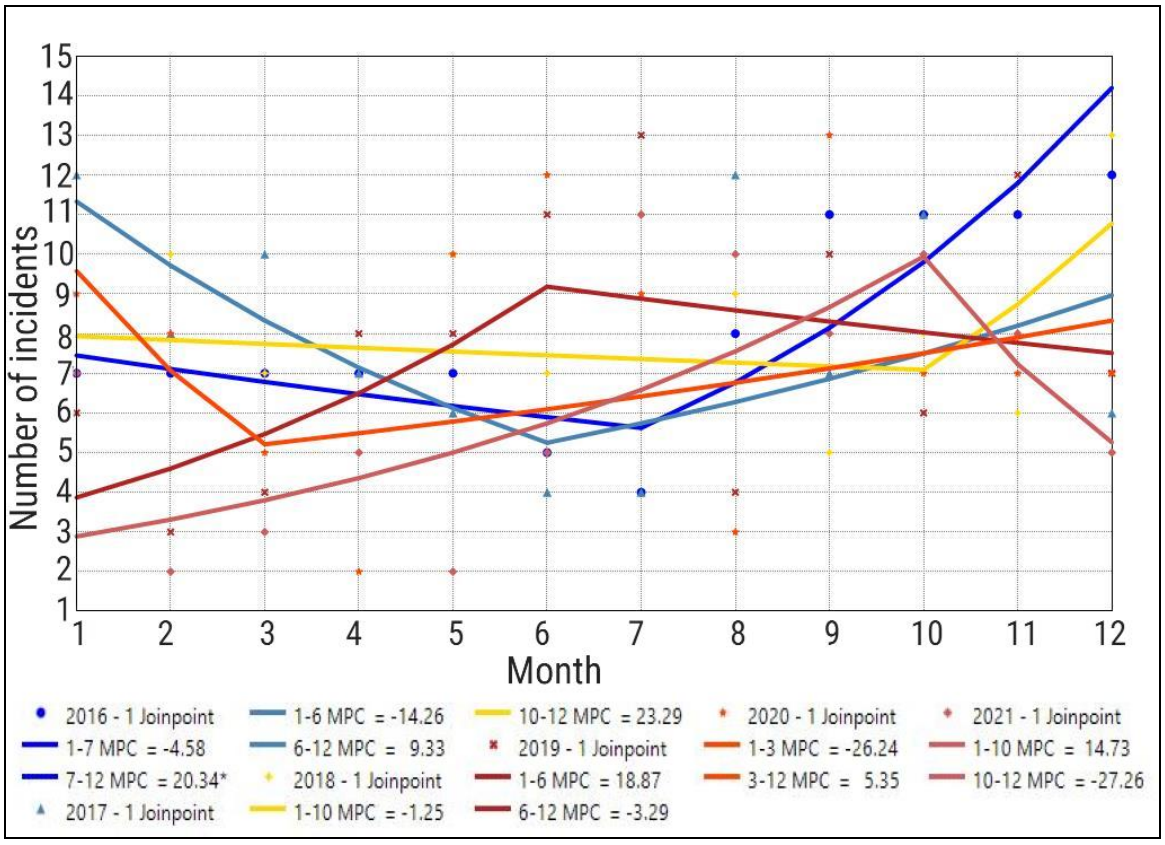

Figure 3. Joinpoint regression analysis of TAM in Belgrade by months, 2016–2021.
Note. Data in the graph are calculated based on Data on traffic accidents by police administrations and municipalities [Data set], by Open Data portal, 2022 (https://data.gov.rs/sr/datasets/podatsi-o-saobratshajnim-nezgodama-po-politsijskim-upravama-i-opshtinama/). In the public domain.

The nature of annual trends is different from the monthly trend when statistically significant change occurs. Thus, in 2016, 2017, 2018, and 2020, decreasing and then increasing trends in TAM were recorded. The months that indicate statistically significant changes marked as turning points are July,

June, October, and March, respectively. The two years when the increasing and then decreasing trend was recorded were 2019 and 2021. The monthly percentage change, decreasing or increasing, differs in all analyzed years. The most significant increase was recorded in 2018, when the MPC was 23.29. Specifically, in two months (from October, when there was a statistically significant change, to December), TAM increased by slightly less than 25%. The highest decreasing rate was recorded in 2021 and amounted to –27.26. Mortality due to traffic accidents in the two months (from October to December) was reduced by slightly less than 30%.

4.2. Spatial and spatiotemporal analysis

The result of the optimized hotspot analysis of TAM is displayed in Figure 4. Only hotspots (shades of red), indicating an increased frequency of deaths at given locations, were detected. A strong statistically significant cluster of incidents hotspots with a confidence level of 99% (the darkest shade of red) covers the territories of all seven central Belgrade municipalities. It completely covers the territories of the municipalities of Stari Grad, Savski Venac, and Vračar. As for the other municipalities, the cluster covers peripheral parts towards these three municipalities. Only one hotspot was detected on the border between the central city municipality of Zemun and the municipality of Surčin, which belongs to the broader area of the city. Coldspots that point to locations with a low frequency of deaths were not detected. Statistical grouping of TAM was not detected in the municipalities belonging to the broader area of the city.

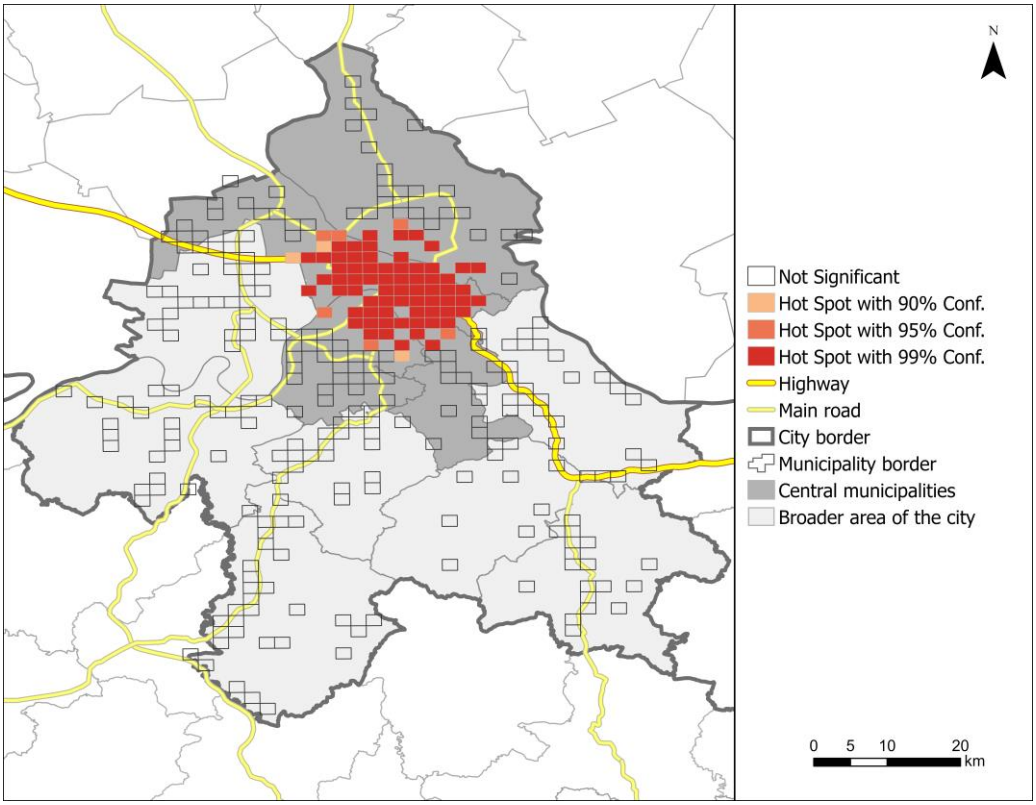

Figure 4. Optimized hotspot analysis of TAM.

Emerging hotspot analysis results indicated two (out of 17) types of hotspots of TAM—Sporadic hotspots and New hotspot, at the different locations (Figure 5a). A significantly higher number of sporadic hotspots, indicating locations marked as hotspots in most cases over time but never as coldspots, can be noticed. Sporadic hotspots have been identified in the municipalities of Surčin, along the international highway and main roads, and in the border part of the municipality of Zemun (central municipality) with the municipality of Surčin, also near the highway (Figure 5b). In the municipalities of Lazarevac (Figure 5c) and Mladenovac (Figure 5d), sporadic hotspots have been identified along the main roads. In contrast, in the municipality of Sopot (Figure 5d), two locations near local roads have been identified as sporadic hotspots. The results of the analysis indicated only one New hotspot (a location marked as a statistically

significant hotspot at the end of the studied period, while in the earlier time step, it was not). It was detected in the central part of the municipality of Surčin (Figure 5b).

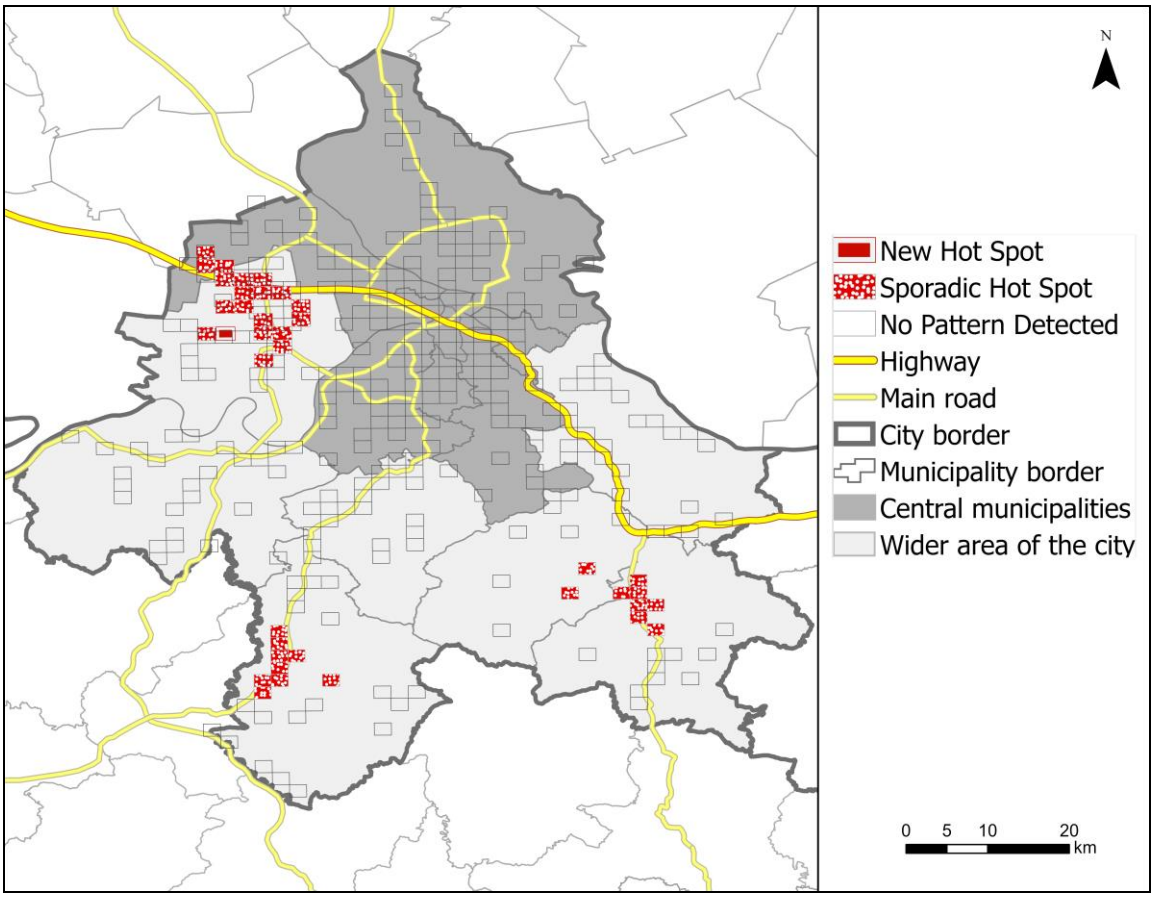

(a)

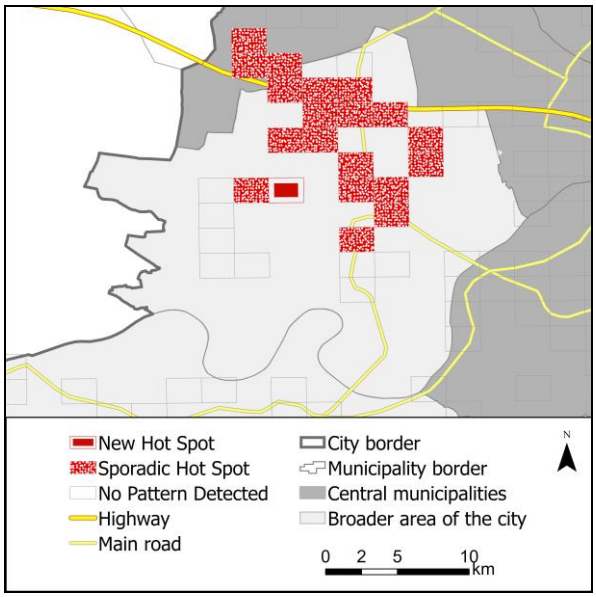

(b)

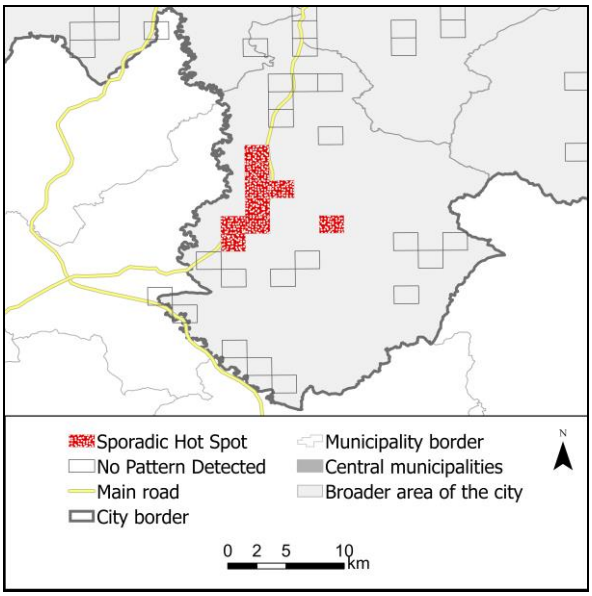

(c)

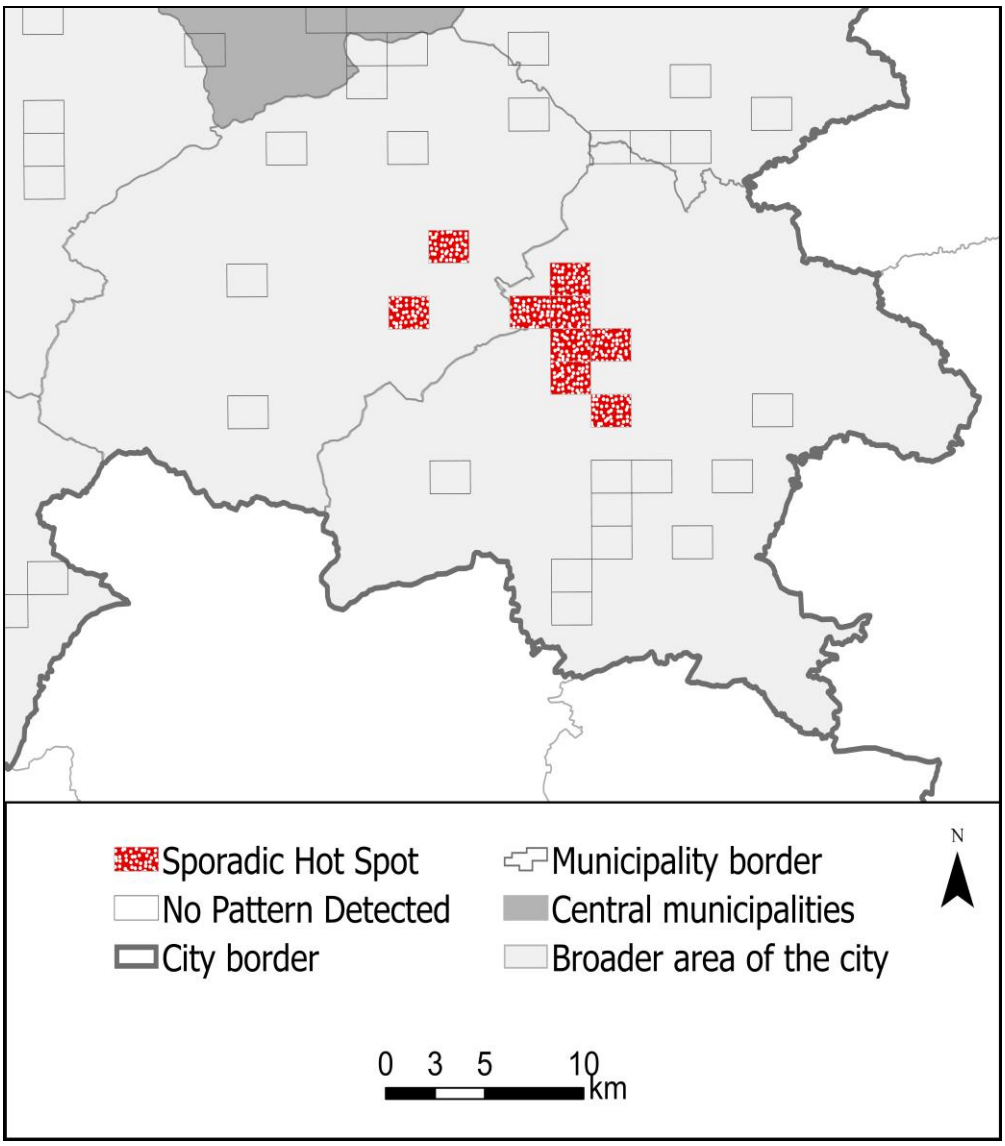

(d)

Figure 5. Space-time cube analysis of TAM for the period 2016–2021, **(a)** The City of Belgrade, **(b)** The municipalities of Surčin and Zemun, **(c)** The municipality of Lazarevac, and **(d)** The municipalities of Sopot and Mladenovac.

5. DISSCUSSION

This study provides a comprehensive assessment of the temporal, spatial, and spatiotemporal variability of TAM in Belgrade, from 2016 to 2021. The variation of the temporal trend by months is achieved through the use of Joinpoint regression analysis, identification of statistically significant hotspots using optimized hotspot analysis, and space-time cube and emerging hotspot analysis are adopted to assess whether hot- and coldspots vary in space over time.

Our findings highlight that the number of deaths during each of the analyzed years differs, as well as during the hours of the day, the day of the week, and the months of the year. Joinpoint regression analysis revealed a statistically significant change in the trend in the number of TAM during the months of the year. In addition, no unique trend was observed for each analyzed year – during the four analyzed years (2016, 2017, 2018, and 2020), the decreasing trend was replaced by an increasing trend. In 2019 and 2021, the opposite change was recorded; the decreasing trend replaced the increasing trend.

The study has also found that a statistically significant spatial concentration of TAM was evident in the study period. A similar study [25] found that deaths caused by driving accidents are spatially grouped in the space, i.e., the distribution of high-risk points is statistically significant. A statistically significant

cluster of hotspots of TAM can be found in the central municipalities of Belgrade. The cluster completely covers the territories of the municipalities of Savski Venac, Stari Grad, and Vračar (Figures 1B and Figure 4). These municipalities are characterized by the continuity of built-up urban areas [60], the highest values of in-migration and out-migrations in recent years [48], and according to current data, a high share of daily migrants among employees is presented [61]. According to the same author, the share of daily migrants in the municipality of Vračar was 80.8%, in the municipality of Stari Grad 88.6%, and the municipality of Savski Venac 92.2%, in 2011. The city core is the place that records the highest concentration of tourist attractions [62]. Besides, the central part of Belgrade is the place with the highest concentration of population and activities [63] and entertainment events [60]. Filipović et al. [64] state that Belgrade is the central part of Serbia's most important daily urban system. These conditions initiate a high daily frequency of people, contributing to the formation of a statistically significant cluster of hotspots on the territory of central Belgrade municipalities. At the same time, optimized hotspot analysis did not indicate any coldspots. Another study analyzing traffic fatalities in Dhaka using spatial analysis also revealed a concentration of hotspots in the core of the city [65].

Finally, the utilization of space-time cube and emerging hotspot analysis pointed to specific temporal variability in the spatial grouping of TAM in the period from 2016 to 2021, which could not be detected by optimized hotspot analysis. By incorporating the temporal dimension, spatiotemporal patterns were obtained. This study has revealed that an increase in the number of deaths over time is evident in municipalities (Lazarevac, Mladenovac, Sopot, and Surčin) belonging to the broader area of Belgrade. Based on the report of the RTSA on the values of public weighted risk of road deaths for 2020 (data on the number of mildly and severely injured and killed were used), the municipality of Sopot is characterized by low [66], the municipality of Mladenovac by medium [67], the municipality of Lazarevac by high [68], and the municipality of Surčin by a very high value of risk [69]. According to the same sources, the municipalities of Mladenovac and Surčin recorded an increase in risk in 2020 compared to the previous year, while the municipalities of Lazarevac and Sopot recorded a decrease. Part of State Road 22, known as Ibarska magistrala, passes through the municipality of Lazarevac. Most of this road is highly risky for road users, and several "black spots" have been identified [70]. A decrease in risk in 2020 can be linked to redirecting part of the traffic to the A2 (Miloš the Great) motorway. This motorway was opened for traffic in 2019, has separate traffic lanes in opposite directions, and enables bypassing the dangerous part of the Ibarska magistrala through the municipality of Lazarevac.

Another spatial characteristic of these hotspots is their concentration along the highway and main roads (Figure 5). This finding is somehow similar to previous studies. Thus, a study conducted by Cheng et al. [35], with the main goal of sustainable development, points out that hotspots are concentrated along main roads and urban road intersections. Analyzing the TAM of motorcyclists Saadat et al. [25] concluded that the highest number of TAM was recorded on the highways. Namely, the part of the International European route, international highway E75 (Corridor 10), passes through the municipality of Surčin. The high frequency of traffic, especially on weekends and holidays, causes an increasing number of traffic accidents, some of which are fatal. The construction of the Belgrade Bypass, which is underway, will enable bypassing of the central Belgrade municipalities and a part of the Surčin municipality. By redirecting traffic, multiple benefits are expected, such as a reduction in noise levels, emissions of toxic gases, traffic frequency, and traffic accidents on the core network of urban roads [71].

Distinct spatial differentiation of hotspots obtained utilizing a geospatial approach indicates spatial disparities of TAM between the urban city core (central municipalities) and the peripheral part of Belgrade (broader city area). Different characteristics of the space, such as land cover, the category of roads, population density, and the different frequencies of the population condition. Accordingly, it is necessary to establish territorial-specific prevention programs to reduce the number of deaths in critical locations. Some measures, like installing cameras and traffic signals and increased control, have already been in force in certain areas with high traffic accidents. Education of younger children also produces significant results [72]. Considering that these measures have given satisfactory results, they can be applied in high-risk areas identified in this study.

6. CONCLUSION

This study is conducted to fill the knowledge gap concerning TAM's temporal, spatial, and spatiotemporal patterns using the potential of Joinpoint regression analysis and geospatial approach to

identify the areas with the highest number of deaths to reduce the number of deaths in traffic accidents and bring them closer to achieving the Target 3.6. Furthermore, a review of the existing literature and obtaining the results of this research showed that implementing prevention measures positively reduces the number of deaths in traffic accidents. In that sense, the results of this study can be a starting point for identifying areas in Belgrade where the adoption of targeted measures to prevent future accidents with fatal outcomes is necessary. Hence, this study represents a significant contribution to the sustainable development of Belgrade and Serbia.

The methodological apparatus used in this study can be applied to other police administrations in Serbia, given the availability of data, but also in other countries where data on traffic accidents and their outcomes are also spatially and temporally determined. The special significance of applying these methods is that they provide insight into the spatiotemporal distribution of the investigated phenomenon at the local level. The obtained results and the conclusions have a practical application because they unequivocally indicate points of interest, i.e., potentially dangerous areas to the population. At the same time, these areas require special targeted policies to reduce TAM in the future.

The limitation of this study is the availability of the data. Namely, due to the incomplete coverage of data from 2015, as the starting year in time-series data, this study adopted 2016. The data available from an earlier period would allow authors to focus further research on a much more extended period.

In addition, it is necessary to analyze the variability concerning different road users, such as pedestrians and motorcyclists, to indicate potentially dangerous areas for each of the studied categories, but also variability among different age groups and genders. Using additional data sources (e.g., digital elevation method) and analysis, such as Viewshed analysis, will contribute to obtaining more complete conclusions to improve traffic safety for the population. Since the portal contains data for all municipalities and police administrations, future research will focus on detecting vulnerable areas in other parts of Serbia.

ACKNOWLEDGMENT

The paper presents the result of work on the III47007 project financed by the Ministry of Education, Science and Technological Development of the Republic of Serbia (Contract No. 451–03–68/2022–14/200172).

REFERENCES

1. World Health Organization. (2021). *Road traffic injuries*. Retrieved from https://www.who.int/publications/i/item/9789241565684
2. The World Bank. (n.d.). *Mortality caused by road traffic injury (per 100,000 population)*. Retrieved from https://data.worldbank.org/indicator/SH.STA.TRAF.P5
3. United Nations. (n.d.). *Sustainable development goals.* Retrieved from https://unstats.un.org/sdgs/metadata?Text=&Goal=3&Target=3.6
4. Road Traffic Safety Agency. (2021a). *Statistički izveštaj o stanju bezbednosti saobraćaja u Republici Srbiji u 2020. godini* [Statistical report on the state of traffic safety in the Republic of Serbia for the year 2020]. Retrieved from https://www.abs.gov.rs/admin/upload/documents/20211221085715-statisticki-izvestaj-o-stanju-bezbednosti-saobracaja-u-republici-srbiji-u-2020.-godini.pdf
5. Zakon o bezbednosti saobraćaja na putevima [The Law on Traffic Safety on Roads], Službeni glasnik Republike Srbije No. 41 (2009). Retrieved from https://www.paragraf.rs/propisi/zakon_o_bezbednosti_saobracaja_na_putevima.html
6. Hadžić, D. & Unković, E. (2013). *Makroekonomski značaj uspostavljanja modela za upravljanje bezbednošću drumskog saobraćaja sa posebnim osvrtom na Republiku Srbiju* [Macroeconomic importance of establishing a model for road traffic safety management with special reference to the Republic of Serbia]. Ekonomski izazovi, 3(2), 1–12. Retrieved from https://scindeks-clanci.ceon.rs/data/pdf/2217-8821/2013/2217-88211303001H.pdf
7. Open Data portal. (2022). *Data on traffic accidents by police administrations and municipalities*. Retrieved from https://data.gov.rs/sr/datasets/podatsi-o-saobratshajnim-nezgodama-po-politsijskim-upravama-i-opshtinama/
8. Statistical Office of the Republic of Serbia. (2022). *Registrovana drumska motorna i priključna vozila i saobraćajne nezgode na putevima, 2021* [Registered road motor and trailer vehicles and traffic accidents on roads, 2021]. Retrieved from https://publikacije.stat.gov.rs/G2022/Pdf/G20221071.pdf

9. Lović Obradović, S., Matović, S., Rabiei-Dastjerdi, H., & Matthews, S. (2022). An ecological study of vulnerability to COVID-19 in Serbia - using Hotspot Analysis for Evidence-Based Population Health Policy. *Forum geografic, XXI*(1), 71–82. https://doi.org/10.5775/fg.2022.103.i
10. Lović Obradović, S., Rabiei-Dastjerdi, H., & Matović, S. (2022). A population-based spatio-temporal analysis of the early COVID-19 dynamic in Serbia. *Stanovništvo, 60*(1), 1–17. https://doi.org/10.2298/STNV2201001L
11. Adesunkanmi, A. R. K., Oginni, L. M., Oyelami, O. A., & Badru, O. S. (2000). Road traffic accidents to African children: assessment of severity using the Injury Severity Score (ISS). *Injury, 31*(4), 225–228. https://doi.org/10.1016/S0020-1383(99)00236-3
12. Gicquel, L., Ordonneau, P., Blot, E., Toillon, C., Ingrand, P., & Romo, L. (2017). Description of Various Factors Contributing to Traffic Accidents in Youth and Measures Proposed to Alleviate Recurrence. *Frontiers in Psychiatry, 8*, 94. https://doi.org/10.3389/fpsyt.2017.00094
13. Bhavan, T. (2019). The Economic Impact of Road Accidents: The Case of Sri Lanka. South Asia *Economic Journal, 20*(1), 124–137. https://doi.org/10.1177/13915614188222
14. Akiyemi, Y. (2020). Relationship between economic development and road traffic crashes and casualties: empirical evidence from Nigeria. *Transportation Research Procedia, 48*, 218–232 https://doi.org/10.1016/j.trpro.2020.08.017
15. Sutlovic, D., Scepanovic, A., Bosnjak, M., Versic-Bratincevic, M., & Definis-Gojanovic, M. (2014). The role of alcohol in road traffic accidents with fatal outcome: 10-year period in Croatia Split-Dalmatia County. *Traffic Injury Prevention, 15*(3), 222–227. https://doi.org/10.1080/15389588.2013.804915
16. Elvik, R. (2013). Risk of road accident associated with the use of drugs: A systematic review and meta-analysis of evidence from epidemiological studies. *Accident Analysis & Prevention, 60,* 254–267. http://dx.doi.org/10.1016/j.aap.2012.06.017
17. Jovic Vranes, A., Bjegovic Mikanovic, V., Milin Lazovic, J., & Kosanovic, V. (2018). Road traffic safety as a public health problem: Evidence from Serbia. *Journal of Transport & Health, 8,* 55–62. https://doi.org/10.1016/j.jth.2017.12.005
18. Wu, P., Meng, X., & Song, L. (2021). Identification and spatiotemporal evolution analysis of high-risk crash spots in urban roads at the microzone-level: Using the space-time cube method. *Journal of Transportation Safety & Security,* 1–21. https://doi.org/10.1080/19439962.2021.1938323
19. Erdogan, S. (2009). Explorative spatial analysis of traffic accident statistics and road mortality among the provinces of Turkey. *Journal of Safety Research, 40*(5), 341–351. https://doi.org/10.1016/j.jsr.2009.07.006
20. Okui, T., & Park, J. (2021). Analysis of the regional distribution of road traffic mortality and associated factors in Japan. *Injury Epidemiology, 8*, 60. https://doi.org/10.1186/s40621-021-00356-4
21. Brazinova, A., & Majdan, M. (2016). Road traffic mortality in the Slovak Republic in 1996–2014. *Traffic Injury Prevention, 17*(7), 692–698. https://doi.org/10.1080/15389588.2016.1143095
22. Melchor, I., Nolasco, A., Moncho, J., Quesada, J. A., Pereyra-Zamora, P., García-Senchermés, C., Tamayo-Fonseca, N., Martínez-Andreu, P., Valero, S., & Salinas, M. (2015). Trends in mortality due to motor vehicle traffic accident injuries between 1987 and 2011 in a Spanish region (Comunitat Valenciana). *Accident Analysis & Prevention, 77*, 21–28. https://doi.org/10.1016/j.aap.2015.01.023
23. La Torre, G., Van Beeck, E., Quaranta, G., Mannocci, A., & Riccardi, W. (2007). Determinants of within-country variation in traffic accident mortality in Italy: a geographical analysis. *International Journal of Health Geographics, 6*, 49. https://doi.org/10.1186/1476-072X-6-49
24. Van Beeck, E. F., Mackenbach, J. P., Looman, C. W. N., & Kunst, A. E. (1991). Determinants of Traffic Accident Mortality in the Netherlands: A Geographical Analysis. *International Journal of Epidemiology, 20*(3), 698–706. https://doi.org/10.1093/ije/20.3.698
25. Saadat, S., Rahmani, K., Moradi, A., ad-Din Zaini, S., & Darabi, F. (2019). Spatial analysis of driving accidents leading to deaths related to motorcyclists in Tehran. *Chinese Journal of Traumatology, 22*(3), 148–154. https://doi.org/10.1016/j.cjtee.2018.12.006
26. Passmore, J., Yon, Y., & Mikkelsen, B. (2019). Progress in reducing road-traffic injuries in the WHO European region. *The Lancet Public Health, 4*(6), E272–E273. https://doi.org/10.1016/S2468-2667(19)30074-X
27. Satria, R., & Castro, M. (2016). GIS Tools for Analyzing Accidents and Road Design: A Review. *Transportattion Research Procedia, 18*(3), 242–247. https://doi.org/10.1016/j.trpro.2016.12.033
28. Wang, D., Krebs, E., Nickenig Vissoci, J. R., de Andrade, L., Rulisa, S., & Staton, C. A. (2020). Built Environment Analysis for Road Traffic Crash Hotspots in Kigali, Rwanda. *Frontiers in Sustainable Cities, 2,* 17. https://doi.org/10.3389/frsc.2020.00017
29. Kang, Y., Cho, N., & Son, S. (2018). Spatiotemporal characteristics of elderly population's traffic accidents in Seoul using space-time cube and space-time kernel density estimation. *PLoS ONE, 13*(5), e0196845. https://doi.org/10.1371/journal.pone.0196845
30. Prasannakumar, V., Vijith, H., Charutha, R., & Geetha, N. (2011). Spatio-Temporal Clustering of Road Accidents: GIS Based Analysis and Assessment. *Procedia - Social and Behavioral Sciences, 21*, 317–325. https://doi.org/10.1016/j.sbspro.2011.07.020

31. Soltani, A., & Ascari, S. (2017). Exploring spatial autocorrelation of traffic crashes based on severity. *Injury, 48*(3), 637–647. https://doi.org/10.1016/j.injury.2017.01.032
32. Pljakić, M., Basarić, Đ., & Gugleta, S. (2018, October 17–18). *Spatial Clustering of Traffic Analysis Zone: A Case Study from Novi Sad, Serbia* [Paper presentation] XIV International Symposium "Road accidents prevention 2018" Novi Sad, Serbia. Retrieved from https://www.researchgate.net/publication/328392920_SPATIAL_CLUSTERING_OF_TRAFFIC_ANALYSIS_ZONE_A_CASE_STUDY_FROM_NOVI_SAD_SERBIA
33. Vaz, E., Tehranchi, S., & Cusimano, M. (2017). Spatial Assessment of Road Traffic Injuries in the Greater Toronto Area (GTA): Spatial Analysis Framework. *Journal of Spatial and Organizational Dynamics, 5*(1), 37–55. http://www.cieo.pt/journal/J_1_2017/article4.pdf
34. Yoon, Y., & Lee, S. (2021). Spatio-temporal patterns in pedestrian crashes and their determining factors: Application of a space-time cube analysis model. *Accident Analysis & Prevention, 161*, 106291. https://doi.org/10.1016/j.aap.2021.106291
35. Cheng, Z., Zu, Z., & Lu, J. (2019). Traffic Crash Evolution Characteristic Analysis and Spatiotemporal Hotspot Identification of Urban Road Intersections. *Sustainability, 11*(1), 160. https://doi.org/10.3390/su11010160
36. Rahman, M. K., Crawford, T., & Schmidlin, T. W. (2018). Spatio-temporal analysis of road traffic accident fatality in Bangladesh integrating newspaper accounts and gridded population data. *GeoJournal, 83*, 645–661. https://doi.org/10.1007/s10708-017-9791-x
37. Bandi, P., Silver, D., Mijanovich, T., & Machinko, J. (2015). Temporal trends in motor vehicle fatalities in the United States, 1968 to 2010 - a joinpoint regression analysis. *Injury Epidemiology, 2,* 4. https://doi.org/10.1186/s40621-015-0035-6
38. Barrio, G., Pulido, J., Bravo, M. J., Lardelli-Claret, P., Jiménez-Mejías, E., & de la Fuente L. (2015). An example of the usefulness of joinpoint trend analysis for assessing changes in traffic safety policies. *Accident Analysis & Prevention, 75*, 292–297. https://doi.org/10.1016/j.aap.2014.12.010
39. Nistal-Nuño, B. (2018). Joinpoint regression analysis to evaluate traffic public health policies by national temporal trends from 2000 to 2015. *International Journal of Injury Control and Safety Promotion, 25*(2), 128–133. https://doi.org/10.1080/17457300.2017.1341937
40. Jovic Vranes, A., & Kosanovic, V. (2016). Road Traffic Accidents in Serbia in 1999–2014. *European Journal of Public Health, 26*(1). https://doi.org/10.1093/eurpub/ckw175.065
41. Rančić, N., Jovanović, M., Lazić, D., & Jakovljević, M. (2012). Korelacija alkoholemije i stope saobraćajnih nezgoda sa fatalnim ishodom [Blood alcohol concentration impact on the traffic accident rates with fatal outcome]. *Medicinski časopis 46*(3), 160–167. https://doi.org/10.5937/mckg46-1315
42. Petrović, A., Jovanović, D., & Stojanović, P. (2020). Promene broja poginulih u saobraćajnim nezgodama u Republici Srbiji [Changes in the number of traffic accidents fatalities in the republic of Serbia]. *Tehnika – Saobraćaj, 67*(4), 479–484. Retrieved from https://web.archive.org/web/20201024194307id_/https://scindeks-clanci.ceon.rs/data/pdf/0040-2176/2020/0040-21762004479P.pdf
43. Simić, S., Popović, N., Erić, M., & Marinković, J. (2014). Economic crisis, transition and health status of the Serbian population. *European Journal of Public Health, 24*(2), 96. https://doi.org/10.1093/eurpub/cku161.113
44. Statistical Office of the Republic of Serbia. (2021a). *Surface area and number of settlements, by NSTU*. Retrieved from https://data.stat.gov.rs/Home/Result/1201?languageCode=en-US
45. Statistical Office of the Republic of Serbia. (2021b). *Estimates of population by age and sex (beginning, middle and end of year)*. Retrieved from https://data.stat.gov.rs/Home/Result/18010403?languageCode=sr-Cyrl
46. Matović, S., & Lović Obradović, S. (2021). Assessing socio-economic vulnerability aiming for sustainable development in Serbia. *International Journal of Sustainable Development & World Ecology, 29*(1), 27–38. https://doi.org/10.1080/13504509.2021.1907629
47. Miletić, R. (2022). Regional specialization in Serbia during the period 2001–2015. *Journal of the Geographical Institute "Jovan Cvijić" SASA, 72*(1), 67–83. https://doi.org/10.2298/IJGI2201067M
48. Lukić, V., Lović Obradović, S., & Ćorović, R. (2022). COVID-19 and internal migration in Serbia—geographical perspective. *Journal of the Geographical Institute "Jovan Cvijić" SASA*, 72(2), 191–205. https://doi.org/10.2298/IJGI2202191L
49. Open Data portal. (2022). *Data on traffic accidents by police administrations and municipalities*. Retrieved from https://data.gov.rs/sr/datasets/podatsi-o-saobratshajnim-nezgodama-po-politsijskim-upravama-i-opshtinama/
50. Road Traffic Safety Agency. (2021b). *Procenat vozača u saobraćajnom toku pod uticajem alkohola u naselju 2020* [Percentage of drivers in traffic under the influence of alcohol in the settlement 2020]. Retrieved from https://www.abs.gov.rs/admin/upload/documents/20210727071224--vozaca-u-saobracajnom-toku-pod-uticajem-alkohola-u-naselju-2020.pdf

51. Statistical Methodology and Applications Branch, Surveillance Research Program, National Cancer Institute. (2021). *Joinpoint Regression Program (Version 4.9.0.0)* [Computer software]. Retrieved from https://surveillance.cancer.gov/joinpoint/download
52. Kim, H. J., Fay, M., Feuer, E. J., & Midthune, D. N. (2000). Permutation tests for joinpoint regression with applications to cancer rates. *Statistics in Medicine, 19*, 335–351. https://doi.org/10.1002/(sici)1097-0258(20000215)19:3<335::aid-sim336>3.0.co;2-z
53. Getis, A., & Ord, J. K. (1992). The Analysis of Spatial Association by Use of Distance Statistics. *Geographical Analysis, 24*(3), 189–206. https://doi.org/10.1111/j.1538-4632.1992.tb00261.x
54. Getis, A., & Ord, J. K. (1996). Local spatial statistics: An overview. In P. Longley and M. Batty (Eds.), *Spatial Analysis: Modeling in A GIS Environment* (261–277). New York: John Wiley & Sons.
55. Rabiei-Dastjerdi, H., McArdle, G., & Hynes, W. (2022). Which came first, the gentrification or the Airbnb? Identifying spatial patterns of neighbourhood change using Airbnb data. *Habitat International, 125,* 102582, https://doi.org/10.1016/j.habitatint.2022.102582
56. Rabiei-Dastjerdi, H., & McArdle, G. (2021). Novel Exploratory Spatiotemporal Analysis to Identify Sociospatial Patterns at Small Areas Using Property Transaction Data in Dublin. *Land, 10,* 566. https://doi.org/10.3390/land10060566
57. McLeod, A. I. (2011). *Kendall Rank Correlation and Mann-Kendall Trend Test*. Retrieved from https://cran.r-project.org/web/packages/Kendall/Kendall.pdf
58. Esri. (n.d.). *How Emerging Hot Spot Analysis works*. Retrieved from https://pro.arcgis.com/en/pro-app/2.8/tool-reference/space-time-pattern-mining/learnmoreemerging.htm
59. Esri. (2020). *ArcGIS Pro* (version 2.5) [Computer software]. Retrieved from https://arcgis.pro/download-arcgis-pro-2-5/
60. Todorić, J., Vuksanović Macura, Z., & Yamashkin, A. (2022). Spatial patterns of entertainment in cities. *Journal of the Geographical Institute "Jovan Cvijić" SASA, 72*(2), 207–220. https://doi.org/10.2298/IJGI2202207T
61. Filipović, M. (2020). Dnevni migracioni system Beograda [Daily migration system of Belgrade] [Unpublished doctoral dissertation]. Belgrade, Faculty of Geography. https://nardus.mpn.gov.rs/bitstream/handle/123456789/18274/Disertacija.pdf?sequence=1&isAllowed=y
62. Pavlović, S., & Jovanović, R. (2021). Geographical index of concentration as an indicator of the spatial distribution of tourist attractions in Belgrade. *Turizam, 25*, 45–54. Retrieved from https://scindeks.ceon.rs/Article.aspx?artid=1450-66612101045P
63. Panić, M., Drobnjaković, M., Stanojević, G., Kokotović Kanazir, V., & Doljak, D. (2022). Nighttime lights—innovative approach for identification of temporal and spatial changes in population distribution. *Journal of the Geographical Institute "Jovan Cvijić" SASA, 72*(1), 51–66. https://doi.org/10.2298/IJGI2201051P
64. Filipović, M., Krunić, N., & Zelenkhova, E. (2020). Functional dependence of settlements and its demographic component in the transition phase of the daily urban system. *Journal of the Geographical Institute "Jovan Cvijić" SASA, 72*(3), 323–339. https://doi.org/10.2298/IJGI2203323F
65. Rahman, M. K., Crawford, T., & Schmidlin, T. W. (2018). Spatio-temporal analysis of road traffic accident fatality in Bangladesh integrating newspaper accounts and gridded population data. *GeoJournal, 83*, 645–661. https://doi.org/10.1007/s10708-017-9791-x
66. Road Traffic Safety Agency. (2021c). *Izveštaj o osnovnim pokazateljima stanja bezbednosti saobraćaja u periodu od 2016. do 2020. godine – Opština Sopot* [Report on basic indicators of traffic safety in the period from 2016 to 2020 – The municipality of Sopot]. Retrieved from https://www.abs.gov.rs/admin/upload/documents/20210714082432-sopot.pdf
67. Road Traffic Safety Agency. (2021d). *Izveštaj o osnovnim pokazateljima stanja bezbednosti saobraćaja u periodu od 2016. do 2020. godine – Opština Mladenovac* [Report on basic indicators of traffic safety in the period from 2016 to 2020 – The municipality of Mladenovac]. Retrieved from https://abs.gov.rs/admin/upload/documents/20210714110250-mladenovac.pdf
68. Road Traffic Safety Agency. (2021e). *Izveštaj o osnovnim pokazateljima stanja bezbednosti saobraćaja u periodu od 2016. do 2020. godine – Opština Lazarevac* [Report on basic indicators of traffic safety in the period from 2016 to 2020 – The municipality of Lazarevac]. Retrieved from https://abs.gov.rs/admin/upload/documents/20210714110547-lazarevac.pdf
69. Road Traffic Safety Agency. (2021f). *Izveštaj o osnovnim pokazateljima stanja bezbednosti saobraćaja u periodu od 2016. do 2020. godine – Opština Surčin* [Report on basic indicators of traffic safety in the period from 2016 to 2020 – The municipality of Surčin]. Retrieved from https://abs.gov.rs/admin/upload/documents/20210714082250-surcin.pdf
70. Galović, N., Kukić, D., Maksimović, V., & Petrović, D., (2013). *Pilot projekat Ibarska magistrala – Ocenjivanje bezbednosnih karakteristika puta i mapiranje rizika u skladu sa IRAP/EuroRAP metodologijom* [Pilot project Ibarska magistrala - Evaluation of road safety features and risk mapping in accordance with the IRAP/EuroRAP methodology]. AMSS – CMV & Agencija za bezbednost saobraćaja, Beograd.

71. Public enterprise Roads of Serbia. (n.d.). *Belgrade Bypass*. Retrieved from https://www.putevi-srbije.rs/index.php/en/belgrade-bypass1
72. Bumbasirevic, M., Lešić, A., Bumbasirevic, V., Zagorac, S., Milosevic, I., Simić, M., & Denic, Lj. (2014). Severe road traffic injuries and youth: a 4-year analysis for the city of Belgrade. *International Journal of Injury Control and Safety Promotion, 21*(4), 313 – 317. https://doi.org/10.1080/17457300.2013.823452